LETTER OF INTENT FOR AN EXPERIMENT AT TEVATRON WITH WIDE BAND NEUTRINO AND ANTINEUTRINO BEAMS IN THE 15' CHAMBER FILLED WITH DEUTERIUM (OR LIGHT NEON), AND WITH AN INTERNAL ELECTROMAGNETIC CALORIMETER.

Ecole Polytechnique - PALAISEAU, FRANCE
University College - LONDON, UNITED KINGDOM

With light liquids (light neon, hydrogen or deuterium) a major limitation on neutrino analysis is the loss of γ-rays and poor detection of electrons. A calorimeter, as described below, would remedy this. Some success has been achieved in developing the solid-argon ionisation chamber with a view to designing a large area calorimeter for the 15' chamber. When these tests have been successfully completed (May-June 1980) we intend to submit a detailed proposal for an experiment using this technique. The physics interest in such an experiment is summarised below.

A - PROPERTIES OF AN INTERNAL ELECTROMAGNETIC CALORIMETER.

The two purposes for which a calorimeter is desirable are the detection and measurement of γ-rays and the identification of electrons. With a hydrogen or deuterium filling in the chamber only about 70% of the hadron energy is measured. If γ-rays can be converted then more than 90% of the energy is accessible. A similar, though smaller, improvement can be gained with light neon. But it is not enough to catch only those γ-rays in the forward direction which carry the highest energy. The direction of a hadron shower is as important as its energy, since much of neutrino ana-

lysis depends upon transverse momentum balance. A study of all the γ-rays detected in a sample of hydrogen events in the WBB hydrogen TST experiment in BEBC(WA 24) shows that 52% of them are emitted at greater than 10°, 24% at more than 20° and 12% at more than 30°. Weighting the events according to the Tevatron energy spectra does not change these numbers by very much: respectively 41%, 18% and 9%(fig. 1A). There is an average of 3.5 gammas per event in the high energy events. The large angle γ-rays have lower average energies but they carry similar transverse momentum to the small angle γ's(fig. 1b). Another study in the same experiment has shown that a non negligeable part of the events in hydrogen which appear from the charged tracks to have no missing longitudinal or transverse momentum are in fact accompanied by gamma-rays. Thus, without γ detection, serious errors will be made in correcting the kinematic variables. It would therefore be desirable that a calorimeter should have two zones. The inner zone would cover the neutrino beam area of $\sim$ 1.2 x 1.2 m^2 with good spacial resolution ($\sim \pm$ 1.5 cm) to measure γ angles and separate γ's from hadrons. It would also have good energy resolution ($\sim \pm$ 10% $\sqrt{E}$) to improve the overall hadron energy measurement. The outer zone would wrap about the back of chamber, giving overall coverage of 2.4 x 3.6 m^2 with spatial resolution to $\pm$ 5 cm and energy resolution to $\sim \pm$ 15% $\sqrt{E}$. Here the area covered is more important than the precision. The results from similar calorimeters (ref. 1) indicate that there would be only $\sim 10^{-3}$ punch through of charged pions misidentified as electrons by comparing the track curvature with the calorimeter measurement.

The Ecole Polytechnique and U.C.L. groups have carried out tests which show that a solid argon chamber can work at liquid hydrogen temperature and further tests are under way to investigate the efficiency of such a chamber. It is proposed to continue this program of testing in order to provide the basis for a calorimeter design which could be mounted inside the 15' bubble chamber.

B. PHYSICS AIMS.

If an electromagnetic calorimeter can be used it should be helpful for any kind of filling of the bubble chamber, but the more at-

tractive liquid to be used is a light liquid, where the target is simple and the measurements are accurate. Nevertheless the problem of statistics is crucial, which makes deuterium more attractive than hydrogen. The yields quoted in all what follows have been computed for deuterium.

In a wide band beam with 800 GeV protons, for a run of 100.000 pictures with $2.5 \cdot 10^{13}$ ppp in D^2, $\sim$ 50 000 ν events can be expected in a volume of $\sim$ 10 m^3, and $\sim$ 15 000 $\bar{\nu}$ in similar conditions (4). The main subjects of interest that can be seen so far are the following :

1 - STUDY OF HADRONIC FINAL STATES.

Bubble chambers are the only place where each individual hadron can be investigated. Each track has to be measured accurately, which can be performed in light liquid and the largest possible part of the energy has to be seen, since most of the feasible tests rely on the fraction of hadronic momentum taken by each hadron : the presence of an electromagnetic calorimeter is essential.

a) Fragmentation functions - QCD tests.

First results on the properties of factorisation and invariance of fragmentation functions in charged particles have been obtained in the BEBC hydrogen experiment, the scaling failure being observed only for hadronic system masses below 4 GeV, which is unexpected. With a calorimeter the total hadronic momentum would be evaluated more accurately, with much smaller corrections, and so would be the evaluations of the D(Z) functions. With the higher Q^2 available at the Tevatron, it should be possible to test the QCD predictions in a more reliable way.

In addition, fragmentation functions for neutral pions should be obtainable.

b) Transverse momentum of single hadrons.

QCD predicts that due to gluon bremsstrahlung, the mean transverse momentum for single hadrons with respect to the total hadronic

momentum, $< p_T^2 >$ should increase with Q^2 or W^2. Effects have been observed in BEBC and 15' experiments in heavy neon, for large values of Q^2. Heavy neon is not suitable for this kind of events at the tevatron energy, because of their complexity. In a light liquid, the calorimeter is necessary to determine the total hadronic momentum with accuracy, which is essential for a good determination of $< p_T >$. This analysis is very interesting to be performed at the Tevatron, since high values of Q^2 are requested.

c) QCD tests with angular variables.

In the study of hadronic final states in deep inelastic scattering, QCD effects appear in two ways :

- scaling violations in structure functions, related to the emission of gluons colinear to the initial quark.
- modifications in the energy emission antenna pattern with respect to the parton model, characterizing hard gluon emission.

Bouchiat, Meyer and Mezard (2) have proposed the choice of inclusive observables connected with the angular distribution of light-cone energy :

$$X_n = \sum_{i=1}^{N} z_i \, |\vec{v}_i|^n$$

The sum is taken over all the final hadrons associated to the fragments of the struck quark, $\vec{v}$ is the transverse light-cone velocity in the Breit frame ($\vec{v} = p_\perp / p_+$) and $z = p_+ / P_+$, P being the total energy-momentum of the final hadronic system.

These observables receive their main contribution from the fragmentation of the quark which has interacted with the intermediate boson. The non perturbative contribution is computed semi-empirically

using the known values of fragmentation functions, and does not depend, at a given Q^2, on the x Bjorken scaling variable. On the contrary, the QCD perturbative contribution appears as a rapidly decreasing function of x, as shown in fig.2A, where the x dependence of $< X_2 >$ is shown for $Q^2 = 10\ GeV^2$.

Experimental tests of these predictions need the individual measurement of all emitted hadrons. Of course, bubble chambers are well suited to this kind of analysis, provided all hadrons emitted forwards in the Breit frame ($|\vec{v}_i| < 1$)are measured. Consequently, it is essential that π°'s are efficiently detected.

The use of a light liquid (H_2, D_2 or light neon) in the chamber equipped with an electromagnetic calorimeter will give simultaneously the necessary accurate measurement of charged particles and the detection of π°'s.

The choice of the best liquid is dependent on conflicting criteria :

- in order to avoid secondary interaction which would disturb the angular and energy distributions, hydrogen would be very desirable.
- high statistics are needed to check significantly the theory which is relevant only for "high" Q^2 events. Events with $Q^2 < 10\ GeV^2$ will have to be rejected, representing $\sim$ 70% of the total statistics. The best way of analysis should be to measure $< X_n >$ at given values of x and Q^2, but the rapid fall-off of the Q^2 distribution will probably lead to integrate over Q^2. In that case, the non-perturbative contribution shows a x-dependence which will make harder the separation with the QCD contribution. The expected values of $< X_2 >$, for $E = 70$ GeV and $Q^2 > 10\ GeV^2$, are shown in Fig.2B.

The analysis of 10^4 events in a wide band beam from 800 GeV protons would provide an accuracy between 0.005 and 0.02 for $< X_2 >$ integrated over Q^2 and measured inside 0.1 width bins of x.

2. *INCLUSIVE REACTIONS.*

Structure functions could of course be determined for a large range of q^2. All what is specific to deuterium ($\sigma n/\sigma p$, Adler sum rule etc...) could be performed at high energy, with the advantage of a good determination of the ν energy.

3. *NEW PARTICLES.*

In spite of the statistics more reduced than in counter experiments, some properties of the new particles, or means of discovering them, can be achieved only in bubble chambers.

a) Charmed particles.

In ν production, large statistics have been obtained so far only for leptonic modes and essentially in counter experiments, where the possible investigations of their properties are limited. The hadronic modes have been seen in very small numbers, most of the time with only charged particles in heavy liquid experiments. In a rather light liquid, with accurate measurements and with a good observation of neutral pions with the calorimeter, it should be possible :

- to compute invariant masses for the hadronic modes.
- for leptonic modes, to detect $\mu\mu$'s with the EMI, and μe's with the calorimeter. In case of no missing baryons, the missing neutrino could perhaps be reconstructed (OC fit) and the charmed particle identified (D or Λ^c).
- for hadronic modes and some leptonic modes, to be able to compute the space-time characteristics of the produced charmed meson or baryon.
  This should allow to investigate their production as a function of energy, in particular to determine their fragmentation function.

With a rate of 5.10^{-2} of the normal charged current events, 2500 charmed events could be expected, 250 of them appearing like $\mu^-\mu^+$ events, about half of which being identified with the EMI, and 250 like μ^-e^+ events

which could be identified with the calorimeter most of the time.
The 2.000 hadronic decays could be seen in case of a visible strange particle being present.

If high resolution cameras can be provided, it should be possible to see some of the decays : a 10 GeV/c charm with a time of flight of 5.10^{-13}s should leave a track of 750 µm. With a resolution of 200 µm, a not so bad accuracy on the lifetime should be obtainable. For such an identified charged event, the calorimeter would be especially useful for measuring the decay products.

b) Beauty

Beauty should be searched for in antineutrino pictures ($\bar{\nu} + u \to \mu^+ + b$). Rates estimated by Phillips (3) to $\sim 10^{-3}$ at 70 GeV lead to $\sim$ 15 B events. The only hope to see them should probably be their direct observation. A 20 GeV/c B particle with a time of flight of 10^{-13}s gives a 100 µ long tract. Some events can be expected with a time of flight greater than the optical resolution. In addition, since most of them should decay in charmed particle, two successive scatters at the beginning of a track or an event with three vertices could sign a $b \to c$ event. Observing them is a matter of luck....

4. ν_e, $\bar{\nu}_e$ *physics*.

If the $\nu_e(\bar{\nu}_e)$ rate in the horn beam is the same as at present energies for the same running time more ν_e's($\sim$ 1000) should be expected in this beam than in specific $\nu_e(K_L^o)$ beam or in beam dump. Light liquid with calorimeter would be ideal for this kind of analysis; the electron could be well measured in the liquid, then would be identified in the calorimeter without possible confusion with pions : the ν_e spectrum is harder than the ν_μ's so the electron is much more energetic than any of the pions. In $\bar{\nu}$ they can differ by an order of magnitude.

So all the ν_e physics for charged currents can be cleanly performed in this experiment. For neutral currents the ν_e/ν_μ ratio would be too low and the analysis can be done only in a specific ν_e beam.

5) NEUTRAL CURRENTS IN HYDROGEN

Most of the analysis of neutral currents have been performed on isoscalar targets. An analysis with hydrogen is the only way to distinguish couplings with u and d quarks. If an experiment with the 15' foot B.C. filled with hydrogen could be performed at the Tevatron, a calorimeter would be highly desirable to get a reliable analysis on neutral currents (if all the hadronic momentum is seen, in principle it is possible to compute completely the characteristics of the events (OC fits).

V. BRISSON , P. PETIAU (Ecole Polytechnique)
F.W. BULLOCK, D.J. MILLER (U.C.L.)

- REFERENCES -

1 - J.A. APPEL, Proceedings of Calorimeters workshop, Fermilab (1975).

2 - C. BOUCHIAT et al., to be published
M. MEZARD, Thesis, Ecole Normale Supérieure, Paris

3 - R.J. PHILIPPS, Nucl. Phys. B 153, 475(1979).

4 - S. MORI, Argonne Neutrino Tevatron workshop, Oct. 1979.

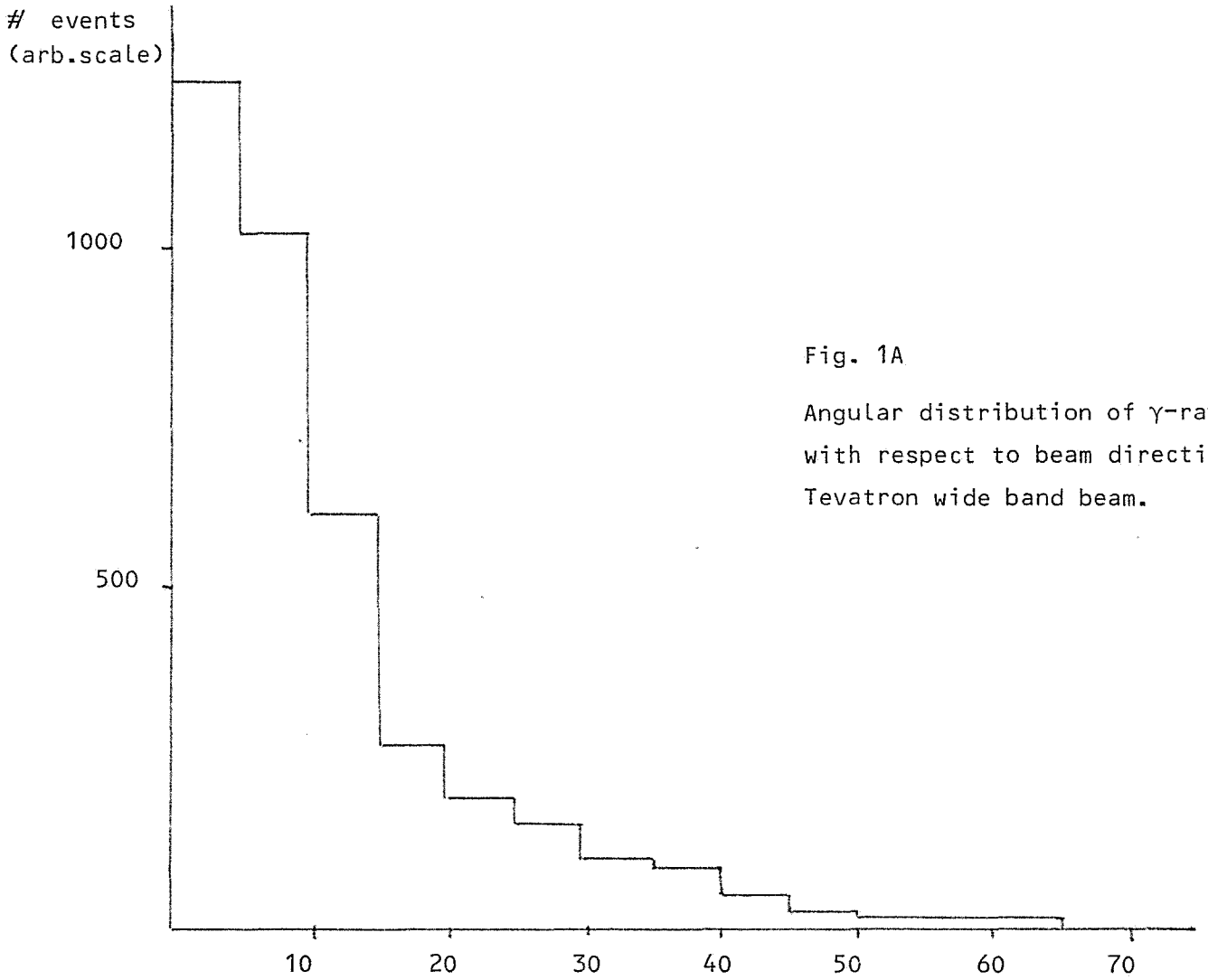

Fig. 1A

Angular distribution of γ-rays with respect to beam direction in a Tevatron wide band beam.

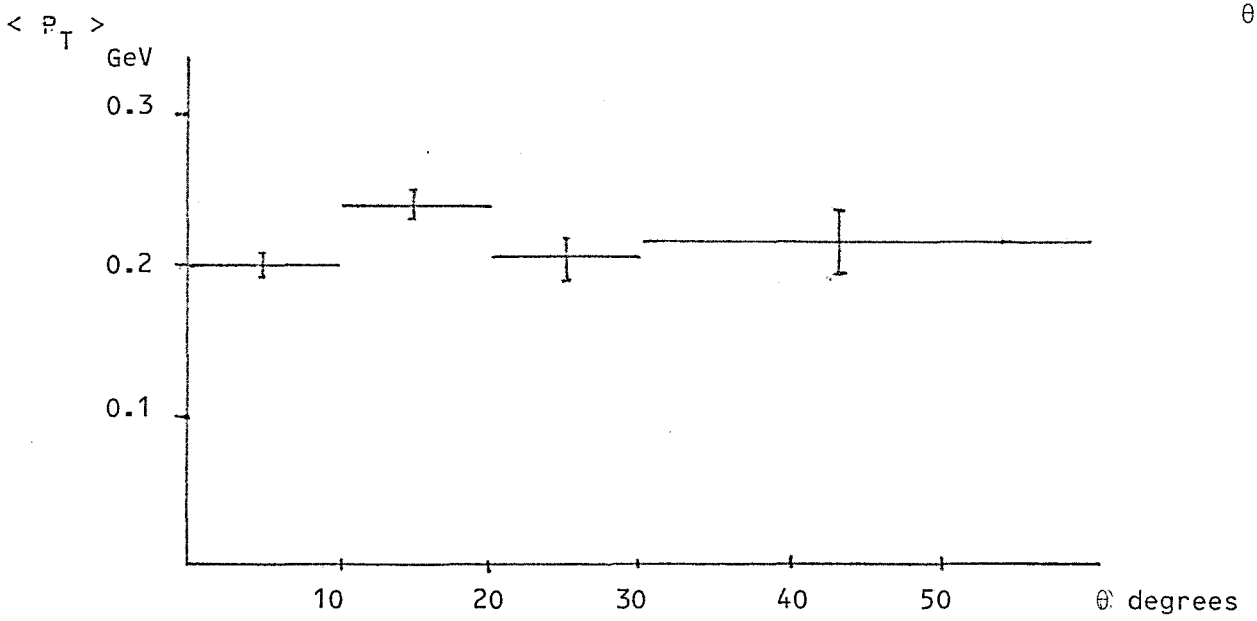

Fig. 1b

Mean transverse momentum of a γ-ray as a function of emission angle θ with respect to beam direction in a Tevatron wide band beam.

Fig. 2 A

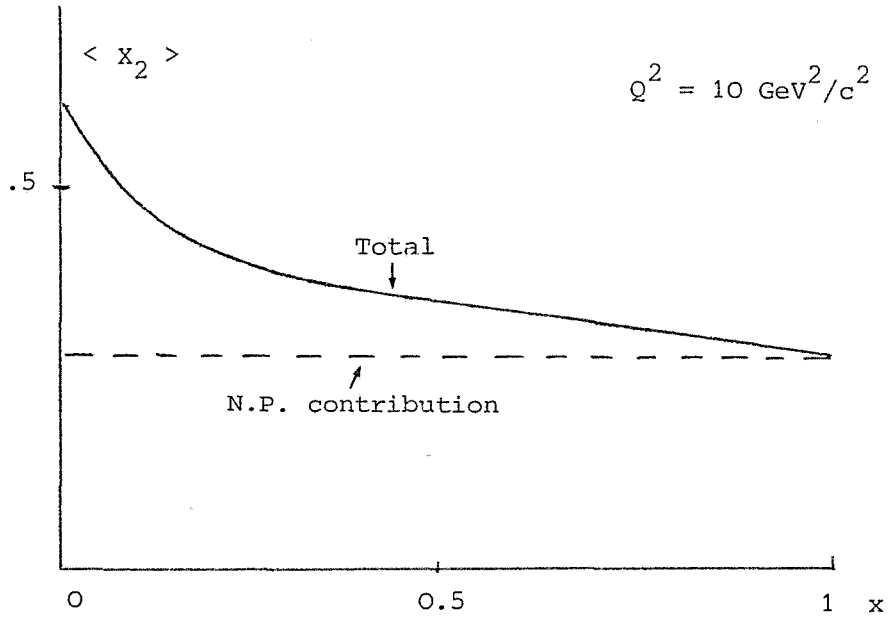

Fig. 2 B

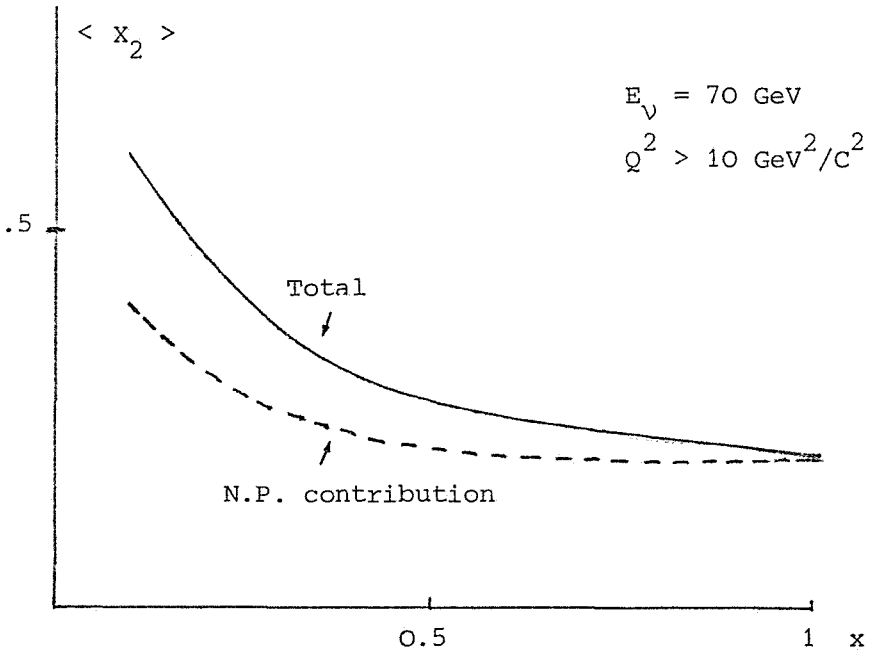

Theoretical Predictions for < X_2 > as a function of x, showing the non-perturbative and the QCD contributions.

February 1982

ADDENDUM TO PROPOSAL 651

A 15' Bubble Chamber Experiment with a solid Argon or Neon Calorimeter*

Ecole Polytechnique, Illinois Institute of Technology, Tufts University, University College London.

INTRODUCTION Since the proposal was first submitted members of our collaboration have continued to work on the solid neon and solid argon technique. We have also been engaged in the analysis of current bubble chamber neutrino experiments. This note will give a brief reminder of some of the advantages of a calorimeter, give further details of how a calorimeter could be built and list desirable improvements to the 15' neutrino facility.

A. Calorimeter Development

1. Fermilab Tests. Since it is not yet clear whether solid argon or solid neon will be the simplest filling for a calorimeter (see below) we have been working on both techniques. As part of the solid neon programme it was shown that neon frozen from a neon-hydrogen mixture (as available in large quantities at the 15' chamber) performs in a small ionisation chamber as well as does pure neon(1).This will lead to a saving of around $100,000 if neon is used,since a new filling of clean neon will not be needed.

2. Calorimeter Tests. A test calorimeter with 40 readout channels has been built at Ecole Polytechnique in order to study the performance of solid Ar and solid Ne in a large unit. The area of the electrodes is 30cm x 60cm. There are 30 gaps, each with 3 mm of solid, separated alternately by Pb ground electrodes and by printed circuit boards carrying the positive high voltage electrodestrips. The strip patterns run in the up-down direction in the front and back layers of the calorimeter and are inclined at $\pm 45^{o}$ in the middle layers. Each channel is connected via a charge-preamplifier (2) to an ADC in CAMAC. The calorimeter is 14 centrimetres thick, with more than eight radiation lengths of Pb and other material. It is now installed in a beam at CERN and a programme of tests is scheduled during February and March.

The purpose of these tests is to show :

a) That large blocks of Ar and Ne, at a suitable temperature for operation inside a bubble chamber, will give reliable and uniform sensitivity to beam particles; both electrons and hadrons.
b) That the pulse-height data from such a calorimeter fits the performance predicted from a Monte Carlo programme. Thus the performance of the larger calorimeter in the 15' chamber(energy resolution, position resolution, ambiguities) can be infered from the same program.
In a preliminary test of the calorimeter and its cryogenics at the Ecole Polytechnique in January 1982 the pulses due to Cosmic Ray particles in solid Ar were very clearly resolved.

3. Design for inside chamber. We have benefited from a continuing dialogue with the BEBC engineers at CERN and they are giving support to

* Spokesperson D.J.Miller, U.C.London

our current tests. In particular, one of them has done a heat-transfer study on the problem of cooling-down and freezing the calorimeter for either an argon or a neon filling. With argon there is a problem that the boiling and freezing points are in the 80°K range where hydrogen cooling-loops cannot be efficiently controled. With neon the only problem is that the liquid freezes at about 25°K (triple point 26.19°K), so that the calorimeter would have to be kept a few degrees colder than the chamber liquid and insulated from it.

It is anticipated that the internal structure of the calorimeter for the 15' chamber would be similar to that of the current test calorimeter, but with at least one layer of square pad electrodes, instead of strips, to help resolve ambiguities. There would also be copper plates to act as thermal pathways during the cooling and freezing periods.

The outer wall of the calorimeter must withstand the full shock of the chamber expansion. It is proposed that the services to the calorimeter should be brought in through a single pipe from the top of the vacuum vessel, through the chamber wall and into the central module. The other two modules would be connected inside the chamber. Within the service pipe as it passes upwards through the vacuum space there will be a temperature gradient from calorimeter temperature to room temperature. To protect against failure of the room temperature plate and feedthroughs on the end of this pipe the walls of the calorimeter itself need to be able to withstand the same overpressure as the chamber. To keep the average front wall thickness down to half a radiation length it will be necessary to place support-rods between the front and back walls of the calorimeter box at 30 cm intervals. These will pass through holes in the electrodes and will help to support the Pb plates. Only a small fraction of the useful area is lost in this way (c.f. BBQ rods in a scintillator calorimeter).

In order to achieve the required granularity, to give both spatial resolution and electron identification, we estimate that at least 3000 channels of readout will be needed. If the pre-amplifiers are kept outside the bubble chamber then there will need to be approximately 5m of twisted pairs between each electrode and its pre-amplifier, adding $\sim$0.5nF to the channel capacitance and increasing the noise threshold accordingly. 3000 twisted pairs will also add a considerable conductive heat load to the chamber. A system of cold pre-amplifiers and cold CCD multiplexers has been proposed and some tests have been made at Ecole Polytechnique and UCL. This shows promise and may allow us to reduce the number of readout connections to around 200.

Special cooling loops will be needed inside the calorimeter to cool and freeze the contents, to carry away heat from cold electronics and to intercept heat conducted along the high-voltage and signal leads.

B. Advantages of Calorimeter for Physics Programme

1. Exposure

We are asking for 2.5×10^{18} protons divided equally between ν and $\bar{\nu}$, with a deuterium filling in the bubble chamber. For the study of hadronic final states in CC events a neutrino beam will give better statistics. For NC studies the $\bar{\nu}$ data will be particularly valuable. We prefer a wide band beam to give better statistics for neutral current studies, but a a quadrupole triplet beam would be acceptable.

2. Quality of Data

Monte Carlo studies of the performance of a calorimeter have shown that it

will make substantial improvements on the determination of the hadron energy in neutrino events. In hydrogen experiments only 73% of the hadron energy is seen. About 20% goes in lost γ-rays. We calculate that only $\sim$3% will be lost in γ-rays with a calorimeter. These calculations have been checked by comparison with the results of the WA24 (H_2 T.S.T. + Neon) experiment at CERN and with E 545 in the 15' chamber.

The deuterium filling is a compromise between event rate and measurability. Already in E546 and WA24 it has become clear that the highest energy events in neon have too many badly measured fast tracks. This effect will be even worse at the Tevatron and it will make the measurement of the highest energy events in P 632 extremely difficult.

3. Charged Current Studies

a) Despite the difficulties of measuring energetic hadrons in neon, E546 has had some success in establishing an excess of transverse momentum in the forward hemisphere of events at large Q^2 and W. This has been interpreted as the observation of gluon bremsstrahlung (3). With 1.25×10^{18} protons we expect 25,000 CC events from a wide band beam (c.f. 5433 in ref.3) of which 5,000 will have $E_\nu > 100$ GeV. This last number would be unchanged if a quadrupole triplet beam is used. These events will be much better reconstructed in deuterium. The calorimeter will addd significantly to the precision with which the hadron direction is defined and the transverse momenta of the fast secondaries will be better resolved.

b) There has been recent interest in the diquark and other higher-twist components of neutrino-hadron scattering. In particular, one would like to know the fragmentation functions for proton production[4]. The variable which is used to identify final-state protons in these studies is $(E-p_\ell)$, both components of which will be better measured with the calorimeter. Both ν and $\bar{\nu}$ data will be needed, the range of W must be large and the cleanliness of deuterium events is important.

c) As well as these two topics there remains an extensive programme of studies to be carried out on CC events; correlation between hadron and Q directions, sphericity, planarity, multiplicity; structure functions with reduced smearing due to better hadron measurement and with the large Tevatron range of ν and Q^2; pion fragmentation functions from p and n with both ν and $\bar{\nu}$ incident; n to p cross-section ratios as a function of x_{Bj}; semi inclusive hadron resonance production in current and target fragmentation (improving upon the E 545 results in D_2 without calorimeter (5)).

4. Neutral Current Studies

The present concern in WA24 is to improve the determination of the u and d quark NC couplings by comparing the cross-sections on neutron and proton, and by looking at semi inclusive pion production. Both of these could be done better in deuterium with a calorimeter. The WA24 collaboration is now achieving a significant improvement in precision (compared with their earlier results[6]) by applying a cluster analysis to the neutral current candidates. This makes use of all the information available for each event, including γ-ray measurements in the neon outside the TST. It would be even more effective in deuterium, with a calorimeter to give precise γ-ray measurements and to reconstruct π^os. An upsteam picket fence (see below) would also help substantially.

C. Improvements to the 15' Neutrino Facility

1. Beam Flux Monitoring

With the calorimeter and deuterium one is in a position to do careful cross-section measurements for both charged and neutral currents as a function of beam energy. This will require better beam monitoring data than has previously been used in 15' WBB experiments. As well as muon counters in the shield and a system of sensors around the horn and target, it would be very useful if pulse-by-pulse data were available on the E.M.I. magnetic tape [7].

2. High Resolution Optics

In the original proposal we pointed out the advantages of using deuterium and a calorimeter for the detection of charm (and beauty). We anticipate that a significant number of charmed decays will be fully reconstructed and if the short lived track (or gap) is well resolved by high resolution optics or holography then each event will be even more valuable.

3. Upstream Internal Picket Fence

The downstream IPF worked very poorly during the 1980/81 run. The calorimeter would in fact perform most of the tasks of the downstream IPF, but we reiterate the need for an upstream IPF in neutral current studies. In WA24 one of the main sources of confusion in identifying neutral current events is the background due to neutron interactons. An upsteam IPF will measure the timeslot for most ($\sim$80%) of the events occuring outside the chamber which cause neutron interactions in the liquid. Neutral current candidates can be rejected if they fall into the same timeslot as an event in the upstream IPF. Such a system is now working in BEBC.

4. E.M.I. and Computer

The existing two-plane E.M.I. will be adequate for this experiment if it has been set up and debugged in good time before the exposure begins. The addition of our calorimeter would mean a major change to the computer program and it is anticipated that other modifications mentioned in ref. 5 would be included in a completely rewritten system incorporating E.M.I., calorimeter and beam monitoring (plus upsteam IPF,if available). Hardware modifications to improve the reliability of the E.M.I. would certainly be welcome.

References

1. W.Cyko et al, "A Particle Detector using Solid Neon Frozen from a Neon-Hydrogen Mixture"; Fermilab neutrino note65, to be published in Nuclear Instruments & Methods. Also V. Brisson et al, "Tests on a Solid Argon Detector at Liquid Hydrogen Temperature", Physica Scripta 23, 688 (1981).

2. W.J. Willis and V. Radeka, Nucl.Instr. and Meth.120, 221 (1972).

3. H.C. Ballagh et al, "Evidence for Hard Gluon Bremsstrahlung in a Deep-Inelastic Neutrino Scattering Experiment", Phys.Rev.Letts.,47,556(1981).

4. L. F. Abbott et al, Phys.Lett.88B, 157 (1979).

5. E545 results reported by W.A.Mann, ν '81 Hawaii, Vol.II. P.162.

6. V.Brisson, ν '81 Hawaii, Vol.II.

7. D.J.Miller "The 15' Bubble Chamber's E.M.I." Fermilab Neutrino Note No.68 (April 1981) and "Future of E.M.I. for 15' Bubble Chamber", Neutrino Note No.66 (August 1981).

PROPOSAL FOR THE DESIGN AND CONSTRUCTION OF A SOLID NEON CALORIMETER FOR INSTALLATION IN THE 15 FT. FERMILAB CHAMBER

Prepared by

Energy Conversion Section of the
Energy and Environmental Systems Division

ARGONNE NATIONAL LABORATORY

Proposal for the Design and Construction of a Solid Neon Calorimeter for Installation in the 15 ft. Fermilab Chamber

1 Background

An international team of high energy physicists from Ecole Polytechnique, Illinois Institute of Technology, Tufts University, and University College London is proposing a neutrino experiment (P-651) in the Fermilab 15 ft. bubble chamber at tevatron energies. An important feature of this experiment would be the introduction of an electromagnetic calorimeter into the bubble chamber. When operated with deuterium filling of the chamber, this solid neon calorimeter would be capable of precise measurements of the electromagnetic as well as the charged particle component of the neutrino interaction. Dr. David Miller of University College who is the lead physicist of the collaboration visited ANL on November 2, 1982 and discussed briefly the calorimeter development. Dr. Miller is aware of ANL cryogenic bubble chamber expertise and he was also directed here by Fermilab who cannot commit themselves to the engineering development at this time.

The present schedule for this experiment is as follows: engineering test of one full size module in the 15 ft. bubble chamber in Spring of 1984 and start the physics run with three modules in January of 1987. Dr. Miller believes that a more realistic date for the engineering test may be January, 1985.

Some initial conceptual work has already been done by G. Passardi at CERN on the construction and cooling of the calorimater. Tests of a small calorimater immersed in a static cryostat have been successfully carried out at Ecole Polytechnique. Dr. Miller inferred that the results of these studies would be made available to ANL at appropriate time.

The physics collaborators have submitted a proposal to Fermilab. The initial phase of the program requires design, construction, installation and test of a single module of the calorimater. Dr. Miller has requested A. Thomas to prepare a proposal that would address the entire design and construction phase with an option to stop after the conceptual design studies. This proposal represents the initial response to the request.

2 Objective

Provide cryogenic bubble chamber expertise and assistance to the international high energy physics collaboration in the conceptual design, detail design, fabrication, and test planning of a solid neon calorimeter. The calorimeter will be installed and operated in the 15 ft. Fermilab bubble chamber with liquid deuterium filling. As presently conceived the final calorimeter would consist of three modules installed through the piston opening. The present proposal addresses the engineering of the calorimeter modules and the construction of a single full size test module.

3 Scope of Work

The work to be performed under this agreement will be under the direction of A. Thomas of the Energy and Environmental Systems Division at ANL. The principal spokesman for the physics collaboration is Dr. David Miller, University College London.

The initial requirements of the calorimeter development program are as follows:

Conceptual Design

a) Collect and review all specific technical background information
b) Study selected design options in consultation with high energy physics researchers
c) Prepare an interim report suitable for safety and design review

Detail Design

a) Specify the final design requirements
b) Conduct detail mechanical design
c) Design cooling system and specify components
d) Prepare fabrication plan
e) Prepare installation and cooldown instructions

Construction of Prototype Module

a) Order materials and parts
b) Fabricate calorimeter structure
c) Install calorimeter internals
d) Complete assembly and leak check

4 Work Plan

ANL will accept technical and program guidance and direction from Dr. D. Miller or his designated representative and provide the required engineering and related services to carry out the tasks. It is ANL understanding that the actual installation of the calorimeter in the bubble chamber, the optics (including the attachment of Scotchlite), the cooldown and the operation will be handled by Fermilab. The calorimeter electronics will be designed and supplied by others to ANL.

ANL will perform the following tasks:

Conceptual Design

Task 1 Collection of Specific Technical Background Information

There has been experimental and engineering, work performed both at CERN and at Ecole Polytechnique related to the development of the calorimeter. Written information will be furnished to ANL by Dr. Miller: this will be reviewed and where appropriate utilized in the conceptual design study. If telephone conferences or correspondence do not yield the necessary information a trip to visit these research centers may be required. Preliminary discussions will be held with Fermilab to discuss the chamber related constraints.

Task 2 Study Selected Design Options

This task must be initiated quite early. The physicists will need to establish specific design goals and options to be studied. It is essential in this kind of support arrangement to focus sharply on very specific goals in order to avoid inefficiency and dilution. The establishment of the specific study goals will require at least one or two iterations between engineers and physicists.

Once the study goals are established ANL will provide layouts, weight estimates, preliminary stress calculations, conceptual installation and attachment methods, fabrication and assembly study, cooldown and warmup concepts, and temperature control. These studies will interface with appropriate Fermilab personnel in order to take into account the chamber limitations on static and dynamic load distribution, installation accessibility, optics, parasitic boiling and optical turbulence, and mechanical fatigue considerations.

Task 3 Prepare an Interim Report

At the end of Task 2 all the significant information will be collected into an Interim Report. The contents of the report will be sufficient for a design and safety review. The Interim Report will also contain cost estimates for the final design and fabrication for each option studied. Submission of the Interim Report will be a point for the high energy physics research group to decide on whether to continue with the calorimeter development. This decision could conceivably be influenced by a variety of factors technical, programmatic, and scientific.

Detail Design

Task 4 Specify the Final Design Requirement

The final design requirement may not necessarily be identical to those studied during the conceptual design phase but the additions or deviations should be of small engineering impact. It is expected that once agreed upon the final design specifications will remain unchanged throughout the detail design. ANL will take action to assure that definitive input information is obtained from both the physics group and the Fermilab bubble chamber group.

Task 5 Conduct Detail Mechanical Design

Mechanical fabrication drawings will be made, stress calculations will be finalized, and attachment method will be specified. The detail design will take into account all the safety requirements, parasitic boiling considerations, and the calorimeter/chamber interactions; (thermally, mechanically and optically.) A significant amount of interfacing with Fermilab will be required during this task.

Task 6 Design Cooling System and Specify Components

A cooling system will be designed based on the concepts developed during the conceptual design. The system will allow proper control of the calorimeter during cooldown, operation and warmup of the bubble chamber. The cooling system will include purging and pressure relief provisions. All components of the cooling system will be designed to withstand required full internal and external pressures so that no breach due to pressure will occur. Flow and temperature control method will be selected in consultation with Fermilab.

Task 7 Prepare Fabrication Plan

A fabrication plan will be prepared which will include a schedule and identify the sequence in which the assembly will proceed. Instructions for the calorimeter internals will be needed during this task. The plan will contain critical checks and tests to be made during assembly The plan will be submitted to the physics group for comment.

Task 8 Prepare Installation and Cooldown Instructions

Written instructions for installation and cooldown will be prepared. The instructions will be suitable for a safety review. The instructions may not be of sufficient detail to be incorporated directly into job lists or operating procedures. Additional effort by Fermilab to detail them to that level may be required.

Construction of Prototype Module

Task 9 Order Materials and Parts

All materials and parts required for the construction and assembly of the calorimeter will be ordered. Arrangements will be made for shipment of calorimeter parts made by other organizations to ANL.

Task 10 Fabricate Calorimeter Structure

The calorimeter structure will be fabricated in accordance with the fabrication drawings. Engineering supervision will be provided to assure that the workmanship meets the required standards and specifications.

Task 11 Install Calorimeter Internals

Calorimeter internals will be installed and checked in accordance with instructions furnished by the organization responsible for the calorimeter instrumentation design and the fabrication plan generated in Task 7. Particular attention will be paid to the mechanical supports and electrical lead attachment and insulation, especially their susceptibility to cyclic fatigue loads.

Task 12 Complete Assembly and Leak Check

The unit will be completed and the entire assembly will be vacuum leak checked prior to shipment to Fermilab for installation.

5 Deliverables

ANL will submit the following deliverables during the course of the entire calorimeter development program:

a) Interim report at the end of the conceptual design

b) Fabrication plan at the beginning of the construction phase

c) Installation and cooldown instructions, at the end of the construction phase

d) A package containing fabrication and assembly drawings and stress and cooldown calculations at the end of the detail design phase.

e) One prototype module of the calorimeter ready for shipment and installation in the Fermilab 15ft bubble chamber.

6 Effort

Maximum estimated staffing requirements in person-months for this project are as follows:

	Conceptual Design	Detail Design	Construction	Total
Lead Engineer	2	2	1	5
Design Engineer	5	6	3	14
Designer	~~10~~ 3 (checked with A.Th.)	6	2	11
Total Staff	10	14	6	31
Secretary	1	1	1	3
Technician	—	—	5	5
Total Weekly	1	1	6	8

7 Cost Estimate

The cost estimates in this proposal cover all three phases of the calorimeter development. The assumptions used in preparing the cost estimate are as follows:

a) The conceptual design will be limited to a small number of design variations from the basic concept.

b) The entire development program will be carried out in a continuous manner so that no reassignment of manpower is involved.

c) Only the fabrication but not material costs need to be included for the lead plates in the calorimeter.

d) The cost estimates for the detail design and construction are stictly preliminary since the entire question of the final design is open. The final costs for these two phases will be made in Task 3 of Conceptual Design.

Conceptual Design

Task No.	Task	Estimated Cost (x1000)
1	Collection of Specific Technical Background Information	14
2	Study Selected Design Options	41
3	Prepare an Interim Report	10
		65
	General and Administrative Cost	15
		$80

Detail Design

Task No.	Task	Estimated Cost$ (x1000)
4	Specify the Final Design Requirements	7
5	Conduct Detail Mechanical Design	44
6	Design Cooling System and Specify Components	17
7	Prepare Fabrication Plan	9
8	Prepare Installation and Cooldown Instructions	13
		90
	General and Administrative Cost	20
		$ 95

Construction of Prototype Module

Task No.	Task	Estimated Cost (x1000)
9	Order Materials and Parts	37
10	Fabricate Calorimeter Structure	40
11	Install Calorimeter Internals	27
12	Complete Assembly and Leak Check	19
		123
	General and Administrative Cost	27
		$150
	Total estimated cost of calorimeter design and fabrication of one test module	$340

8 Schedule

It is estimated that the work described in this proposal can be accomplished in about 16 months, provided no major changes in requirements surface during the design stages. Upon initial agreement the work would proceed as follows:

Phase	Completion
1. Conceptual Design	5 months after agreement
2. Detail Design	6 months after approval
3. Construction	app. 6 months after detail design depending on the features of final design

Fermilab Proposal 651
(Revised and updated)
Spokesman : D.J. Miller

NEUTRINO-PROTON AND NEUTRINO-NEUTRON INTERACTIONS IN THE FERMILAB 15-FOOT BUBBLE CHAMBER WITH A SOLID NEON CALORIMETER

Ecole Polytechnique
V. Brisson, P. Petiau

Illinois Inst. of Technology
R. Burnstein, J. Hanlon, H. Rubin.

Tufts University
T. Kafka, W.A. Mann, A. Napier, J. Schneps.

University College London
F.W. Bullock, D.J. Miller

February, 1983

Table of Contents

I. INTRODUCTION

In 1981 this collaboration submitted a Letter of Intent to carry out neutrino-deuterium physics in the 15-foot bubble chamber equipped with a solid argon (neon) calorimeter; this Letter, which became Proposal P651 was followed in February, 1982 by an addendum of a few pages, and in May 1982 by detailed answers to questions from the PAC. The purpose of this revised and completed version is to bring all the earlier documentation into one coherent whole, while adding new material and expanding on some of the previous . It is our contention that there is little point to carrying out further large neutrino-deuterium (hydrogen) exposures without effective detection of neutral particles and electrons. Present experiments have, or will soon have, reached the point where the limitations due to this lack prevent the accumulation of much further knowledge.

We are proposing a 2.5×10^{18} proton quadrupole triplet neutrino exposure, half ν, half $\bar{\nu}$, on deuterium, in order to study νn, νp, $\bar{\nu} n$ and $\bar{\nu} p$ interactions as well as interactions on an isoscalar target. To sharpen νp physics, that is to eliminate any nuclear effects, we propose following this wih a comparable neutrino-hydrogen exposure. We envision the bubble chamber facility becoming an almost complete hybrid vertex detector system by the inclusion of high resolution optics (HRO), a completed internal picket fence (IPF), an improved external muon identifier (EMI) and the solid neon calorimeter (SNC). In addition to the detection of short decay tracks, timing information, muon identification, and the detection of photons and electrons which this system makes possible, we show that the calorimeter will also enable us to achieve a substantial amount of proton identification and the detection of neutrons and K^o_L.

The main physics aims of these experiments will be:

a) To measure $\sin^2\theta_w$ in semileptonic interactions to an experimental precision of about 0.005.

b) To determine the neutral current couplings of the u and d quarks with greatly increased precision.

c) To determine the charged-current structure functions, and hence the quark distributions, of the proton and neutron using hydrogen and deuterium; without "EMC effects".

d) To study QCD effects taking advantage of the highest available range of Q^2 values.

e) To study charmed final states and to look for beauty, putting

tighter constraints on the Kobayashi-Maskawa couplings.

f) To investigate the hadronic final states as a function of quark flavour, with good resolution in the z variable.

See Sections V and VI of this document for some of the other worthwhile physics which can also be done.

That a solid neon (or argon) calorimeter works at the operating temperatures of hydrogen bubble chambers has now been demonstrated on three occasions. Small modules were built and tested in particle beams at Saclay and at Fermilab[1]. More recently a large module, constructed at Ecole Polytechnique, was tested in a beam at CERN and showed all the properties necessary for good calorimetry; long term stability, good pion-electron separation, and resolution comparable to that obtained in liquid argon calorimeters[2]. The preliminary results of these tests were presented at the PAC open meetings of April 1982.

In the following sections we state our proposal, review the particle identification properties of the calorimeter, the advantages which lead us to consider deuterium as probably the first bubble chamber fill, and discuss the physics to be done on the assumptions that in addition to the SNC, the EMI, IPF and HRO will be part of the 15-foot facility. Technical details on the calorimeter are given in the final section.

II. PROPOSAL

We propose to begin the calorimeter programme with a 2.5×10^{18} proton exposure of the deuterium filled 15-foot bubble chamber, equally divided between ν and $\bar{\nu}$ at the highest available Tevatron energy, the bubble chamber to be equipped with an EMI, IPF, HRO and, in particular, the solid neon calorimeter (SNC) which is the vital part of this proposal. This would be followed by a comparable neutrino-hydrogen exposure. We would use a quadrupole triplet beam for both exposures.

The expected event rates for the deuterium exposure are 25,000 CC events and 7500 NC events for neutrinos, and 8000 CC events and 3200 NC events for antineutrinos. The Q^2 and W^2 distribution of the CC neutrino events is shown in Table I. It is noteworthy that more than 2/3 have $W > 5$GeV, where separation of target and current regions becomes very good. The number with $W^2 > 100\text{GeV}^2$ and $Q^2 > 50\text{GeV}^2$ is 1352.

III. THE SOLID NEON CALORIMETER - ENERGY DETECTION AND PARTICLE IDENTIFICATION

The solid neon calorimeter will detect photons and electrons coming from neutrino interactions in the bubble chamber. It is also capable of detecting the substantial fraction of the neutrons and K_L^o produced in those interactions, which interact in the calorimeter material. These properties make it possible to achieve an enormous improvement in the measurement of neutrino energies on an event-by-event basis, to identify individual neutral particles such as π^o, η and neutrons or K_L^o, and furthermore, to achieve a substantial amount of proton identification.

Using a calorimeter arrangement as indicated in Figure 1, we have carried out Monte-Carlo calculations to study these questions using data from both the E545 νd experiment and the WA24 TST experiment as input. We find that 90% of all γ's either enter the calorimeter or convert in the chamber liquid, and only 10% escape. However, those which escape tend to be low energy γ's, and we find that 98% of all γ energy is deposited in either the calorimeter or the liquid. For 80% of π^o's both γ's are detected, whereas for only 5% do both γ's escape. We find that $\sim$ 60% of all neutrons and K_L^o produced in neutrino interactions will give visible interactions within the calorimeter, in addition to about 20% which will produce secondary interactions within the chamber liquid.

In charged current interactions in a hydrogen or deuterium experiment in the bare chamber $\sim$ 73% of the hadronic energy is seen. Some 20% is lost in γ rays and the rest in neutrons and other hadronic particles (K_L^o, $\Lambda \rightarrow n\pi^o$, etc.). The standard procedure for determining the neutrino energy of a CC event is to assume the ratio of neutral hadronic to charged hadronic longitudinal momenta is the same as the ratio of transverse momenta. This leads to a considerable smearing in our knowledge of neutrino energy and therefore in all the kinematic quantities that depend on it. This is illustrated in Fig.2, where we show the energy smearing for a bare hydrogen experiment, and a Monte Carlo calculation for the calorimeter, and in Fig.3, where we show the transverse momentum ratio p_T^H/p_T^μ for bare H_2, BEBC with TST and the calorimeter.

In Fig. 4 we show a plot of $\gamma\gamma$ invariant masses from Monte-Carlo generated neutrino events. We see a clean π^o peak over a combinatorial

background. The full width of the peak at half height is about 60 MeV. However, this does not take into account any fitting process used with CC events ($\sim$ 40% will be fittable), which will improve the identification and measurement of the π^o's greatly. A similar result is obtained for η's, but the width of the peak is broader, $\sim$ 110MeV.

We now turn to the question of neutron (or K_L^o) detection. We expect $\gtrsim$ 20% of neutrons from neutrino events to produce visible secondary interactions in the bubble chamber liquid. Using timing information from the track hitting the calorimeter itself or the IPF, it will be possible to associate these secondaries with primary neutrino interactions. Of the remaining neutrons our Monte-Carlo shows that $\sim$ 3/4 will interact in the calorimeter material producing a detectable pulse. Again, using timing information from the IPF and the SNC, we will be able to associate these neutrons with neutrino primaries. Although we will not be able to measure the neutron energy, the location of the pulse in the calorimeter will give us the neutron direction. In some cases this will enable us to fit an event; in all cases it will enable us to improve the determination of the neutrino energy. This is illustrated in Fig. 5, where a reduction in the tails of the smearing distribution is noted.

Next, for CC events, we consider the question of proton identification with the SNC. We remark that the lack of proton identification in earlier experiments has lead to serious distortions in π^+ fragmentation functions and in charge flow measurements, and produced false Q^2 and W^2 dependences. It has not been possible to address a number of interesting questions concerning baryon production except using Λ particles, in which case low statistics are a limiting factor. On the other hand, the detection of a large fraction of the neutral hadronic energy makes the situation quite different. We propose to use the same method recently employed by the BEBC TST collaboration (in which two of our groups participate).

The core of this method is the longitudinal quantity

$$\varepsilon = \sum_i (E_i - P_{L_i}) - m_N$$

where the sum is over the outgoing particles. For a neutrino interaction, if all outgoing particles are detected ε will be zero. However, if a proton is identified as a π^+ ε will be negative. The method then is to try each positive particle in an event as a proton, and to choose as the

proton that which makes ε most nearly zero. If no positive particle makes ε zero within a predetermined amount (110 MeV in the TST experiment) then it is assumed the event contains a neutral baryon. In the TST experiment, of all protons below 1 GeV/c which were identified by other means (ionization, stopping), 90% were successfully identified by this method. For all momenta, it was possible to determine statistically the fraction of events with protons, which was 75 ± 5%. However, of those tracks chosen as protons 26% were actually π^+. Using the selected protons, and correcting for the known π^+ contamination, it was possible to determine x_F and z distributions and to obtain a clear Δ^{++} signal.

The chief limitation on this method in the TST experiment was that only 60% of the γ's were detected. Thus a correction had to be made to each event for missing $E-P_L$ which leads to a smearing in ε. With the SNC in the 15-foot chamber we will detect $\sim$ 90% of all γ's as well as $\sim$ 80% of neutrons and K_L^o's. Thus the corrections to ε will be much smaller resulting in even better proton identification.

In the case of neutral current events the energy determination is naturally not as good, but still quite reasonable. The method is to assume that the calorimeter detects all the neutral hadronic energy and momentum, and to do a zero constraint fit to the event. This gives the incident neutrino energy as well as the energy and direction of the outgoing neutrino. In Fig.6 we show a Monte-Carlo distribution of the ratio of the energy obtained by this method to the true energy. It is seen that 62% of the events are within 20% of the true energy. (Neutron detection is not included, but should improve this to $\sim$80%). Thus we shall be able to obtain distributions of x and y and examine Q^2 and W^2 dependences to a level which will enable us to check theoretical ideas concerning neutral currents (See Section VI). It will also be possible to study the hadronic final state in much the same way as is done for charged current events. Such a study is impossible without the estimate of the hadron energy which can only be obtained by using the calorimeter.

Another unique feature of the calorimeter with deuterium or hydrogen is superb electron identification and measurement. The alternative bubble chamber techniques are much poorer. A neon-filled chamber can identify electrons quite well but cannot make reliable measurements on electrons above 20 GeV/c because of bremsstrahlung. A bare hydrogen or deuterium chamber does not recognise most of the

electrons. Counter experiments also have great difficulties with ν_e events.

Our calorimeter will be divided into a number of longitudinal sampling layers so that it will be possible to observe the difference between the buildup of electromagnetic and hadronic showers. On the basis of our CERN test we expect a pion rejection of better than 1000 : 1 at about 5 GeV/c. This will be sufficient to pick out electronic charm-decay candidates with less than 50% background before cuts.

At higher energies there are fewer background pions so the high energy electrons from ν and $\bar{\nu}_e$ events will be very cleanly identified and well-measured in the calorimeter. This experiment will probably accumulate the best sample of clean ν_e and $\bar{\nu}_e$ events that has ever been analysed (See Section V.D below).

IV. DEUTERIUM AND HYDROGEN TARGETS - RESCATTERING AND FERMI MOTION

The main physics advantages of the deuterium target come from the opportunity to study ν and $\bar{\nu}$ reactions on the ideal isoscalar target while at the same time studying the reactions νn, νp, νn and $\bar{\nu} p$. One gets automatic flux normalization between νn and νp and between $\bar{\nu} n$ and $\bar{\nu} p$. While measurement accuracy is comparable to that in hydrogen, one gains a factor of three in event rate for neutrino and 3/2 for antineutrinos. In comparison with heavy liquids, such as neon-hydrogen mixtures, the event rate is lower, but measurement errors are smaller, vertices are clearer, which is important with HRD, and it is possible to fit individual events. With the SNC added to the bubble chamber, the ability to detect γ's and $e^{\pm}$ will be even better than in the heavy liquids. Furthermore, recent results from the European Muon Collaboration, which indicate important nuclear effects when structure functions are measured in heavy nuclei, seem to indicate that neutron and proton structure function measurements can only be made on neutron and proton targets, that is on hydrogen and deuterium.

In this section we consider two disadvantages usually associated with deuterium experiments; rescattering on the second nucleon and Fermi motion. We shall show that the former can be largely eliminated and discuss where the latter may be important. We also discuss the reasons for complementing the deuterium experiment with a comparable hydrogen one.

The method of separating neutron from proton reactions in a neutrino-deuterium experiment is simply to separate the events into even and odd prong categories (where even includes odd prong events where one prong is interpreted as a spectator proton). This in fact gives a very clean sample of νn events. However, since the probability of a rescattering in the deuteron is $\sim$ 10%, and since such double scattered events are odd prong, the νp sample is contaminated by about 25% double scatters in the neutrino case and about 13% in the antineutrino case. The Fermilab E545 νd collaboration (including two of the groups on this proposal) has developed a method to deal with this based again on the longitudinal quantity.

$$\varepsilon = \sum_i (E_i - P_{L_i}) - m_N$$

where the sum is over visible outgoing particles. Missing neutral particles and treating protons as pions both have the effect of reducing ε, which would otherwise have the value 0 for single scatters and m_N for double scatters. Thus ε varies from $-m_N$ to 0 for single scatters and from $-m_N$ to m_N for double scatters (See Fig.7). A comparison of the distribution of ε for odd prong events with the distribution from neutrino-proton interactions shows that $\sim$ 85% of double scatters have $\varepsilon > 0$. By cutting out these events the contamination of odd prong events by double scatters is reduced to $\sim$ 5%. With the SNC's high efficiency for detecting neutral outgoing particles we estimate that $\sim$ 95% of the double scatters will have $\varepsilon > 0$. This will reduce the contamination of the νp sample to the order of 1%. Present estimates of the fraction of events which rescatter are $\sim$ 10 $\pm$ 3%. With the SNC the error will be $\sim$ ½%. This is particularly important for determining NC/CC ratios, since this fraction must be known well in order to properly correct the odd and even prong NC events.

With the calorimeter then the problems connected with double scattering in the deuterium can be dealt with very well, which brings us to the question of Fermi motion effects and the benefits of high resolution optics.

Fermi motion is a problem only when the spectator nucleon, or nucleons, is not seen. Thus, in a counter measurement of structure functions in a heavy nucleus such as iron, there is essentially no reliable way to account for distortions due to Fermi motion. However, for the case of deuterium in a bubble chamber the situation is quite different. For νn interactions the spectator protons are either seen and measured or their range is too short to be seen. With HRO this situation is improved for it may be possible to see stubs due to spectators down to a range of $\sim$ 200 microns, which corresponds to $\sim$ 50 MeV/c. Thus one expects to be able to see and measure 40 - 50% of spectators from νn events, and those which are too short to measure are just those which have the least effect. For νp interactions in deuterium the situation is rather different. Spectator neutrons cannot be seen and therefore the proton is treated as if it were at rest. Smearing in the measured variables can be quite large in some cases. The Bjorken variable x, for example, can vary by as much as 20% from its true value, although the average is about 4%. We note that deuterium is

the one nucleus where we have a good knowledge of Fermi motion. Thus one can improve measured distributions by unfolding the Fermi motion using, for example, the Hulthén distribution. Event fitting, which we expect to carry out on a relatively large scale, should be quite good for νn events with visible recoils but may be only modest for νp.

If nuclear effects in structure functions are important, as suggested by the EMC experiment, then they would be expected to show up as a difference between neutrino measurements made in deuterium and hydrogen. If such a difference exists it may be small enough that one would need the accuracy provided by the SNC to detect it. Since such nuclear effects may be complex, a comparison between hydrogen and deuterium is undoubtedly the best hope for understanding them (see Section V A).

V. CHARGED CURRENT PHYSICS

A. Structure Functions and Parton Distributions

Neutrinos and antineutrinos are ideal probes for studying the distributions of quarks in the nucleon. The neutrino interacts only with d, $\bar{u}$ and s quarks, whereas the antineutrino interacts with u, $\bar{d}$ and $\bar{s}$. Experiments to measure structure functions with ν and $\bar{\nu}$ have been carried out at both CERN and Fermilab with large statistics counter experiments on heavy nuclei, and with lower statistics bubble chamber experiments on hydrogen and deuterium. In the heavy nuclei one is not separately measuring the u and d valence quark distributions in the proton (or neutron) but one has believed that the results still reflected these distributions as would be expected from an isoscalar target. However, the recent measurements, using muons, of the ratio of the structure function in Fe to that in D_2 reported by the EMC collaboration (Fig. 8) make this doubtful.[3] Fermi motion cannot explain the narrower distribution in iron, and it seems likely that what one is observing is a basic nuclear effect, perhaps the internucleon parton distribution. Therefore, if we are going to "photograph the nucleon" it will have to be done in experiments using hydrogen and deuterium. The 15-foot bubble chamber with the SNC is certainly the best available tool for doing this at the Tevatron with neutrinos. In the following we discuss some of the major points in this area.

a) σ_n/σ_p for ν and $\bar{\nu}$

In the naive quark-parton model of the nucleon, where only valence quarks are taken into account, the neutron-proton ratio is exactly $R \triangleq 2$ for ν and $R = 0.5$ for $\bar{\nu}$. Sea quark contributions and QCD effects will change these values. For example, using quark structure functions deduced by Field and Feynman[4,5] gives values $R = 1.89$ and $\bar{R} = 0.58$. To avoid nuclear effects the best way to make this measurement would be with a deuterium target (assuming nuclear effects in deuterium are small) since one gets automatic flux normalization between νn and νp. The results of the measurements in present D_2 experiments are the following :

			ν	$\bar{\nu}$
15-foot	νd	5	$2.03 \pm 0.08 \pm 0.27$	$0.51 \pm 0.15 \pm 0.07$
BEBC	$\nu d, \bar{\nu} d$	6	$2.22 \pm 0.12 \pm 0.25$	$0.51 \pm 0.01 \pm 0.03$

The dominant error is the systematic error associated with lack of knowledge of the rescattering fraction in deuterium. With the SNC, using the method described in Section IV, the rescattered events will be removed except for a very small number whose amount is measured. The errors will be predominantly statistical $\sim \pm 0.03$ for R and $\sim \pm 0.01$ for $\bar{R}$.

b) The quark densities d(x) and u(x) in the proton

The quark distributions d(x) and u(x) tell us something about how nucleons are made from quarks. In principle, a fundamental theory of the strong interaction would yield these functions, as well as $\bar{u}(x)$, $\bar{d}(x)$, s(x), etc. While such a calculation has not as yet been possible some interesting features, particularly as $x \to 1$, have been noted. The naive quark-parton model predicts $d(x)/u(x) = 0.5$ for all x. In the limit $x \to 1$ QCD requires that $d/u \to 0.2$ [7], isospin arguments[8] and SU(6) symmetry breaking effects [9,10] have $d/u \to 0$, and a model in which scattering from diquarks accounts for all scale breaking effects [11,12] has $d/u \to \sim 0.27$.

Two methods have been used to measure these distributions on single nucleons, and we propose a third. In the valence quark region, $x > 0.2$,

$$F_2^{\nu p} = 2 x d(x)$$

$$F_2^{\nu n} = 2 x u(x)$$

and $$F_2^{e,\mu p} = \frac{4}{9} u(x) + \frac{1}{9} d(x)$$

The methods which have been used are

1) Measuring $F_2^{\nu p}/F_2^{\nu n}$ as a function of x in deuterium.

2) Comparing $F_2^{\nu p}$ from a hydrogen measurement with $F_2^{e,\mu p}$ to avoid rescattering and Fermi motion effects.

We propose also

3) Comparing $F_2^{\nu n}$ from deuterium with $F_2^{\nu p}$ from hydrogen.

Method 1) can be repeated as soon as we have our deuterium data, taking advantage of the reduced smearing with the SNC, as explained below.

Method 2) can also be used with νp events from either our deuterium or our hydrogen exposure.

However, method 3) could eventually be better than both, since it needs no input from ep or μp experiments and it uses the νp data from hydrogen which is less smeared than νp from deuterium.

The main limitations in a bubble chamber experiment in the region $x > 0.6$ are first, statistics are lowest there; second, resolution in x due to the smearing in neutrino energy is worst; and third, in deuterium Fermi motion effects are largest.

Myatt[13] has recently shown Monte-Carlo results on the effect an SNC would have in reducing the smearing corrections on neutrino-H_2. Fig.9 shows the corrections in the bare chamber (a) and in the chamber with SNC(b). Figure 10 shows the uncertainty in smearing corrections as well as statistical errors for a 30,000 event experiment. The reduction in smearing in Fig.9 is seen to be a factor $\gtrsim 2.5$ for $x \gtrsim 0.7$. Thus in Fig.10 we see that the smearing uncertainties become comparable to the statistical errors, or less. It will be possible to make measurements to $\sim$ 10-15% accuracy at $x = 0.8$ which may enable us to choose between a QCD model in which d/u goes to 0.2 at $x = 1$ and the Feynman - Field model in which d/u goes to zero. (Since Myatt's Monte-Carlo did not take into account the detection of neutrons by the SNC the situation will actually be somewhat better than he calculated.)

With regard to Fermi motion we have already pointed out that for the νn sample in deuterium the effects are small because the spectator protons are observed (especially well with HRO). The effects of smearing should only be in the few percent range. On the other hand, for νp in deuterium one would have to rely on an unfolding using a hypothetical distribution such as the Hulthén. For this reason we have suggested an eventual third alternative: $F_2^{\nu n}$ from deuterium and $F_2^{\nu p}$ from hydrogen.

c) The quark densities $\bar{u}(x)$, $\bar{d}(x)$, $\bar{s}(x)$

There has been some evidence from the BEBC $\bar{\nu}d$ experiment that the total $\bar{d}$ content in the proton is greater than the $\bar{u}$ content. A large asymmetry in the sea is not expected and the possibility of it makes a study of the sea distributions even more interesting. The best way to do this, as in the BEBC experiment, is with $\bar{\nu}$ on deuterium. The differential cross-sections on proton and neutron are (assuming charge symmetry)

$$\frac{d^2\sigma^{\bar{\nu}p}}{dxdy} = \frac{G^2_{ME}}{\pi}\, 2x \left[u(x)\ (1-y^2) + \left[\bar{d}(x) + \bar{s}(x)\right]\right]$$

$$\frac{d^2\sigma^{\bar{\nu}n}}{dxdy} = \frac{G^2_{ME}}{\pi}\, 2x \left[d(x)\ (1-y^2) + \left[\bar{u}(x) + \bar{s}(x)\right]\right]$$

One takes advantage of the decrease in the valence quark distribution at high y. The BEBC $\bar{\nu}d$[14] result was (integrating over x)

$\bar{d} + \bar{s} = 0.034 \pm 0.004$ from $\bar{\nu}p$

$\bar{u} + \bar{s} = 0.021 \pm 0.003$ from $\bar{\nu}n$

This result, though interesting, suffers from two defects. The proton sample includes contamination from all the double scatters, and the smearing in y is important. As we have already noted, both these factors are greatly improved with the SNC.

d) QCD Effects

It is now believed that Q^2 dependences of structure functions in deep inelastic lepton-nucleon scattering have been observed. Although the counter experiments may not be observing nucleon (as opposed to nucleus) structure functions, the Q^2 observations remain valid, and those experiments will always enjoy a large statistical advantage over light liquid bubble chamber experiments, except in certain regions more accessible to the bubble chamber, namely low Q^2, high x. The Q^2 dependences seen seem to be consistent with the predictions of leading order QCD. However the value of the parameter Λ is still not precisely known and the situation concerning non-perturbative, or higher twist, QCD terms remains unclear. In fact, it is just the low Q^2, high x range which is crucial for seeing higher twist effects, which go as $(1/Q^2)^n$.

Of course, the wider range of Q^2 available at the Tevatron is going to be an enormous advantage to these studies, and it is our intention to analyze the structure functions over the entire range available to us, taking advantage also of the improvement in Q^2 resolution we will have in comparison to past bubble chamber experiments.

Eventually, a νp experiment may be best for this analysis, since Fermi motion effects, largest at high x, would hamper a moments analysis in any other nucleus. From the point of view of ever understanding higher twist contributions we quote a remark of J.Morfin made at the Neutrino '82 Conference[15]. "The ideal higher twist experiment would have minimal high x smearing (Fermi motion) corrections, a large sample of high x events and good hadron energy resolution down to O (1GeV). This would suggest an enormous amount of running time using a hydrogen target within a detector which, considering the required hadron energy resolution, has yet to be developed." The 15-foot bubble chamber with the SNC may very well be that detector.

e) The EMC Effect

We have mentioned this effect with frequency in this Section and now turn to the question of what might be contributed to an explanation by

a comparison of deuterium and hydrogen data.

We feel intuitively that the effect is somehow connected with nucleons being densely packed together in a nucleus. However, several possible explanations as to the source of the effect have been offered. We mention some here - higher twist effects in which the incident particle interacts with several quarks coherently; nucleons being distorted within the nucleus, that is changing their mass and radius, and thus their quark distributions; multiquark states of 3, 6 or 9 quarks within the nucleus; a modification of the pion cloud in the nuclear environment, that is, in addition to the valence and sea quark distributions within the nucleon, which remains basically unchanged, there is an additional sea quark distribution in the internuclear space.

Some experiments suggested to investigate the effect further, in addition to studying A dependences are the following [16] :

- Drell Yan Effect comparing pp with pA in the same experimental setup
- J/ψ muon production on $\underline{P}, D_2$, F_e
- Measurement of $\dfrac{F_2^{\nu p} + F_2^{\bar{\nu} p}}{F_2^{\nu d}}$

We are concerned with this last. On the assumption that $F_2^{\nu n} = F_2^{\bar{\nu} p}$ the ratio should be flat except for Fermi motion effects in the deuterium, which one can consider unfolding using the Hulthén distribution, but which in any event oppose the EMC effect. How large the EMC effect is in deuterium is, of course, unknown. On the basis of the difference in nucleon densities between deuterium and iron one might guess the effect may be an order of magnitude smaller. In any case, it is clear that one will need the maximum resolution if it is to be observed, and the SNC is therefore a crucial element , and both deuterium and hydrogen experiments will be needed.

We point out that the ability of the SNC to separate νn from νp very well, and the ability of HRO to observe spectators may make a more detailed analysis of the EMC effect possible in deuterium. That is, the former will enable us to separately compare νn and νp from deuterium with $\bar{\nu} p$ and νp from hydrogen. If the effect comes from internucleon pions [17] events in which a neutrino scatters from one of these pions will leave the two nucleons as spectators, in some cases both protons.

B. Production and Decay of Charm and Beauty

The combination of HRO and the SNC provides a powerful tool for charm detection and analysis. In the following we discuss the questions of charm and beauty production and charmed particle properties. Hadronization of charmed quarks is discussed in the next Section.

a) Charm Production Rates in CC Reactions

It is only in $\nu(\bar{\nu})$ interactions that we can study flavour changing processes at high energy. Measurements of the rates of such processes are crucial input, for example, for determining the mixing angles of the Kobayashi-Maskawa 6-quark model. In the neutrino case single charm production takes place on valence as well as sea quarks, whereas in the antineutrino case only on sea quarks

$$\nu + (d,s) \rightarrow \mu^- + c \text{ with couplings } (U_{cd}, U_{cs})$$
$$\bar{\nu} + (\bar{d},\bar{s}) \rightarrow \mu^+ + \bar{c} \text{ with couplings } (U_{cd}, U_{cs})$$

Charm production rates have been measured in the CDHS counter experiments[18] (opposite sign muon pairs), in the Fermilab emulsion experiment E53[19] (observation of decays), and in bubble chamber experiments[20] (e^+ decays and hadronic modes). The former two methods find overall rates of $\sim$10%, whereas the bubble chamber finds $\sim$13% from e^+ and suggests even higher rates from hadronic decay modes. Furthermore two bubble chamber experiments[21,22] find 2 ± 1% for $\Lambda_c^+ \rightarrow \Lambda$ X production rate times branching ratio, which when $\bar{K}^o$ decay modes are taken into account suggests an overall charmed baryon rate of $\sim$5%. On the other hand, the counter experiment assumes only $D^{+,o}$ production. Clearly, the knowledge of charm production rates is still rather crude, and more precise and detailed data are needed. We must also point out that the use of these counter data to obtain the amount of strange sea in the nucleon may be misleading, since the experiments are done on nuclei.

In the proposed neutrino part of this experiment, assuming a 13% production rate, we will produce $\sim$ 3300 charmed particles, $\sim$2500 of which are D-mesons. Assuming lifetimes of 4×10^{-13} sec. and 9×10^{-13} sec. for D^o and D^+ respectively[23], and an average D-meson energy of $\sim$5 GeV, we find a mean length of $\sim$300 μ for D^o and $\sim$700 μ for D^+. In order to estimate the fraction which will be observable with holography we will be optimistic and assume that HRO will cover most of the fiducial volume and reach a resolution of 50μ. We would then expect to see $\sim$30%($\pm$10%) of D^o and $\sim$60% of D^+, that is $\sim$375 D^o and 750 D^+. The question then becomes how many of these will be identifiable as D's. The clearest identification

would come from a fit to the decaying particles. The fraction of D's decaying into final states with only charged particles or K^o's is $\sim$ 15%. Thus $\sim$ 160 events could be identified in this way. It would also be possible to identify as D's those which decay into a μ^+, giving a total rate of $\sim$ 20%, or $\sim$ 200 events. With the SNC we would in addition be able to fit all the modes with a single π^o and to identify the e^+ decays as well. A rough estimate is that we would identify $\sim$50%, or $\sim$ 550 events. This should allow a determination of the overall D production rate to 5 - 10% accuracy.

The average path lengths for $F^\pm$ and Λ_c will be $\sim$ 200 μ and 150 μ and we would expect to see $\sim$ 15% and 10% respectively. If Λ_c rates are in the 3-5% range we will produce 750 - 1250 of them, and we will be able to see $\sim$ 100. Of these, with the SNC, we should be able to analyze $\sim$ 50, and determine the Λ_c production rate to an accuracy of $\sim$ 15 - 20%. For $F^\pm$ a rough estimate of the rate is 340 events, of which we would see $\sim$ 50 and reconstruct $\sim$ 25.

We have been conservative in determining the fraction of particles we can see, assuming a minimum path length of 5-10 times the resolution will be necessary. The fact that vertices will be very clean in deuterium and measurements very good will also be a great advantage.

b) Properties of Charmed Particles

1) Lifetimes

The ability to analyze a large fraction of charm decays gives us momentum information which will allow lifetime measurements to be made. The measurement of these lifetimes is not one of our primary objects since this may be done better in smaller high resolution chambers (of the type of LEBC, BIBC, SLAC). Nevertheless, a lifetime measurement will be a very important check on the validity of our methods.

2) Masses

The ability, with the SNC, to fit a large number of complete events, will allow very accurate mass measurements to be made. This will be more important in the case of the charmed baryons, where world data is still meager. It is worth noting that the best Λ_c^+ mass value comes from just a few complete νp events in a bubble chamber.

3) Branching Ratios

The calorimeter will enable us to obtain branching ratios into $e^{\pm}$ and into hadronic final states with one or more π^{o}'s. The EMI will detect $\mu^{\pm}$ decay modes. A glance at the Particle Data Book tables shows that much of this information hardly exists at present.

4) Charmed Resonances

With the detection of almost all the hadronic final state particles we can use the events with a visible D or F or Λ_c^+ to search for mesonic and baryonic resonances. Once again the event fitting should lead to more accurate mass values than could be obtained with simple invariant mass plots. One advantage neutrinos have is that charm production is single, whereas in hadro - or photo -production, or in e^+e^-, it is in pairs, which certainly complicates the fitting process.

6) Beauty and Charm in $\bar{\nu}$ Interactions and the Strange Sea

The detection of bare beauty in present antineutrino experiments is extremely difficult because of the large number of final state particles resulting from the prevalent decay chain $b \to c \to s$. This situation could be dramatically changed in the 15-foot chamber (plus HRO, SNC and EMI) with the ability to simultaneously detect charm decays, $e^{\pm}$, $\mu^{\pm}$ and π^{o}'s. The $\bar{\nu}$ events with visible charm decays provide an enriched sample from which to search for beauty.

To give an idea of what we can accomplish we make some rough estimates. In a recent paper it is shown that the coupling parameter $|U_{ub}|^2 < 0.03$ from the $\mu^+\mu^+$ rate in $\bar{\nu}$ reactions, and $|U_{ub}|^2 = .004 \pm .004$ based on the relation $|U_{ub}|^2 = 1 - |U_{ud}|^2 - |U_{us}|^2$ where $|U_{ud}|^2$ and $|U_{us}|^2$ come from β-decay and strange particle decay. Let us assume a B-production rate of 1%. Then from 8000 $\bar{\nu}$ CC events in this experiment we expect $\sim$ 80 B's, half B^- and half B^o. The branching ratio into leptons is $\sim$ 25% [24] (half e^-, half μ^-).

$$B^{o} \to D^{+} \ell^{-} \bar{\nu} \qquad \sim 20 \text{ events}$$

Using the numbers for D identification in part (a) of this Section we ought to clearly see $\sim$ 10 of these events. These are events with a candidate D decay and a μ^- or e^- from the $\bar{\nu}$ interaction vertex. In $\sim$ 5 of the 10 cases the D would be clearly analysed. If no candidates are seen this would correspond to an upper limit $|U_{ub}|^2 \lesssim 0{,}001$ or $|U_{ub}| \lesssim 0.03$ to be compared to $|U_{ub}| < 0.18$ and $|U_{ub}| < 0.1$ from the two results mentioned above.

Of the remaining 60 B's, which decay hadronically, $\sim$ 12 will have clearly analyzed D's. One could combine these with particles from the $\bar{\nu}$ vertex to look for B masses. Background D's would come from $D\bar{D}$ pair production , so whether one could see a B mass peak would depend on how large this process is. This also suggests to us another method for obtaining a limit on B production, namely finding the difference between D and $\bar{D}$ production in the non-sea region.

Finally we note that a measure of $\bar{D}$ production in the low x region detects the strange sea and determines $\bar{S}(x)|U_{cs}|^2$.

C. The Hadronic Final State

There are a large variety of very interesting topics to be studied in the hadronic final state, and there are several features which make the proposed experiment particularly well suited. First, there is the higher Tevatron energy which gives about 75% of all events having $W > 4$ GeV. This value of W is needed to get good separation between current and target regions. Second, the ability to identify protons, as discussed earlier, avoids serious distortions which can be caused when protons are treated as π^+ mesons and provides crucial information on baryon production. Third, the detection of most of the neutral energy allows a substantial increase in the resolution of the fragmentation function parameters, x_F and z; of the W boson direction; and also allows the reconstruction of π^o's and thus resonant states decaying to them. In the following we discuss some selected topics of special interest and simply list some others.

a). Fragmentation functions

Fragmentation functions are the vital input into understanding the question of how quarks turn into hadrons, usually referred to as hadronization or fragmentation of quarks. This is just the reverse of the question, how are hadrons made of quarks, described by structure functions. In principle it is equally fundamental, but because of the complexity one has had to rely on empirical models, of which there are now several,[25,26,27] the earliest being that of Field and Feynman, and perhaps the most popular at present being the Lund model. These models make a large number of predictions and involve several parameters which

must be determined empiracally. Among the predictions are the fragmentation functions, $D_q^h(z)$ or $F_q^h(x_F)$ of the particles observed in the hadronization process: π mesons, K mesons, baryons, charmed particles and even beauty. In order to test these models the functions should be determined for every identifiable outgoing particle, since, among other things their shape is mass dependent. $F(x_F)$ is a sharper discriminant than $D(z)$, since it separates the current and target regions.

One of the great advantages of ν and $\bar{\nu}$ experiments is that with a suitable cut ($x_B \geq 0.2$) the outgoing quark is uniquely identified. In fact there is no other way of observing d quark hadronization except from antineutrino interactions. In present experiments fragmentation functions for π^+ and π^- have been determined for both ν and $\bar{\nu}$ interactions. These are contaminated by K^+, p and K^-, $\bar{p}$ respectively, the most serious contamination being the p in the π^+ distribution (a backward proton treated as a π^+ often ends up in the forward direction). The only attempt to correct for this[28] involved using a model (the Lund model), but it is not very desirable to correct the distribution using a model which is to be tested by that same distribution.

With the SNC it will be possible to remove the protons from the π^+ sample, to obtain the proton fragmentation function itself, to obtain the π^o fragmentation function, possibly that for neutrons, and, based on $\sim$ 500 D's the charm fragmentation functions. These latter will provide very good tests of models because of the large mass of the D's. It is worth noting that while these are available from the flavour changing $\nu(\bar{\nu})$ interactions, they are not available from muon experiments, except via pair production

In addition to making more fragmentation functions available the SNC will significantly improve the resolution, just as in the case of structure functions. A comparison of $h^+ + h^-$ fragmentation functions from an H_2 experiment and Ne-H_2 experiment, where the fraction of hadronic energy detected was 70% and 87% respectively shows a systematic difference[29] (see Fig. 11). There are two possible explanations: Inadequate corrections for neutral energy in the hydrogen, or internal scattering in the neon. With the SNC detecting > 93% of the hadronic energy this will no longer be a problem. This improved resolution will be particularly important in testing for QCD effects in fragmentation, since the fragmentation function must, according to QCD, have a Q^2 dependence, $D(z,Q^2)$.

In connection with this we remark that by a careful comparison of singlet and non-singlet fragmentation functions

$$D_S = \frac{1}{3}\,(D_u^{\pi^+} + 2D_u^{\pi^-})$$

$$D_{NS} = D_u^{\pi^+} - D_u^{\pi^-}$$

it is possible to extract gluon fragmentation moments[30].

Clearly, to study QCD effects we need the wide Q^2 range the Tevatron gives us, but to take full advantage of it we need the resolution which the SNC will bring.

b). Resonance Production

If the fragmentation function D_q^h is to represent the fundamental process of hadronization it should describe hadrons h which arise directly from the fragmentation of quark q. For the meson fragmentation functions discussed in the previous section, namely pionic, but also $D^{K^o+\bar{K}^o}$, this is not the case. It is very likely that most of the pions arise from the decay of vector mesons which are produced directly in the hadronization process. In fact the models used to describe hadronization include a parameter which is just the ratio α of vector to pseudoscalar meson production. This parameter is usally determined by fits to the shape of the pionic fragmentation functions. Values found in this way vary from 1 to 3 and depend on which model is being used. What would settle the matter is obviously a direct measurement of vector meson production. This would allow a straightforward determination of α, the removal of pions arising from resonance decay from pion fragmentation functions, thus giving fundamental fragmentation functions, and the determination of the resonant fragmentation functions.

In present experiments only the ρ^o and K^{o*} production has been measured and the z distributions determined. Indirect evidence for resonance production of ω^o and z has come from an E545 study of the $\pi^+\pi^-$ invariant mass distribution[31]. With the SNC we shall be able to determine production rates for all the vector mesons; $\rho^{+,-,o}$, ω^o, $K^{*+,o}$, $\bar{K}^{*-,o}$ and even ϕ. For the pseudoscalars we shall be able to measure η and $\pi^{+,-,o}$, $K^o+\bar{K}^o$, but not K^+,K^- ($\phi \to K^+K^-$ is identifiable since K^+K^- treated as $\pi^+\pi^-$ will show the ϕ at a lower mass with a broader peak). With the reasonable assumption that $K^++K^- = K^o+\bar{K}^o$ we shall be able to determine α separately for nonstrange and strange particles

and determine fragmentation functions for all particles except K^+ and K^-.

These results will allow excellent tests of the fragmentation predictions of the models.

c). Diquark Studies

As Sukhatme has pointed out[32] the diquark is the only example of an extended coloured hadron which we have a chance to study. Neutrino and antineutrino interactions are ideal for this in that the diquark system emerging in the target region is uniquely defined if we operate in the valence range ($x_B > 0.2$).

$$\nu p \rightarrow (u\,u)$$

$$\nu n\,,\ \bar{\nu} p \rightarrow (u\,d)$$

$$\bar{\nu} n \rightarrow (d\,\bar{d})$$

Interestingly enough the study of diquark fragmentation may shed light on nucleon structure, particularly as to whether a diquark-quark structure is predominant. A variety of analyses which investigate this[33] conclude that if such a model holds the nucleon consists primarly of an I = 0, S = 0(ud) diquark core plus an outer quark. The I = 1 diquark contribution is zero or very small. If we assume this model, then,since the neutrino interacts with a d quark, in a proton the (ud) core is always broken up and the recoiling uu system would not be expected to be highly correlated. In the νn case the core would be broken up half the time, but in the other half, when the outer d quark is struck, a tightly bound (ud) would emerge in the target region. In the $\bar{\nu}$ case we have a similar situation with the roles of proton and neutron reversed.

Now the fragmentation of the diquark may take place in two different modes, known as coherent and independent fragmentation (see diagrams)

$Di \rightarrow B + \bar{q}$ $\qquad$ $Di \rightarrow M + D$

In the former the diquark goes directly into a leading (fast backward) baryon, while in the latter the baryon will be formed further down the

hadronization chain, with a less hard distribution.

If the diquark-quark model described above were to hold then we might expect the ud diquark to show considerably more coherent fragmentation than the uu or dd. It is also clear that one needs to be able to identify baryons.

In present experiments the only identifiable baryon is the Λ particle. One interesting result from the E545 experiment[34] shows that the uu diquark undergoes about 50% coherent and 50% independent fragmentation. This comes from comparing Λ to Y^{*+} production in νp interactions. The Λ's which do not arise from Y^{*+} or Λ_c^+ decay must come from independent fragmentation. However very little can be said about the ud diquark from νn interactions.

With the SNC a variety of new studies involving baryons from diquarks becomes possible. A comparison of $\Sigma^0 \to \Lambda\gamma$ production to Λ production is a measure of $(ud)_{I=1}$ vs. $(ud)_{I=0}$ production. If the ud emerges primarily in the I=0 state we would expect to see very little $\Delta^{+,0}$ production in νn interactions in comparison to νp . To identify $\Delta^0 \to p\pi^-$, $\Delta^+ \to p\pi^0$ and $\Delta^{++} \to p\pi^+$ we must have the power to identify p and π^0. A comparison of the hardness of the x_F distributions of the baryons will also be related to the relative rates of coherent and independent fragmentation. This cannot be done well with Λ's because of limited statistics, and thus requires proton (and neutron) identification (proton rates are $\sim$ 10-15 times Λ rates).

We see that how a diquark fragments depends on how the two quarks emerge from the nucleon. Since we consider these two quarks as spectators to the $\nu(\bar{\nu})$ interaction, how they emerge presumably reflects how they were moving in the nucleon before the collision. Thus the diquark fragmentation process will also contribute to "photographing the nucleon".

d). Distribution of P_t^2

If QCD effects are important it is expected that due to gluon emission the current region jet in νN interactions will have a broader P_t^2 distribution than the target region jet. The advantage of neutrino interactions is that the jet axis is uniquely defined as the W boson direction and does not depend on the final state particles. In present experiments this jet widening has been observed in plots of $\langle P_t \rangle^2$ vs W where the current jet shows a clear increase in width over the target jet

as W increases above 8 GeV.

There are important reasons for redoing this analysis at the Tevatron with the SNC. First, it is important to extend the range of W, which will also more cleanly separate target and current jets, and to look at Q^2 dependences. Second, the observation of neutral energy in the SNC will significantly reduce smearing in the determination of the jet axis, which smearing contributes to the measured $\langle P_t^2 \rangle$.

e). Higher Twist Effects

The role of higher twist (non-perturbative) terms in the QCD expansion remains an enigma. These are usually searched for by looking for $(1/Q^2)^n$ dependences in the structure functions. If these terms exist it would seem that one is looking for a very small effect on top of the larger leading (perturbative) term, which in itself has been hard work to find. We propose here a simple way to look for one higher twist term, the so-called twist-4, and to separate it from the leading term. The twist-4 term corresponds to the interaction of the neutrino coherently with a diquark in the nucleon. This will produce forward going diquarks which will give rise to forward going baryons. The rate of production of forward baryons as a function of Q^2 would then enable us to identify the twist-4 term, if it is there, and to measure its magnitude. The backgrounds to be dealt with are 1) baryons from the backward region leaking forward and 2) baryon-antibaryon pairs produced by a single current quark. The first can be dealt with by going to sufficiently high W to well separate current and target regions, the second by determining the rate of antibaryon production. In any event, the backgrounds would not give rise to the dramatic $1/Q^4$ dependence of the twist-4 term.

With the SNC, although we cannot identify individual forward protons, we can statistically determine their rates. The same method could be tried to find antiprotons from the second background. Whether any effect will be seen will depend on its size, but in any case, we should be able to determine an upper limit.

f). Some other Topics

There are so many topics involving the hadronic final state that we feel obliged only to list a few others:

1. Charge flow in current and target regions.
2. Angular energy flow to study QCD effects.
3. P_t balance within events to check primordial P_t effects.
4. Λ polarizations - Lund model predictions.
5. Fragmentation of 4-quark target remnants left when a sea quark is struck.
6. Azimuthal dependences of final state hadrons for QCD effects.
7. Multiplicity studies, particularly for large W.

D. Electron Neutrino Physics

The quadrupole triplet beam will have a "contamination" of electron neutrinos from K decays of between 1 and 2%. These events are at a higher average energy than the ν_μ events so their cross-section should be greater. Thus, corresponding to 25,000 ν_μ CC events we should see $\sim$ 500 ν_e CC events. There should also be $\sim$ 150 $\bar{\nu}_e$ CC events in the $\bar{\nu}$ half of the run.

As mentioned above, the SNC gives the only known method for cleanly identifying and measuring ν_e events over the whole final-state electron spectrum. With these statistics it will be possible to obtain reasonable (x,y) distributions and to test universality by comparing them with the ν_μ distributions. If differences are seen then there will be sufficient clean data for the ν_e structure-functions to be extracted.

VI. NEUTRAL CURRENT PHYSICS

A. Physics Considerations

The discovery of neutral currents in νN scattering in the Gargamelle bubble chamber [35] was the first step toward confirmation of the unified theory of electromagnetic and weak interactions which has come to be known as the Standard Model. Since then a variety of experiments has tested the predictions of this theory without finding any clear contradictions. Now, with the possibility that the charged intermediate vector bosons have been detected, the next major test of the theory may be at hand. However, discovery of the $W^{\pm}$ and Z and the measurement of their masses will still not conclusively establish SU(2) x U(1) as the true electroweak theory. To go further in distinguishing this theory from others with similar leading order behavior it will be necessary, and require a new level of precision, to test the predictions of second order effects. In discussing these matters in a recent paper [36], Llewellyn Smith has given four examples to indicate what the required precision is in measurements of $\sin^2\theta_W$. Summarized briefly these are the following :

1) Radiative corrections change $\sin^2\theta_W$ as determined from $R_\nu = \sigma(\nu N \to \nu X)/\sigma(\nu N \to \mu X)$ from the average value 0.220 ± 0.015 to $\sin^2_{\overline{ms}}\theta_W = 0.215 \pm 0.015$. In ed scattering the change is from 0.223 ± 0.015 to 0.215 ± 0.015. The radiative correction is ∿0.008. One would like to measure these with a precision which is about half this value.

2) Since R is sensitive to different radiative corrections from $R_{\nu e} = \sigma(\nu_\mu e \to \nu_\mu e)/\sigma(\bar{\nu}_\mu e \to \bar{\nu}_\mu e)$ it should be measured to a precision giving $\delta(\sin^2\theta_W)$ to the same accuracy as may be achieved in $\nu_\mu e$ experiments, ∿0.005.

3) Lowest order theory gives, based on the value of R_ν, $M_z = 89.0^{+2.2}_{-2.0}$ GeV, $M_W = 78^{+2.7}_{-2.5}$ GeV. Radiative corrections and the second order mass formulae give $M_Z = 93.8^{+2.5}_{-2.2}$ GeV, $M_W = 83.1^{+3.1}_{-2.8}$ GeV. An improvement of a factor of three in the errors would provide a clear distinction between the two.

4) Consider a fit of R_ν and $R_{\bar{\nu}}$ to two parameters, $\sin^2\theta_W$ and ρ^2 (the NC/CC strength parameter). Radiative corrections give $\sin^2\theta(M_W) = \sin^2\theta_{exp} - 0.004$ and $\rho^2 = 1 - 0.016 + 4 \times 10^{-3}(M_t/M_W)^2$.

All of the above criteria, Llewellyn Smith concludes, indicate that a precision of $\sim$0.005 in $\sin^2\theta_W$ would permit really significant tests of SU(2) x U(1). He then considers theoretical uncertainties in the interpretation of $\sin^2\theta_W$. The error due to possible deviations from the QCD parton model is shown to be less than 0.002 when $\sin^2\theta_W$ is measured on an isoscalar target. The largest error is due to ignorance of the coupling $|U_{cs}|$ and the strange sea. Using present limits gives an uncertainty of ±0.008. However, accepting the common view that $|U_{cs}| \approx 1$ reduces this to ±0.004. Given that improvements in $|U_{cs}|$ or in S(x) will eventually occur, the conclusion is that there are no theoretical obstacles to tests of second order effects if $\sin^2\theta_W$ can be measured to an accuracy of 0.005.

In addition to $\sin^2\theta_W$ a measurement of the neutral current coupling constants from NC/CC ratios in νn, νp, $\bar{\nu} n$ and $\bar{\nu} p$ will be of great interest, as well as the determination of x and y distributions of neutral current events. In fact, the observation of strange particle production in NC events together with the measurement of x, provides a way to determine S(x) directly (in CC measurements it is the product $S(x)|U_{cs}|^2$ which is measured).

Other tests of the standard model which we should be able to carry out in this experiment involve π^+/π^- and $\pi^\circ/\pi^\pm$ ratios in NC final states and coherent π° and η° production. These will not give the precision discussed above on $\sin^2\theta_W$ but will provide useful information on coupling constants. In addition, we should be able to establish some limits on flavor changing NC processes.

B--Determination of $\sin^2\theta_W$

Assuming only $u, d, \bar{u}, \bar{d}$ quarks and Cabibbo angle equal to zero, for an isoscalar target one has

$\sigma_{nc}^{\nu(\bar{\nu})} = (\frac{1}{2} - Z + \frac{5Z^2}{9})\,\sigma_{cc}^{\nu(\bar{\nu})} + \frac{5Z^2}{9}\,\sigma_{cc}^{\bar{\nu}(\nu)}$ + small corrections where $Z = \sin^2\theta_W$. The small corrections, which are dealt with in detail in the paper by Llewellyn Smith referred to above, take into account contributions from strange quarks, charmed quarks, K-M mixing angles and deviations from the QCD parton model. For our purpose in this section, which is to discuss the precision with which $\sin^2\theta_W$ can be measured, we can ignore them.

In terms of ratios the above equation is equivalent to :

$$R^{\nu} = \frac{1}{2} - Z - \frac{5Z^2}{9} + \frac{5Z^2}{9}\,r$$

and

$$R^{\bar{\nu}} = \frac{1}{2} - Z - \frac{5Z^2}{9} + \frac{5Z^2}{9}\,\frac{1}{r}$$

where $R^{\nu(\bar{\nu})} = \sigma_{nc}^{\nu(\bar{\nu})} / \sigma_{cc}^{\nu(\bar{\nu})}$ and $r = \sigma_{cc}^{\bar{\nu}} / \sigma_{cc}^{\nu}$.

A world average of r based on a recent summary[37] gives $r = 0.49 \pm 0.02$. Since r (or 1/r) is multiplied by a small quantity in the above equations, its contribution to the error in $\sin^2\theta_W$ is quite small in comparison to that due to $R^{\nu(\bar{\nu})}$. The question then becomes how well can we measure R ? It is just here where the SNC makes a dramatic difference from what is possible in the bare bubble chamber. In present experiments[38,39] measurements of R are severely limited by systematic errors due to the following factors :

(1) Hadronic background in NC.
(2) Unidentified muons (affects NC and CC).
(3) ν_e background in NC
(4) $\bar{\nu}$ background in NC
(5) Hadrons identified as muons (affects NC and CC).

The corrections due to all these effects together are $\sim$5% on the number of CC events and $\sim$20% on NC events. The precision with which those corrections are known is such that systematic errors in the numbers of events are

~1% for CC and ~5% for NC. The severe cuts which are used to achieve this also increase the statistical error in the experiments and introduce biases for which further corrections must be made.

We propose to use a new method developed by Van Doninck[40] for the WA24 BEBC TST experiment, a method which will only work with neutral particle identification. This is known as the multivariant discriminant analysis, or more simply, the cluster analysis. The method makes use of the different behavior of outgoing particles from hadron induced events, CC events and NC events. One chooses a variety of kinematic quantities (which describe outgoing particles) as the coordinates of an n-dimensional space, and one finds the three classes of events cluster in different regions of this space. Figure 12 shows an example of this using data from the TST experiment. Not only does the method separate the three classes of events well, but it does not require cuts (therefore preserving statistics and avoiding bins) nor does it require muon identification to separate CC from NC events. Thus items (1), (2) and (5) above are no longer sources of systematic error. Item (3) is not a large effect but is beautifully handled using the SNC, which will detect ν_e CC events. NC events from ν_e and from $\bar{\nu}$ (item 4) can be removed using known (to first approximation) NC/CC ratios.

Van Doninck has scaled the WA24 data to a 30.000 event νp experiment and finds that R_p^{ν} can be determined to 1.2% accuracy. We expect to do better than this for two reasons : first, the SNC is a considerably better neutral particle detector than BEBC with TST, and second, the IPF will detect a large fraction of the hadronic events. This not only removes these events from the sample to which the cluster analysis will be applied, but also provides a clean sample of hadronic events whose properties will provide imput to the cluster analysis, thus improving its efficiency. In fact, Van Doninck's work shows that the error in R will be little more than the statistical error. In our case this means ~1.5% for R^{ν} and ~2.8% for $R^{\bar{\nu}}$, corresponding to errors in $\sin^2\theta_W$ of ~0.008 and 0.014 respectively, or 0.007 combined. We have assumed here that the cluster method will work as well at Tevatron energies as at CERN energy. Based on this we conclude that in the proposed experiment, we can very nearly meet the criterion for accuracy in $\sin^2\theta_W$ suggested by Llewellyn Smith to test second order effects of

electroweak theory. Of course, increasing the exposure would reduce the error further.

C. Neutral Current Coupling Constants

By measuring the NC/CC ratios, not on an isoscalar target, but on n and p separately it is possible to obtain a great deal of information on the neutral current coupling constants. Using the form introduced by Sehgal[41], measurements of R_p^ν, R_n^ν, $R_p^{\bar\nu}$ and $R_n^{\bar\nu}$ allow a determination of the values of the squares of the four constants u_L^2, d_L^2, $u_{R_2}^2$ and d_R^2. In the standard model these are precisely defined in terms of $\sin^2\theta_W$, $u_R^2 = (\frac{2}{3}\sin^2\theta_W)^2$, $d_R^2 = (\frac{1}{3}\sin^2\theta_W)^2$, $u_L^2 = (\frac{1}{2} - \frac{1}{3}\sin^2\theta_W)^2$, $d_L^2 = (\frac{1}{2} - \frac{2}{3}\sin^2\theta_W)^2$. Any variation from the standard model leads to different values. In the present ν-d experiments such analyses have been carried out. These are based on the four relations :

$$R_k^\nu = f_1^k\, u_L^2 + f_2^k\, d_L^2 + f_3^k\, u_R^2 + f_4^k\, d_R^2$$

$$R_k^{\bar\nu} = g_1^k\, u_L^2 + g_2^k\, d_L^2 + g_3^k\, u_R^2 + g_4^k\, d_R^2$$

where k = p,n and the coefficients f_i^k are ratios of integrals over quark density distributions in the nucleon. In addition to the systematic errors listed in the previous sections, which contribute to the errors in measuring R_k^ν and $R_k^{\bar\nu}$, there is also the systematic error from the rescattering in the deuteron which contributes an additional uncertainty of ∿3%.

With the calorimeter, as pointed out in the last section, we essentially eliminate the former, and as we have discussed earlier, the rescattering error is reduced to ∿1/2%. Thus the errors on the NC/CC ratios will be predominantly statistical, ∿2% on $R_{p,n}^\nu$ and ∿3% on $R_{p,n}^{\bar\nu}$.

The present results on u_L^2 and d_L^2 are shown below :

	u_L^2	d_L^2	u_R^2	d_R^2
E545[38]	0.19 ± 0.06	0.13±0.04		
WA25[42]	0.145±.027±.012	0.183±.025±.017	0.031±.018±.005	-0.08±.018±.005

One sees the errors are still quite large, not even quite sufficient to test the standard model prediction $d_L^2 > u_L^2$, let alone the predicted values. It must be pointed out however that the errors come not only from the statistical and systematic errors discussed, but also from errors in the coefficients f_i^k which come from uncertainties in our knowledge of the quark distributions (the uncertainty in f_1^p, for example, is $\sim$10%). With the SNC these may become the dominant uncertainties, however the improved measurements on quark distributions discussed in section V will reduce these too. We would expect to reduce the errors on u_L^2 and d_L^2 from the 15-30% range of present experiments to the 5-10% range, and to achieve comparable improvements for u_R^2 and d_R^2. The values obtained may be further constrained from measurements of final state particles as discussed in section E(a) below.

D. Distributions in x and y

We expect to be able to measure x and y on an event by event basis for neutral current events. The method used is to assume that all hadronic energy is seen and do a zero-constraint fit to obtain the incident neutrino energy and the outgoing neutrino energy and direction. Naturally the smearing will be considerably worse than in CC events, and will depend very much on how much neutral energy is lost in the form of neutrons, K_L^o's, and strange particles which decay into neutral modes. The ability to detect neutrons (although not to measure their energy) will be very helpful in this respect. We are continuing our Monte-Carlo calculations to study the smearing effects in detail.

The x and y distributions, as in the CC case, depend on the form of the current and on the parton distributions in the nucleon. The technique will also give quantities such as W, Q^2, Z and x_F.

E. Final state particles; the strange sea; flavor changin NC.

a) π^+/π^- ratio ; $\pi^o/\pi^\pm$ ratios

The π^+/π^- ratios in NC events depends on the relative rates of interaction on u, d, $\bar{u}$ and $\bar{d}$ quarks. Since π^+ and π^- fragmentation functions

are known for u and d quark separately from ν and $\bar{\nu}$ CC interactions, this provides a measure of the NC coupling constants or, assuming the standard model, of $\sin^2\theta_W$. We should do this better than present experiments because of the larger and purer NC sample and because of better fragmentation functions from CC currents as discussed in Section V. The same can be done for the $\pi^\circ/\pi^\pm$ ratios, which of course cannot be done at all in present experiments. These ratios give two equations in addition to the four of Section D, adding further constraints on the values of the coupling constants. In fact, these may be quite powerful, since they do not involve the uncertainties of the structure function integrals.

b) Coherent π° and η° production.

Coherent π° and η° production from an I = 0 nucleus are measures of the isovector and isoscalar parts respectively of the neutral current[43]. If it is appreciable in deuterium we should be able to observe it with the SNC.

c) The strange sea

Llewellyn Smith[36] has pointed out that uncertainty in the knowledge of the strange sea contributes to the theoretical uncertainty in the interpretation of $\sin^2\theta_W$. In CC interactions, where charm production is used to study the strange sea, it is the product $|U_{cs}|^2\, s(x)$ which is measured and thus the uncertainty in $|U_{cs}|^2$ contributes significantly to the uncertainty in S(x). In the case of neutral current events, interactions on S or $\bar{S}$ quarks will lead to strange particle pair production, and in principle to a determination of S(x) directly. A best estimate of the sea quark content is given by $2S/U+D = 0.080 \pm 0.035$[36] however, the background of pair production from u and d quark fragmentation is expected to be even greater than this. Therefore any attempt to sort out the sea contribution from the fragmentation will require a study as a function of x, and this in turn will depend on how good a resolution in x we can achieve, as discussed in (b) above.

d) Flavor changing neutral currents

If neutral currents contain flavor changing components, $|\Delta S| = 1$ or $|\Delta C| = 1$, these would lead to events in which a single strange or charmed particle is produced. Because of the inability to identify $K^{\pm}$ and the indistinguishability of K° and $\bar{K}^{\circ}$ decays, it will not be possible to put a useful limit on single strange particle production. On the other hand the situation is better in the case of charm. The rate of charm pair production from the sea and from fragmentation is expected to be only a few percent. Assuming it to be $\sim$5% and assuming, with HRO and the SNC, an overall rate of $\sim$20% for identifying charm decays (as in section V) we would be able to set an upper limit of $\sim$2-3% on single charm production.

VII THE SOLID NEON CALORIMETER (SNC)- TECHNICAL CONSIDERATIONS

Sufficient tests have now been done for us to be able to describe the calorimeter to be built for the 15' chamber in some detail. Bubble chamber engineers at Fermilab, CERN and elsewhere have contributed advice but no complete design has been made. A number of the details mentioned below will surely be changed before the calorimeter is finally built, but a calorimeter with these features can be constructed and would work.

A. Size and Construction and Safety

The calorimeter must be mounted close to the back wall of the chamber inside the chamber liquid. Because it will be inserted through the piston hole each module must be less than 180cm wide. We wish to cover a large solid angle in the forward direction, over the whole cross-section of the neutrino beam, so we propose to have three separate modules, each 150cms across, 240 cms high and 70 cms thick (see Fig. 1). The modules will be welded together in situ to ensure the smallest possible dead region where they meet.

The services to the modules will be brought in through stainless steel trunks that pass through the chamber wall and go vertically through the vacuum space above the chamber, emerging through the vacuum tank in between the camera ports. [Previous plans envisioned one trunk serving all three modules, but the 15' technical team advised that we should try to avoid making inter-module connections for services inside the chamber. The solution with three separate trunks was suggested by them.]

The services include three separate filling and venting lines (see below for details), upper and lower cooling loops for freezing the calorimeter and keeping it at a steady temperature, resistance-thermometer cables, high voltage cables for the detector electrodes, twisted pair signal cables from the electrodes, and test-pulse cables. We anticipate having ~1700 signal lines from each module. These will require feedthroughs to the external world. All the feedthroughs will be mounted on room-temperature boxes outside the vacuum tank. There will be a temperature gradient over the vertical length of the service trunks, in the vacuum tank, from chamber temperature at the bottom to room temperature at the top. The heat load due to conduction will be a few tens of watts; not a serious problem.

In the worst conceivable failure-mode the service trunks could provide a direct dump line from the chamber to atmosphere if the calorimeter were to rupture, so the calorimeter box itself must be built to full pressure-vessel safety specifications. This implies either a very thick front face, presenting many radiation-lengths to particles from the liquid, or a network of stiffening connections between the front and back faces. The BEBC engineers have calculated that the front wall can be kept to an acceptable thickness if it is fabricated from a stainless steel or an aluminium plate, with a grid of square section beams welded to the inside, and with glass-reinforced plastic rods carrying compressive loads from the front face to the back wall, through holes in the electrode structure. (see Fig. 13). It can be seen from the table on Fig. 13 that the front face of a steel box will have 3.8 times as many radiation-lengths as the front face of an aluminium box.

The trunk-connections inside the chamber will also need to be constructed and tested to the full pressure-vessel safety standard. The estimated overall weight of the calorimeter will be about 28 tons divided into three roughly equal modules. This weight will be supported by flanges which must be welded to the inside of the chamber body in the region of the supporting cone (see Fig. 1) which takes the weight of the chamber down to the legs.

B. Thermodynamic Considerations

1) Why Neon?

We are quite definite in our preference for solid neon over solid argon. This is based on our experience with the calorimeter test-module in 1982 where we saw electrical breakdowns in both solids if they were cooled to far below their freezing points. These breakdowns were eliminated by substantially reducing the high voltage on the electrodes. It was then still possible to see particle pulses, but they were of reduced size. Solid-state physicists report that the rare-gas solids are extremely ductile just below their freezing points and become increasingly brittle as they are cooled. They also have very large coefficients of thermal expansion; much bigger than any containing structure. Thus, when the test calorimeter was

running at maximum power. Cooling loops at the top of the calorimeter would be run at 26°K to condense boil-off. Once the calorimeter is full of liquid, a cooling loop at the bottom of each module will be turned on at the lowest possible temperature (∿ 23°K) and freezing will begin slowly from below. The electrode-sandwich (see below) will contain a number of 10mm and 13mm thick copper plates which will act as thermal pathways for freezing. The lower cooling loops will be brazed directly onto these plates. The filling and freezing process will take about two days and use up to 1 Kwatt of cooling power in the calorimeter. Faster freezing than this should be avoided since it is possible to trap liquid under a plug of solid and then create voids when the trapped liquid shrinks and freezes.

As the liquid freezes the neon will expel the liquid hydrogen from the mixture [44] This hydrogen-rich fraction must be syphoned off from the top of the calorimeter through extraction-lines and replaced by more of the neon-rich mixture through the filling lines.

The service-trunks will be open to the inside of the calorimeter boxes at all times and will be connected into them about 50cms below the tops of the boxes. The trunks will fill up with liquid for a short distance as the calorimeter is filled, and will have a thermal gradient in hydrogen-rich gas from the liquid surface up to where they reach the vacuum tank at room temperature. The extraction, filling and emptying lines will all be vacuum-jacketed lines coming down the trunks. The extraction lines will then rise again inside the modules at the very tops of the calorimeter boxes. The filling-lines will empty into the calorimeter boxes at a slightly lower level. The emptying lines will go to the very bottom of each module. The sensitive volume of solid neon will extend up to the level of the filling lines, but there will be a hydrogen-rich liquid layer at the very top of each module, in the region between the filling and extraction lines.

C. Electrode Structure

In our tests with the calorimeter module at CERN we used the sandwich structure given in Table II, with alternative lead sheets as ground electrodes and with two-faced printed circuit boards (p.c.b.s) as high voltage electrodes. The solid neon layers were 3mm thick and the charge was

collected from the neon by a pattern of copper strips on the printed circuit boards.

Some liquid argon calorimeters have used a similar system [45], but others have segmented their lead plates to make strip or square high voltage electrodes [46]. This latter approach has the advantage of packing more radiation-lengths into a given thickness but it is extremely delicate to assemble and could give trouble if strong shrinkage forces in the solid cause individual small plates to break free from their mountings.

We therefore propose to use the more robust structure, with alternative lead (or copper) and p.c.b. electrodes, as before. The copper plates will extend the whole height of the calorimeter to give continuous thermal pathways from the lower freezing loops. The lead plates and p.c.b.s will be cut into smaller areas in order to avoid differential contraction problems and will be supported by the glass-reinforced plastic rods that connect the front faces to the back walls of the boxes. Small plastic spacers will be stuck to the plates to ensure an even 3mm thickness of solid neon.

Five major requirements can be placed upon the performance of the calorimeter.

i) It must have good energy resolution for electromagnetic showers ($\sim 13\%/\sqrt{E}$). Our tests, and liquid argon experience, show that this requires twenty radiation-lengths of lead plates with thickness of about 3mm, and solid layers about 3mm thick.

ii) It must be capable of resolving muon signals from noise in all channels, in order to give a running check on the pulse-height calibration. This can be achieved if the capacitance per solid layer, in the set of layers summed on one preamplifier, is less than about 500 pF (We cannot use coupling-transformers in the bubble chamber field). Allowing (say) 500 pF for the twisted-pair connection and (say) 6 layers per channel, with $\varepsilon = 1.7$ for solid neon, this limits the area of each electrode to less than about 1000 cm^2.

iii) It must have sufficiently good spatial resolution to be able to separate the two gammas from most π^os and to give good separation between most of the charged and neutral particles from a fast hadron jet from the middle of the bubble chamber - i.e. 1.5 metres away. Our Monte

Carlo studies have shown that the resolution needs to be better than ± 2cm if the confusion at Tevatron energies is to be kept at an acceptably low level[47].

iv) Multiple sampling over the depth of a shower is needed for particle identification. This is particularly important for electron-pion separation, where the longitudinal development of the shower can give more than an extra order of magnitude of pion rejection. We will also use it to identify neutral hadron interactions (neutrons and K_L^o, see v) below). It will, in addition, allow us to make measurements of electromagnetic shower directions.

v) Recent Monte Carlo results have shown that catching the neutrons and K_L^o in the calorimeter will make a worthwhile improvement to the measurement of E_{hadron} (see Fig. 13). It is therefore proposed to increase the number of inelastic collision-lengths in the calorimeter from about 1.0 (including the front face, $20X_o$ of lead etc.) to about 1.8, by adding thick copper plates at the back.

Bearing in mind these considerations, we propose a structure with five sampling layers :- a) Tracking region
b),c),d) Electromagnetic calorimetry region
e) Extra hadron detection region

In layer a) there will be (see Tables III and IV) 1 cm wide vertical electrode strips (Ø strips) each of which runs half the height of the detector. These will give good resolution on clear tracks and on early conversions. The next two layers will have three sets of electrode strips 2cm wide. The set of z strips will run horizontally over the whole 1.5 m width of a module. The other two sets are near vertical, but in small-angle stereo to resolve ambiguities (Ø and Ø'). Layer d) is similar, but has 3mm strips, more gaps and thicker lead plates to contain and measure the largest part of an electromagnetic shower at high energy. Layer e) provides the extra hadron conversion efficiency, with a similar strip pattern to layer d). In all cases there will be two sets of Ø and Ø' strips each covering half the height of the calorimeter.

This scheme requires 1700 readout channels per module (see table IV) (Some groups who have reconstructed jets in calorimeters have suggested that

at least one layer of square pads would be advisable, instead (say) of the strips in layer c) ($\sim 4X_o$ to $8X_o$). These would give a clearer starting point for pattern recognition, but would not give the same position-resolution as strips unless a very large number of channels were provided.)

D. Electronics

1. Preamplifiers

All of our tests have been carried out using charge pre-amplifiers of the Willis-Radeka type[48], borrowed from various European liquid-argon groups. They have an intrinsic noise level of about 700 electrons with zero input capacitance, and the effective noise increases with the detector capacitance. We plan to use similar preamplifiers with the SNC, taking advantage, if possible, of more recent developments in noise reduction [49].

An alternative, which we discussed earlier, is to build cold pre-amplifiers which can be mounted inside the calorimeter, thus eliminating ~500 pF per channel of twisted-pair capacitance (and noise-pickup). But our experience in the test at CERN shows that this is not essential. It will not be a good idea to bury 1700 preamplifiers per module in an almost totally inaccessible place unless a clear benefit can be obtained in return for the risk taken.

2. Readout

A new kind of readout system will have to be developed for the calorimeter. The standard Fermilab "wormbox" will not do because of its dead time. The neutrino beam spill lasts about 2 nseconds and the system must be able to record every hit during that period with a time-resolution of about 1μs (typical preamplifier shaping time). The analogue to digital converters, at least for layers c) and d) (see Table III) (>1000) will need a wide dynamic range so that they can digitise either a single muon, for calibration purposes, or the peak of a 300 GeV electron shower. Genuine hits will be very sparse both in position (~10 to 500 channels hit out of ~ 5,100) and in time (~ 200 events per burst, most of them muons) so the readout system will need to reject noise pulses and suppress zeros in hardware before reading out the channel coordinates, pulse heights and hit times.

This specification is not met by any existing readout system that we are aware of but it certainly can be achieved by variants of existing systems. The Ecole Polytechnique group, for instance, is investigating a technique with flash - A.D.C.s and fast microprocessors in CAMAC. The problem of large dynamic range may be overcome by running a number of cheap ADCs in parallel with different input gains, rather than by making one super 12 bit unit per channel.

After on-line zero suppression, time sorting and pulse-height digitisation, it can be estimated that the calorimeter readout hardware will hand on to the E.M.I. computer a total of 36,000 words of information per frame (assuming conservatively:- a) 200 muons per picture, each giving 20 hits in the calorimeter; plus b) 10 ν interactions in walls, chamber and calorimeter, each giving the equivalent of 40 muon tracks; and c) each hit is encoded with 12 timing bits, 13 address bits and 12 pulse-height bits into three 16 bit words).

E. Cost

We estimate the cost of the complete calorimeter to be $1,700,000. This is based on an estimate made by the BEBC engineers, with adjustments for differences between their assumptions and those outlined above. It is increased from the estimate given last year [50] because we have added an extra layer of copper plates to convert more neutral hadrons. In principle, a significant fraction of this cost might be borne by the grant-awarding authorities in the U.K., France and other (potential) collaborating countries, but it is impossible to guarantee such contributions at this stage. These authorities are aware of our proposal but cannot make any commitments until the programme is more clearly defined.

REFERENCES

1. V. BRISSON et al. Physica Scripta 23, 688 (1981)
   W. CYKO et al., Nuc. Instr. and Meth. 196, 397 (1982)
2. V. BRISSON, Performance of a Prototype Solid Neon and Solid Argon Calorimeter, (to be published in Nucl. Inst. and Meth.)
3. EMC Collaboration, see Rapporteurs Report (D. Haidt) 21st International Conference on High Energy Physics, Paris, p. C 3-5 (1982)
4. R. FIELD and R.P. FEYNMAN, Phys. Rev. D15, 2590 (1977)
5. J. HANLON et al., Phys. Lett 45, 1817 (1980)
6. D. ALLASIA et al., Phys. Lett. 107B, 148 (1981)
7. G.R. FARRAR and D.R. JACKSON, Phys. Rev. Lett. 35, 1416 (1975)
8. R.P. FEYNMAN, Photon-Hadron Interactions (Benjamin 1972) p. 150
9. F.E. CLOSE, Phys. Lett. 43B, 422 (1973)
10. R. CARLITZ, Phys. Lett. 58B, 345 (1975)
11. A. DONNACHIE and P.V. LANDSHOFF, Phys. Lett. 95B, 437 (1980)
12. F.E. CLOSE and R.G. ROBERTS, Rutherford Lab. report RL-80-058 (1980)
13. G. MYATT, Private communication
14. ABBPST Collaboration, See Rapporteurs Report (G. Snow), Proceedings Neutrino 81, Hawaii (1981) p. 427
15. J.G. MORFIN, Proceedings of Neutrino 82, Balaton, Supplement p. 87 (1982)
16. J.J. AUBERT, Talk at CERN , Fixed Target Workshop, Dec. 1982
17. C. LLEWELLYN SMITH, A Possible Explanation of the Difference between the Structure Functions of Iron and Deuterium (to be published)
18. H. ABRAMOWICZ et al., Preprint CERN-EP/82-77 (1982)
19. N. USHIDA et al., Phys. Lett. 121B, 187 and 292 (1983)
20. C. BALTAY, Proceedings of Neutrino 82, Balaton, Supplement p. 109 (1982)
21. H. DEDEN et al., Phys. Lett. 67B, 474 (1978)

22. D. SON et al., Phys. Rev. Lett. 49, 1128 (1982)

23. G. KALMUS, 21st International Conference on High Energy Physics, Paris p. C3-431 (1982)

24. K. KLEINKNECHT and B. RENK, Zeit. Für Phys. C 16, 7 (1982)

25. R.P. FIELD and R.P. FEYNMAN, Nucl. Phys. B136, 1 (1978)

26. B. ANDERSSON et al., Z. Phys. C1, 105 (1979); C3, 223 (1980); C6, 235 (1980); C9, 233 (1981); C12, 49 (1982); Nucl. Phys. B178, 242 (1981)

27. A. BLONDEL and F. JACQUET, Baryon Production in Jets, preprint LPNHE/X-82/03 June 1982

28. P. ALLEN et al., ABCMO Collaboration, An Investigation of Quark and Diquark Fragmentation in νp and $\bar{\nu} p$ CC Interactions in BEBC, submitted to Nuclear Physics

29. G. MYATT, private communication

30. P. ALLEN et al., Phys. lett. 96B, 209 (1980)

31. W.A. MANN, IMSTT Collaboration, Proceedings of Neutrino 81, Hawaii (1981)

32. F.P. SUKHATME et al., Phys. Rev. D25, 2975 (1982)

33. M. ZRALEK et al., Phys. Rev. D19, 820 (1979)
Z. DZIEMBOWSKI, Z. Phys. C10, 321 (1981)
G.R. GOLDSTEIN and J. MAHARANA, N.C. 59A, 393 (1980)
S. FREDRIKSSON et al., TRITA-TFY-81-20 (preprint)

34. C.C. CHANG et al., A Study of Diquark Fragmentation into Λ and Y^{*+} (preprint)

35. F.J. HASERT et al., Phys. lett. 46B, 138 (1973)

36. C.H. LLEWELLYN SMITH, On the Determination of $\sin^2\theta_w$ in Semileptonic Neutrino Interactions, Oxford preprint (1983)

37. P. IGO-KEMENES, Proceedings of Neutrino 82, Balaton, Sypplement p. 69 (1982)

38. T. KAFKA et al., Phys. Rev. Lett. 48, 910 (1982)

39. ABBPPST Collaboration, Proceedings of Neutrino 82, Balaton, Vol. II p. 51 (1982)

40. W. VAN DONINCK, Various memoranda including CERN Proposal P152

41. L.M. SEHGAL, Phys. Lett. 71B, 99 (1977)

42. ABBPPST Collaboration, Presented at CERN Fixed Target Workshop, Dec. 1982

43. H. FAISSNER, Proc. XVI Rencontre de Moriond (1981)
F. NIEBERGALL, Proc. Neutrino 82, Balaton, Vol. II, p. 62 (1982)

44. W. CYKO et al. (ref. 1): C.S. BARRETT et al., J. Chem. Phys. 45, 834 (1966)

45. J.H. COBB et al., Nucl. Instr. and Meth. 158, 93 (1979); C. NELSON et al., Fermilab Pub. 83/41 Exp.

46. V. KADANSKY et al., Physica Scripta 23, 680 (1981)

47. J. HANLON and W.A. MANN, I.I.T. HEP-81-08, J. HANLON and H.A. RUBIN, I.I.T. HEP-81-03

48. W.J. WILLIS and V. RADEKA, Nucl. Instr. and Meth. 120, 221 (1974)

49. R. STEPHENSON, Rutherford Laboratory report, RL-82-082

50. See answers to questions from PAC, 1982.

TABLE I

Q^2 vs W^2 for 25,000 WBB Neutrino Events

W^2 ↑	0 – 25	25 – 50	50 – 100	100 – 200	200 – 400
400	69	52	35	26	17
200	338	312	355	87	43
100	1604	676	572	165	52
50	4594	1274	468	87	0
0	12517	1369	277	9	0

Q^2 →

TABLE II

Structure of Calorimeter Sandwich

Unit-thicknesses			Zones
Thickness of lead plates		2mm = 0.36 X_o	y1 & u-v
		4mm = 0.72 X_o	y2
Thickness of stainless steel plates		6mm = 0.33 X_o	y1 & y2
Thickness of a solid Ar or Ne layer		3mm = 0.02 X_o	all
Thickness of printed circuit board		2mm = 0.06 X_o	all

Material in each Zone

y1 zone	1 stainless-plate	6mm = 0.33 X_o
	4x2mm lead plates	8mm = 1.44 X_o
	10 layers Ne or Ar	30mm = 0.2 X_o
	5 pcbs	10mm = 0.3 X_o
	Total y1	54mm = 2.27 X_o
u-v zone	5x2mm lead plates	10mm = 1.8 X_o
	11 layers Ne or Ar	33mm = 0.22 X_o
	6 pcbs	12mm = 0.36 X_o
	Total u-v	55mm = 2.38 X_o
y2 zone	5x4mm lead plates	20mm = 3.6 X_o
	10 Layers Ne or Ar	30mm = 0.2 X_o
	5 pcbs	10mm = 0.3 X_o
	Total y2	60mm = 4.1 X_o
Total sensitive thickness		169mm = 8.75 X_o

Table III Thickesses of Neon and Electrodes

Region a) Tracking (Ø only)	Thickness (mm)	Radiation Lengths	cumulative Thickness (mm)	cumulative Radiation Lengths
6 x mm gaps of solid Ne	18	0.71		
2 x 2mm Pb electrodes	4	0.12		
3 x HT$^+$p.c.b.s and initial plain ground p.c.b.	8	0.24		
	30	1.07	30	1.07
Region b) E.M. Calorimetry				
12 x 3 mm gaps of solid Ne	36	0.24		
1 x 10 Copper electrode(first)	10	0.7		
5 x 2mm Pb electrodes	10	1.8		
6 x HT$^+$p.c.b.s(2Z,2Ø,2Ø')	12	0.36		
	68	3.1	98	4.17
Region c) E.M.Calorimetry				
Same as b),but with 5 x 3mm Pb plates	73	4.0	171	8.17
Region d) E.M.Calorimetry				
Same as c),but with 40 gaps, 19 x 3mm Pb plates and 20 x HT$^+$ p.c.b.s	227	12.9	398	21.07
Region e(Extra Neutral Hadron Detection				
12 x 3mm gaps of solid Ne	36	0.24		
6 x 13mm copper electrodes	78	5.45		
6 x HT$^+$ p.c.b.s.(2Z,2Ø,2Ø')	12	0.36		
	126	6.05	524	27.0

i.e. Total Active Thickness = 52.4 cms

Number of Radiation lengths = 27

Table IV Electrode Patterns and Capacitances

Region a) Tracking	Area of one electrode $(cm)^2$	Number of channels	Capacitance per channel (pF)*
Ø electrodes, 1cm wide x 1.2m high x 6 gaps per channel	120	300	908
Region b) E.M.Calorimetery			
Z Electrodes, 2cm high x 1.5m across x 4 gaps per channel	300	120	1180
Ø and Ø' electrodes, 2cm wide x 1.2m high x 4 gaps each per channel	240	300	1044
Region c) E.M.Calorimetry			
Z electrodes similar to b)	300	120	1180
Ø and Ø' electrodes similar to b)	240	300	1044
Region d) E.M.Calorimetry			
Z Electrodes, 3cm high x 1.5m across x 14 gaps per channel	450	80	4070
Ø electrodes, 3cm wide x 1.2m high x 14 gaps per channel	360	100	3356
Ø' electrodes, 3cm wide x 1.2m high x 12 gaps per channel	360	100	2948
Region e) Extra Hadron Detection			
Z electrodes, 3cm high x 1.5m across x 4 gaps per channel	450	80	1520
Ø and Ø' electrodes, 3cm wide x 1.2m x 4 gaps each per channel	360	200	1316
		Total Channels = 1700 per module	

*Including 500 pF twisted pairs.

FIGURE CAPTIONS

1 - The 15-foot bubble chamber with calorimeter.

2 - Monte Carlo distributions of the ratio of estimated hadronic energy to true hadronic energy for the bubble chamber without and with the calorimeter.

3 - The ratio of the transverse momentum of the hadrons to that of the muon in a bare hydrogen bubble chamber, in the BEBC TST experiment, and from a Monte Carlo study of the bubble chamber with calorimeter.

4 - Monte Carlo study of $\gamma\gamma$ invariant mass spectrum for bubble chamber with calorimeter. A π° peak over combinatorial background is seen.

5 - Monte Carlo studies of the ratio of visible hadronic energy to true hadronic energy for (a), the bare bubble chamber and the bubble chamber with calorimeter but no neutron detection; and (b) the bubble chamber with calorimeter, without and with neutron detection.

6 - Monte Carlo of the ratio of neutral current event energy(determined from a zero-constraint fit)to true energy .

7 - Distribution of $\epsilon = \Sigma\ (E-P_L)_i - m_N$ for odd prong events ("νp") from deuterium experiment E545 and from a hydrogen experiment. The two distributions are normalized for $\epsilon < -0.5$.

8 - The ratio of the structure function F_2 of iron to that of deuterium from the EMC experiment.

9 - The smearing correction on x: (a) bare bubble chamber and (b) bubble chamber with calorimeter.

10 - The uncertainty in smearing in the bare chamber (solid curve), and statistical error on a 30,000 event experiment (dashed curve). The reduction of smearing with the calorimeter would bring the solid curve down to the level of the dashed one. Also shown are SLAC and EMC uncertainties for electron and muon experiments.

11 - Comparison of the z distributions for $h^+ + h^-$ for a hydrogen and a neon-hydrogen experiment.

12 - Clusters of CC, NC and hadron induced events formed using the Van Doninck Multivariant Discriminant Analysis.

13 - Detail sketch and section through front face of calorimeter box.

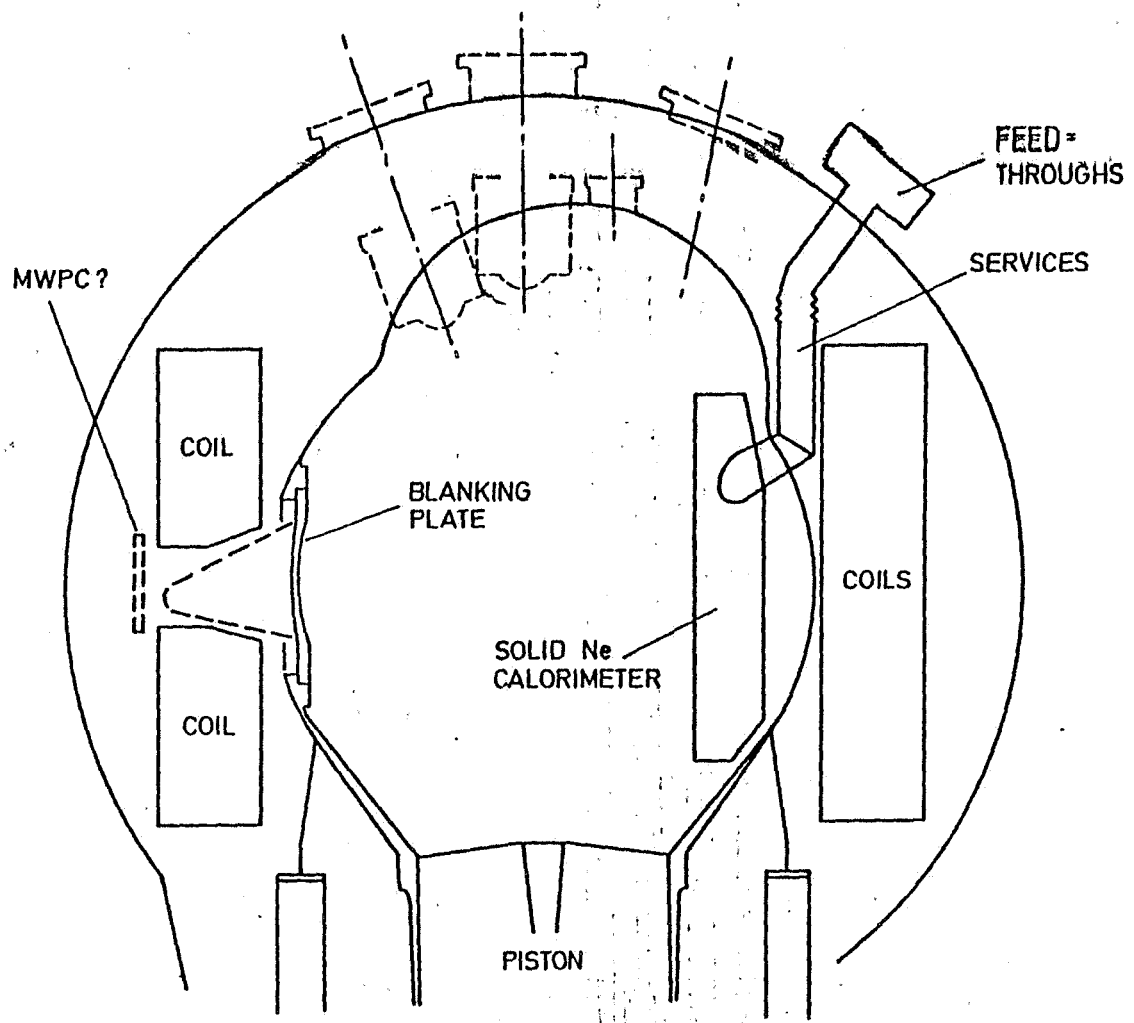

Figure 1 THE 15' BUBBLE CHAMBER WITH CALORIMETER

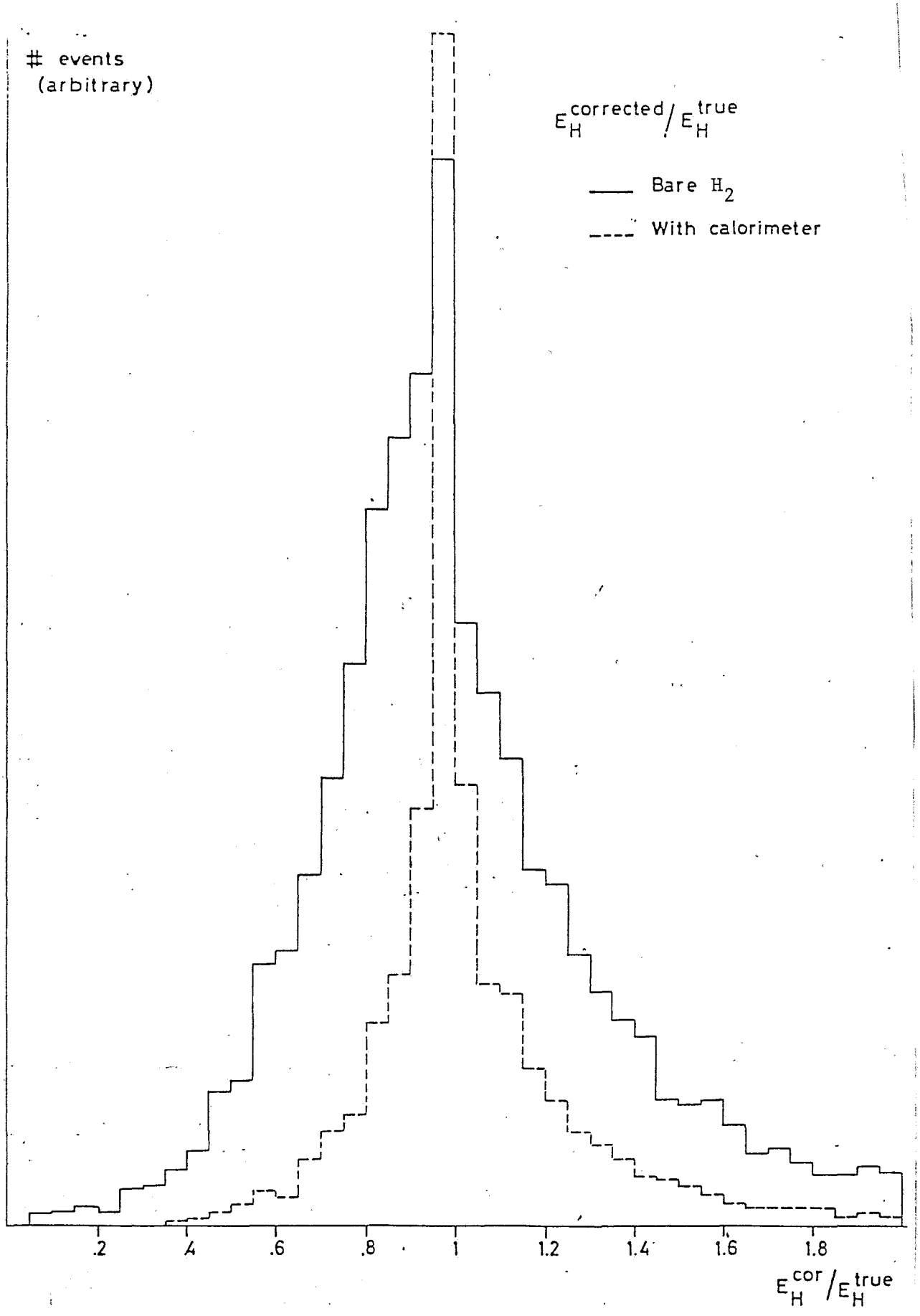
events
(arbitrary)
$E_H^{corrected}/E_H^{true}$
Bare H_2
With calorimeter
.2
.4
.6
.8
1
1.2
1.4
1.6
1.8
E_H^{cor}/E_H^{true}

Fig. 2

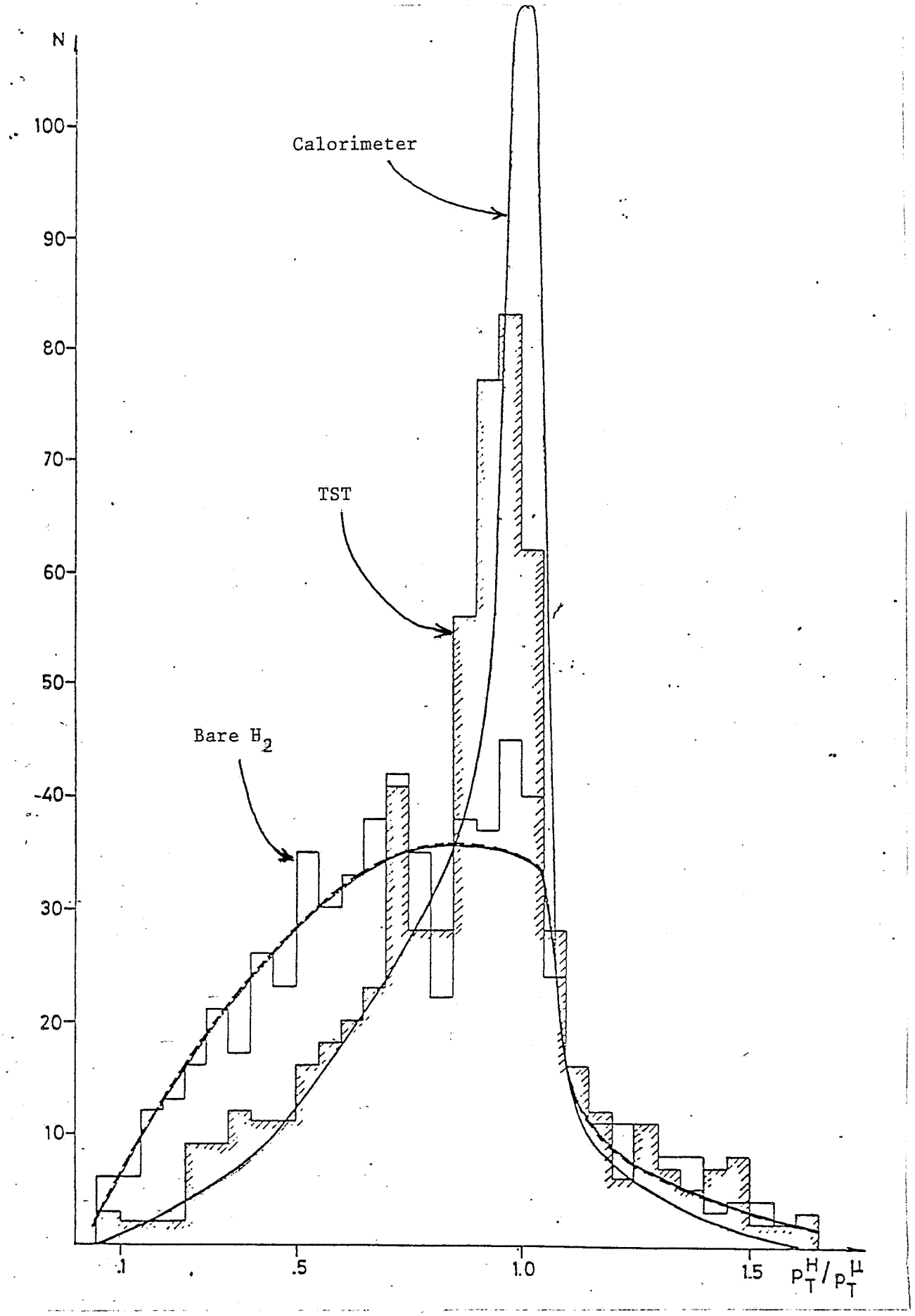
N
100
90
80
70
60
50
40
30
20
10
Calorimeter
TST
Bare H_2
.1
.5
1.0
1.5
p_T^H / p_T^μ

Fig. 3

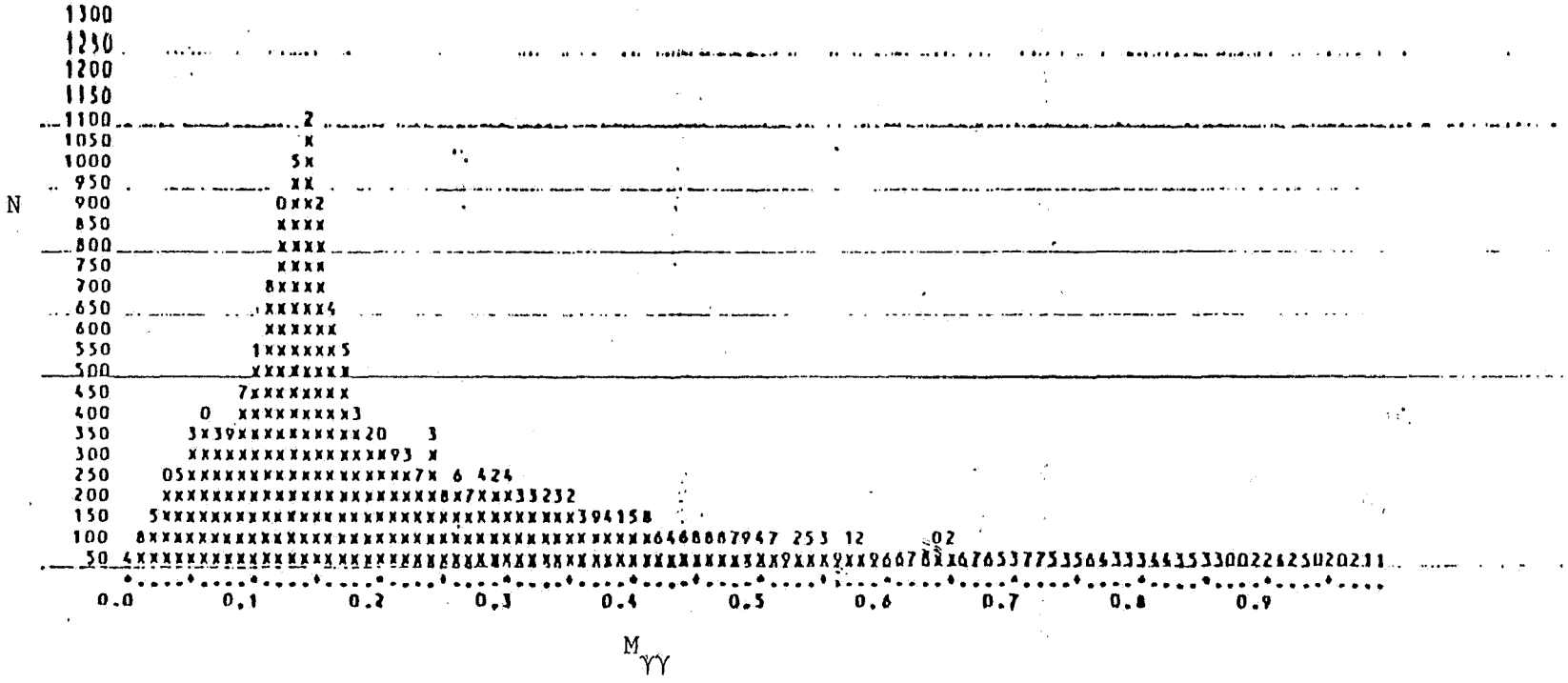
N
1300
1250
1200
1150
1100
1050
1000
950
900
850
800
750
700
650
600
550
500
450
400
350
300
250
200
150
100
50
0.0
0.1
0.2
0.3
0.4
0.5
0.6
0.7
0.8
0.9
M γγ

Fig. 4

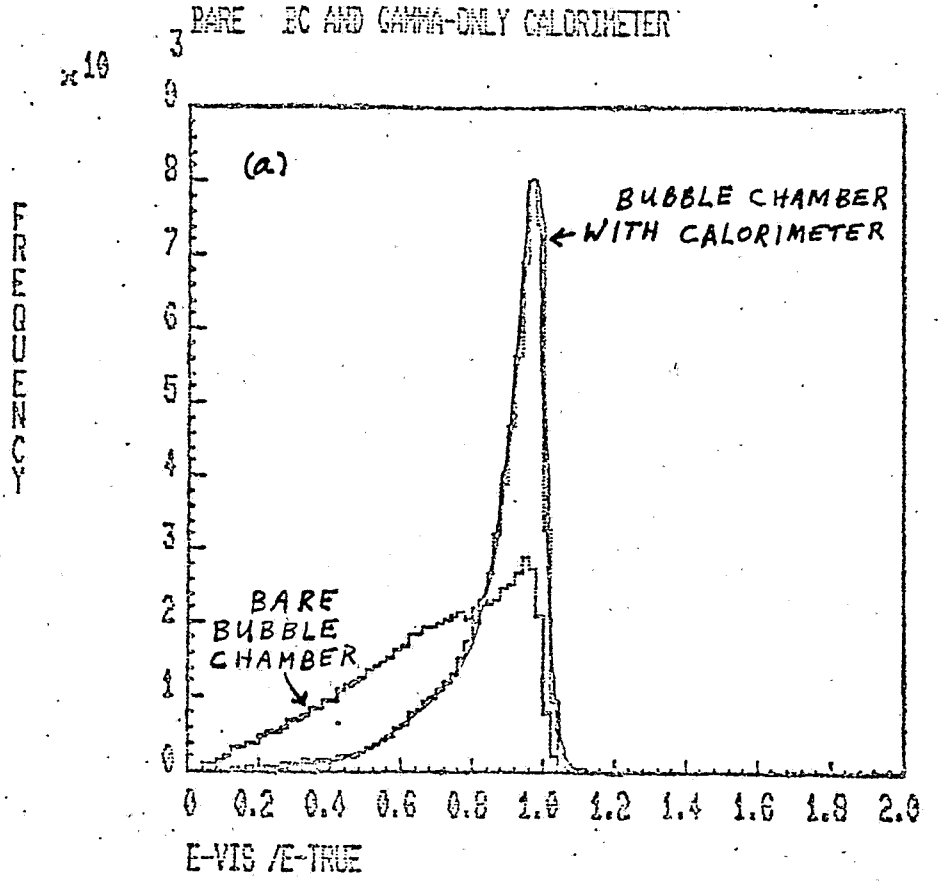
BARE EC AND GAMMA-ONLY CALORIMETER
x10 3
FREQUENCY
(a)
BUBBLE CHAMBER
WITH CALORIMETER
BARE
BUBBLE
CHAMBER
0 0.2 0.4 0.6 0.8 1.0 1.2 1.4 1.6 1.8 2.0
E-VIS /E-TRUE

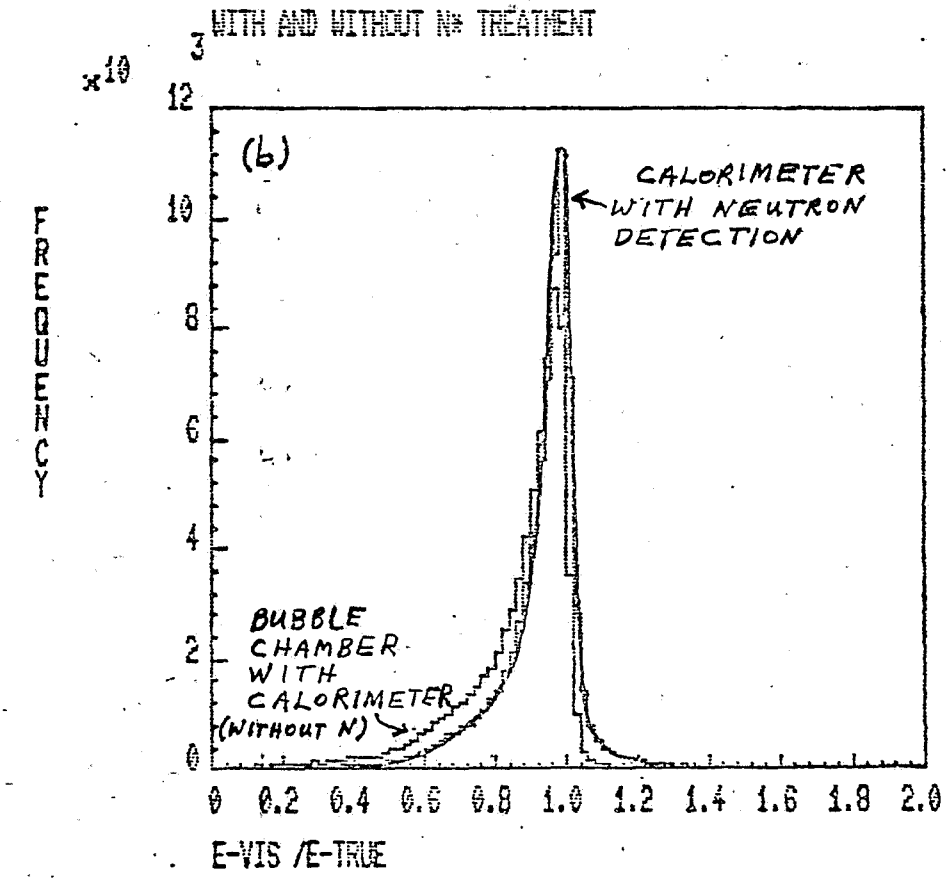
WITH AND WITHOUT N* TREATMENT
x10 3
FREQUENCY
(b)
CALORIMETER
WITH NEUTRON
DETECTION
BUBBLE
CHAMBER
WITH
CALORIMETER
(WITHOUT N)
0 0.2 0.4 0.6 0.8 1.0 1.2 1.4 1.6 1.8 2.0
E-VIS /E-TRUE

Fig. 5

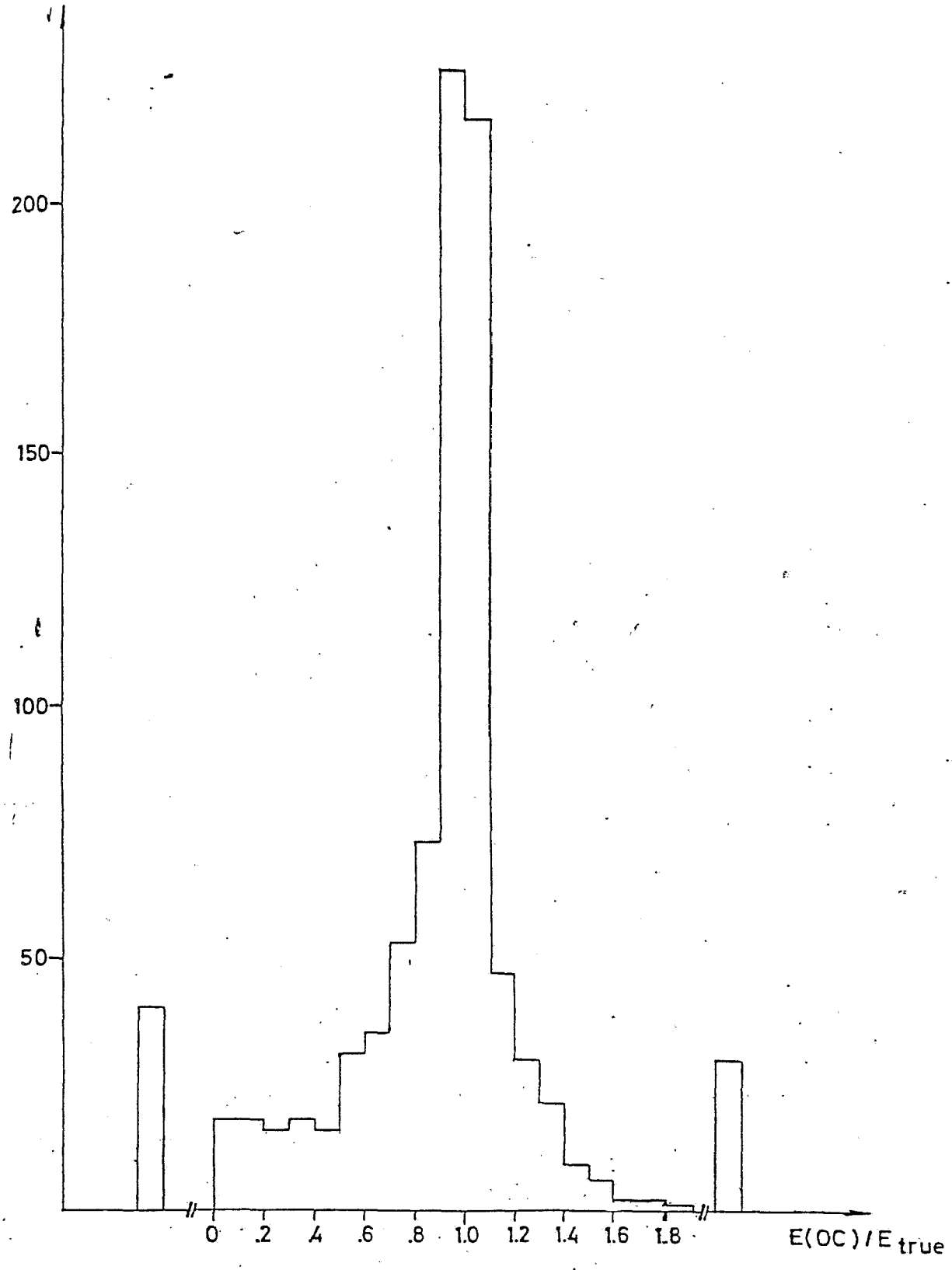

Fig. 6

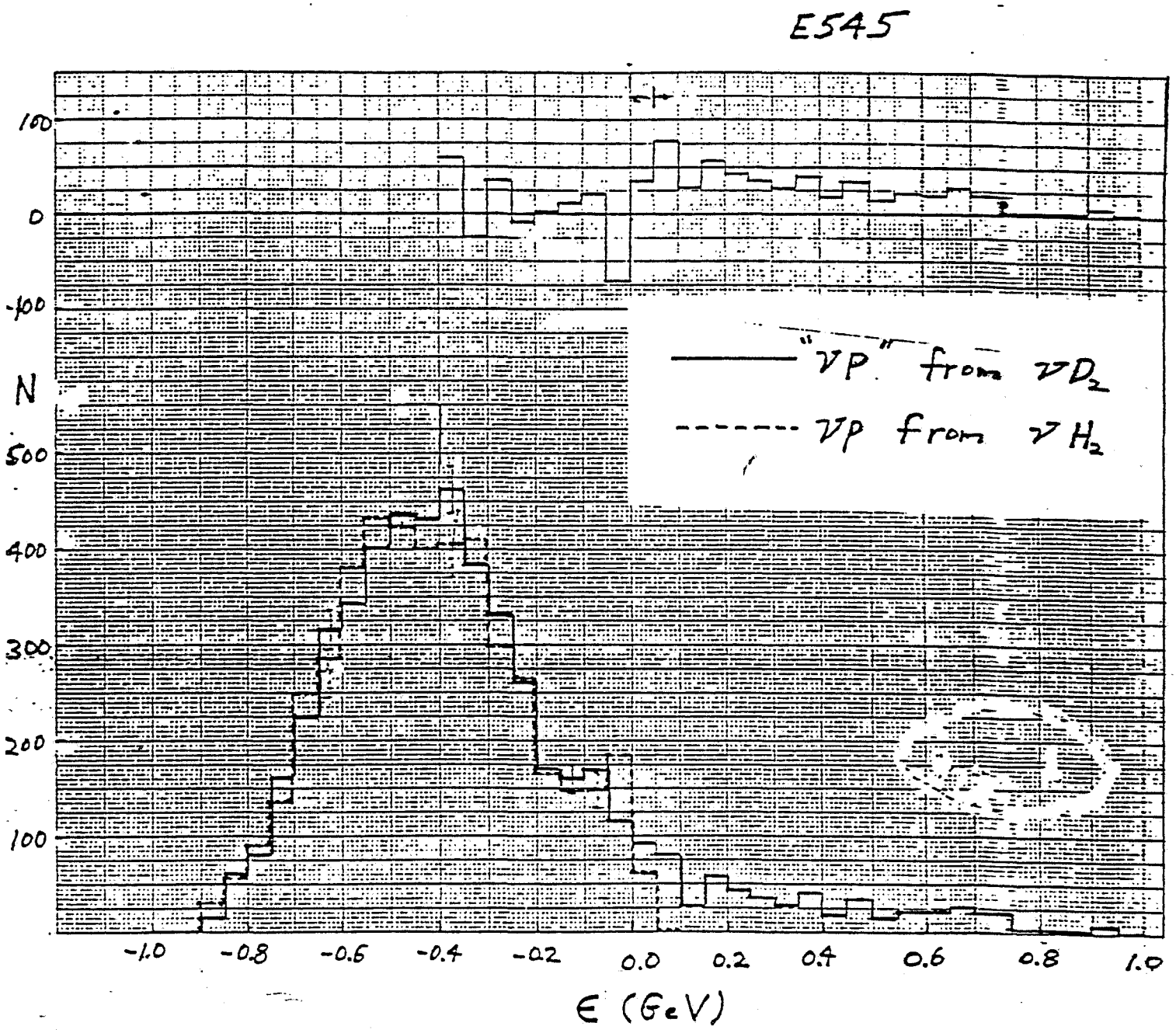
E545
100
0
-100
N
500
400
300
200
100
"νp" from νD₂
νp from νH₂
-1.0
-0.8
-0.6
-0.4
-0.2
0.0
0.2
0.4
0.6
0.8
1.0
ε (GeV)

Fig. 7

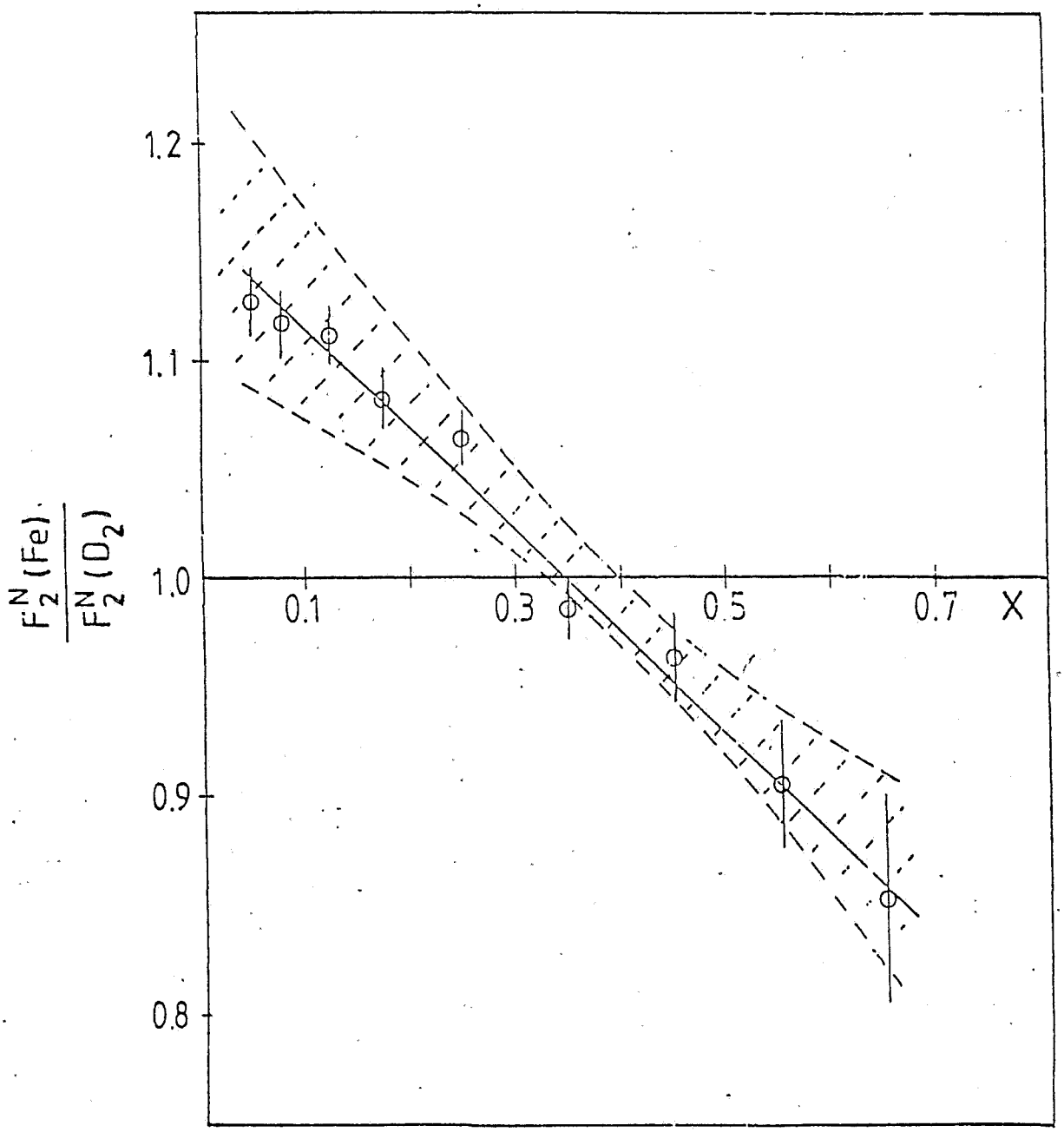

Fig. 8

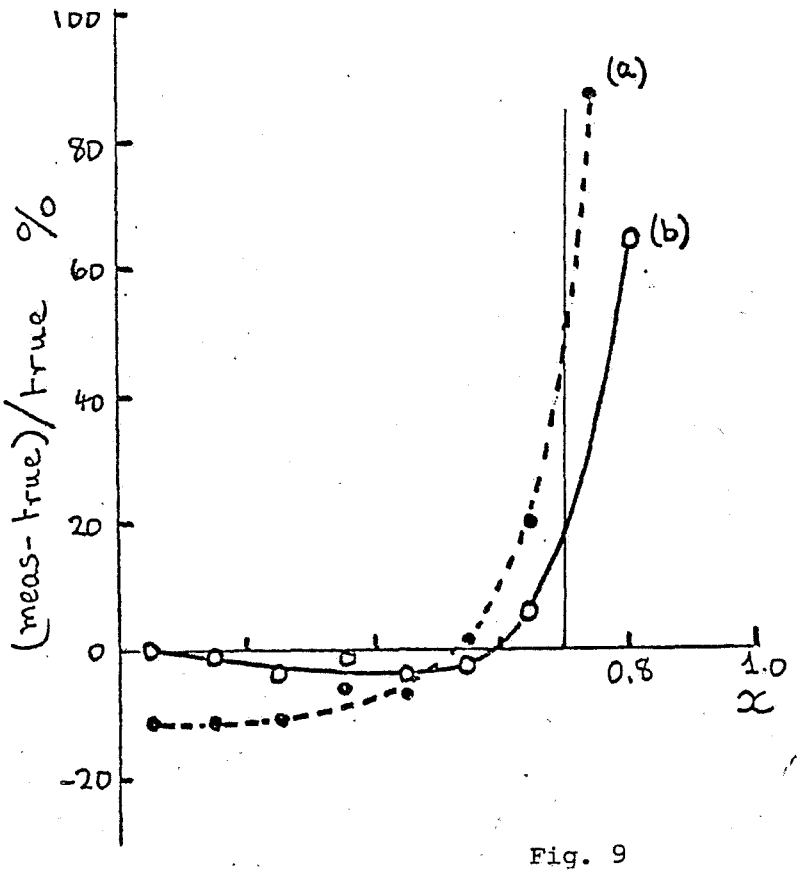
100
80
60
40
20
0
-20
(meas-true)/true %
(a)
(b)
0.8
1.0
x

Fig. 9

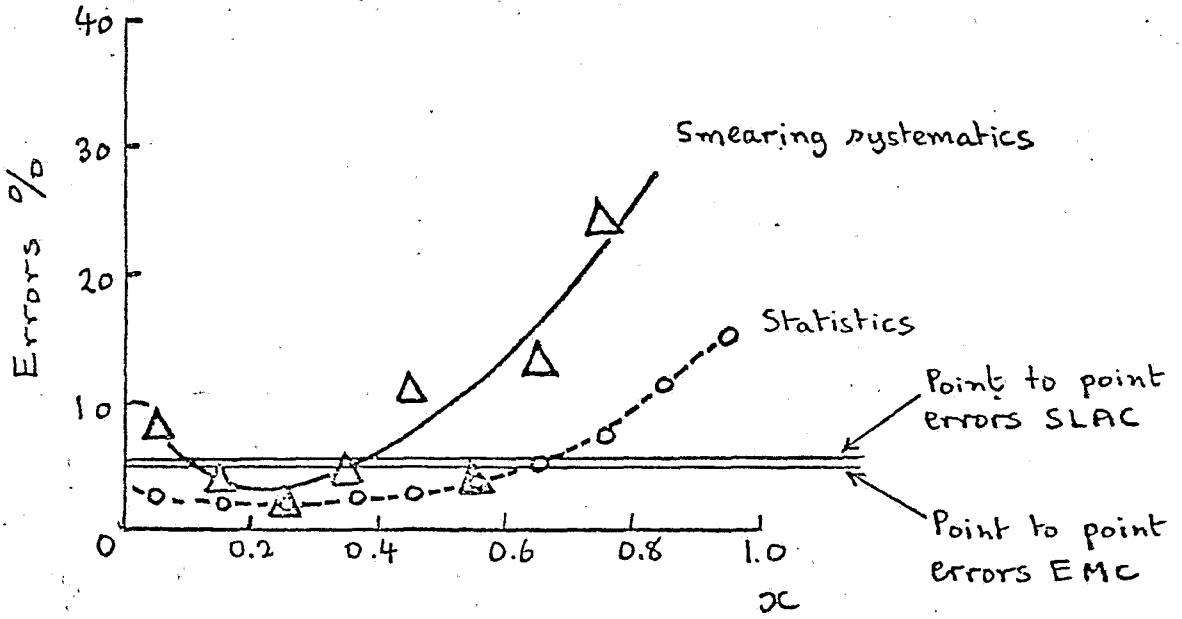
40
30
20
10
0
Errors %
Smearing systematics
Statistics
Point to point errors SLAC
Point to point errors EMC
0.2
0.4
0.6
0.8
1.0
x

Fig. 10

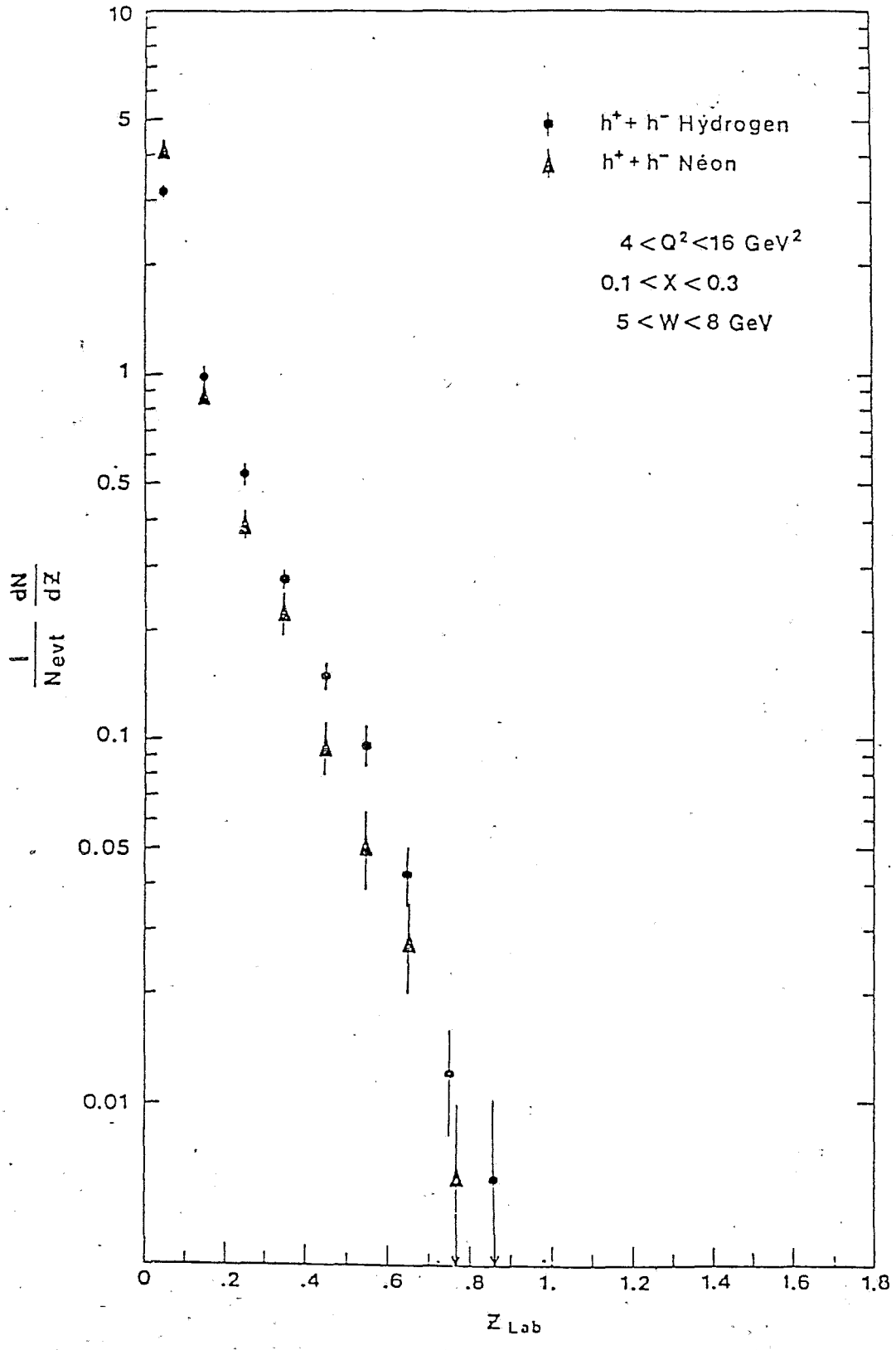
10
5
1
0.5
0.1
0.05
0.01
0
.2
.4
.6
.8
1.
1.2
1.4
1.6
1.8
$\frac{1}{N_{evt}} \frac{dN}{dZ}$
Z_{Lab}
$h^+ + h^-$ Hydrogen
$h^+ + h^-$ Néon
$4 < Q^2 < 16$ GeV^2
$0.1 < X < 0.3$
$5 < W < 8$ GeV

Fig. 11

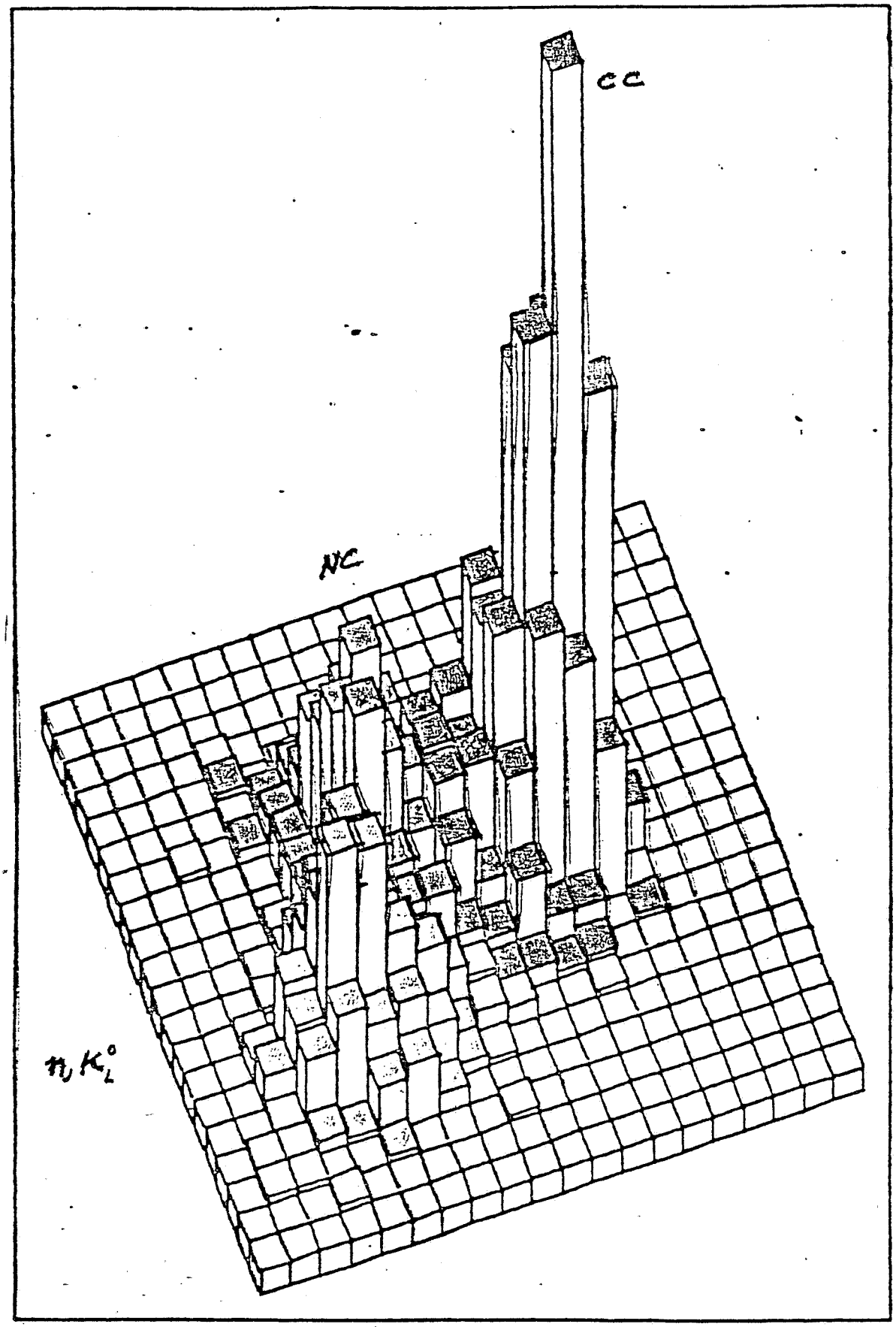

Fig. 12

Detail Sketch and Section Through Front Face of Calorimeter Box

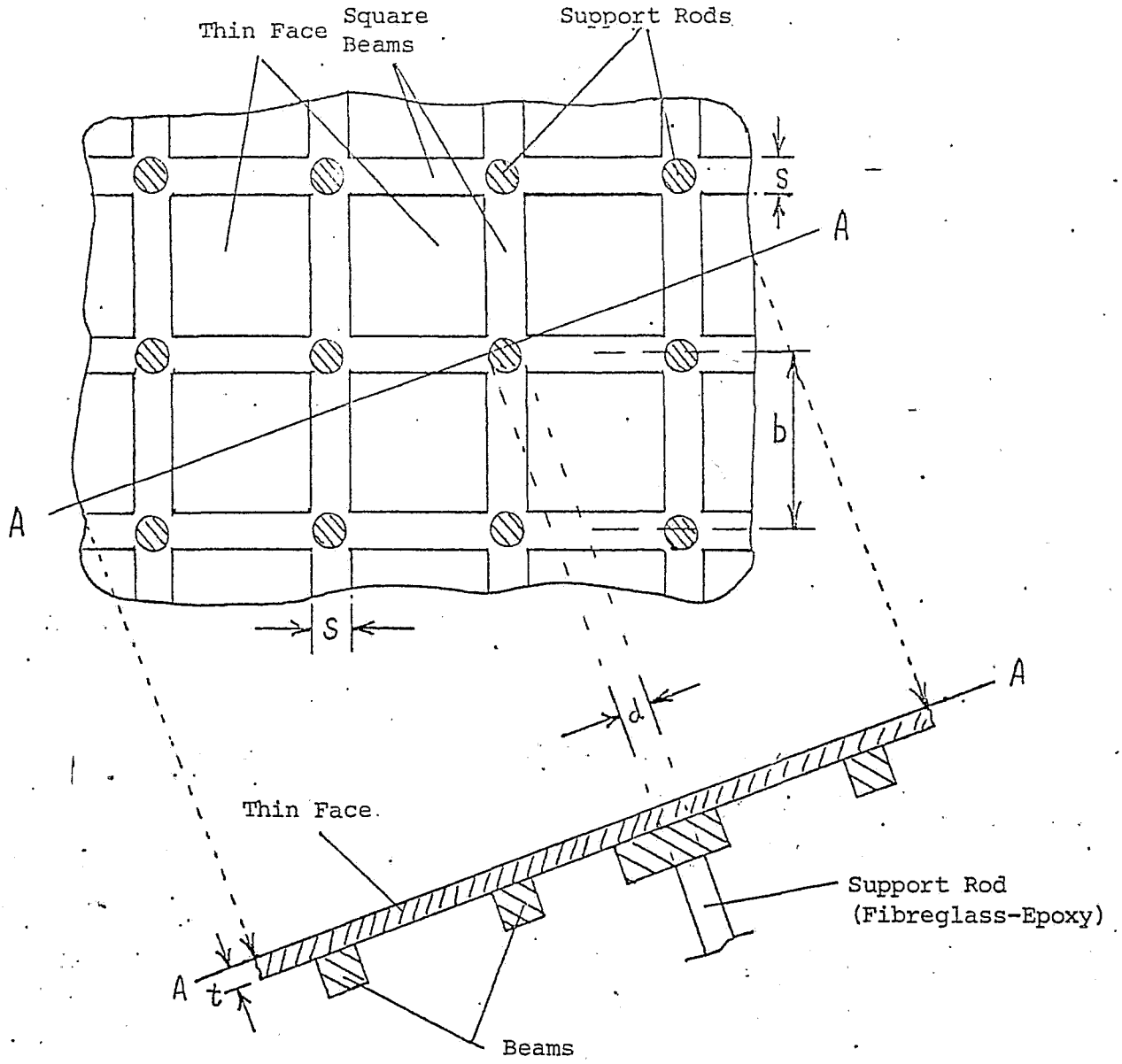

Some Allowed Dimensions (stress calculated by G.Passardi,BEBC)

Material	Aluminium			Stainless		
Beam spacing b cms	50	30	20	50	30	20
Beam thickness s cms	10	6	4	8.6	5	3.3
Thickness of face t cms	4	2.5	1.6	3.2	1.8	1.3
Diameter of rods d cms	7	5	3.5	7	5	3.5
Fraction of area with beam	36%	36%	36%	31%	31%	31%
Fraction of area with rod	1.5%	2.2%	2.4%	1.5%	2.2%	2.4%
Mean thickness (face + beam) cms	7.6	4.7	3.0	5.9	3.3	2.3
Mean number of radiation-lengths	0.83	0.52	0.34	3.4	1.9	1.3
Mean collision-lengths (inelastic)	0.19	0.12	0.08	0.35	0.2	0.14

Fig. 13

PROPOSAL P651

NEUTRINO-PROTON AND NEUTRINO-NEUTRON INTERACTIONS IN THE FERMILAB 15-FOOT BUBBLE CHAMBER WITH A SOLID NEON CALORIMETER

ECOLE POLYTECHNIQUE

ILLINOIS INST. OF TECHNOLOGY

TUFTS UNIVERSITY

UNIVERSITY COLLEGE LONDON

FERMILAB

OBJECT: TO INVESTIGATE ν AND $\bar{\nu}$ INTERACTIONS ON THE SIMPLEST TARGETS WITH A POWERFUL HYBRID VERTEX DETECTOR SYSTEM INCLUDING

THE 15-FOOT BUBBLE CHAMBER
IMPROVED EMI
COMPLETE IPF
HRO - HOLOGRAPHY
SOLID NEON CALORIMETER

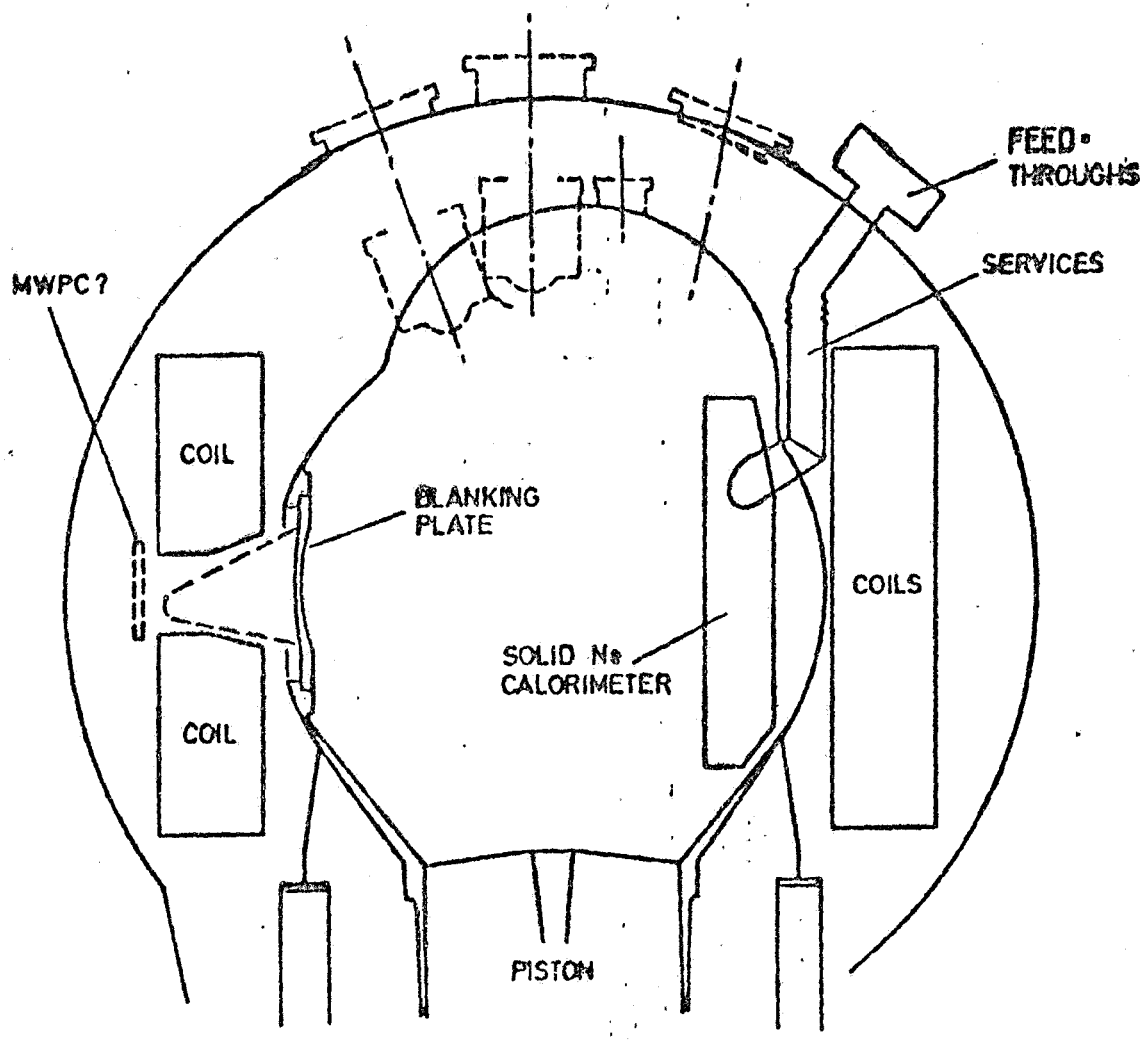

Figure 1 THE 15' BUBBLE CHAMBER WITH CALORIMETER

MAIN PHYSICS AIMS

- MEASURE $\sin^2\theta_W$ TO A PRECISION APPROACHING 0.005 TO TEST SECOND ORDER EFFECTS IN ELECTROWEAK THEORY.
- DETERMINE NEUTRAL CURRENT COUPLINGS OF u and d QUARKS WITH INCREASED PRECISION
- DETERMINE THE STRUCTURE FUNCTIONS AND QUARK DISTRIBUTIONS OF NEUTRONS AND PROTONS USING HYDROGEN AND DEUTERIUM — WITHOUT "EMC EFFECTS"
- STUDY QCD EFFECTS USING THE HIGHEST AVAILABLE RANGE OF W^2 and Q^2 - i.e. THE TEVATRON
- STUDY THE PRODUCTION AND DECAY OF CHARMED PARTICLES — SEARCH FOR BEAUTY
- INVESTIGATE THE HADRONIC FINAL STATE WITH BETTER PARTICLE IDENTIFICATION AND BETTER PRECISION

THIS PROPOSAL -

2.5×10^{18} protons equally divided between ν and $\bar{\nu}$ - QT Beam.

DEUTERIUM fill in the chamber yielding

ν	$\bar{\nu}$
25000 CC events	8000 CC events
7500 NC "	3200 NC "

We envision this as the first experiment in a program of neutrino physics using this facility. Further experiments might be ν and $\bar{\nu}$ on hydrogen.

WHAT THE SNC DOES FOR US

1. DETECTS ELECTRONS
2. DETECTS PHOTONS
~90% OF ALL γ's FROM π^0 INTERACTIONS - 98% OF γ ENERGY
3. MEASURES THE ENERGY WITH A RESOLUTION ~ $13\%/\sqrt{E}$
4. DETECTS NEUTRONS - UP TO ~80% OF ALL NEUTRONS INTERACT IN LIQUID OR SNC

THIS ENABLES US TO

1. IDENTIFY ν_e INTERACTIONS AND HEAVY QUARK β-DECAY
2. SIGNIFICANTLY REDUCE THE SMEARING IN ALL KINEMATIC VARIABLES E_y, x, y, Q^2, W^2, x_F, etc.
3. IDENTIFY π^0's and η's. DETERMINE RESONANCE PRODUCTION: ω, ρ, K^*, etc.
4. IDENTIFY SLOW PROTONS (≤ 1 GEV/c)
5. ACHIEVE CLEAN SAMPLES OF νn AND νp EVENTS BY REMOVING ~90% OF DOUBLE SCATTERS IN DEUTERIUM.
6. USE THE MULTIVARIANT DISCRIMINANT ANALYSIS (MDA) TO ACHIEVE EXCELLENT SEPARATION OF CC, NC AND HADRON BG WITHOUT DRASTIC CUTS WHICH INTRODUCE BIASES AND LARGE STATISTICAL LOSSES.

THE SNC together with the EMI, IPF and HRO make possible a program of neutrino physics which could not be approached with the bare bubble chamber.

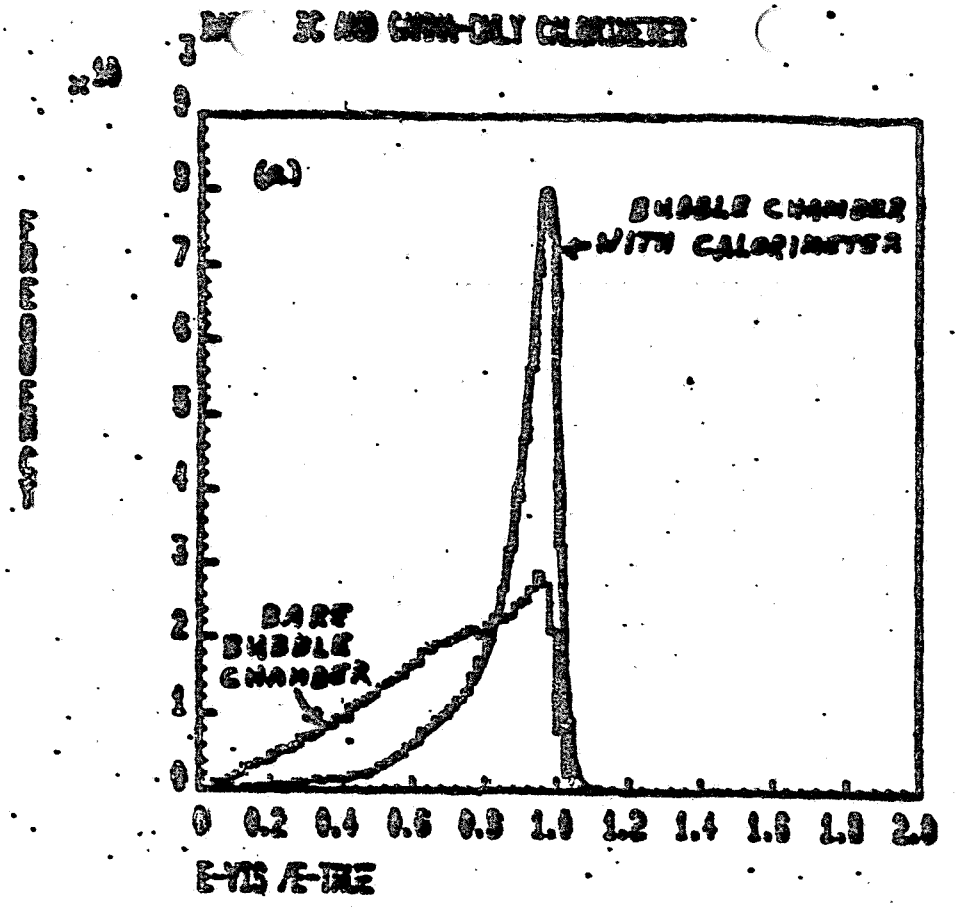
(a)
BUBBLE CHAMBER
WITH CALORIMETER
BARE
BUBBLE
CHAMBER
0 0.2 0.4 0.6 0.8 1.0 1.2 1.4 1.6 1.8 2.0

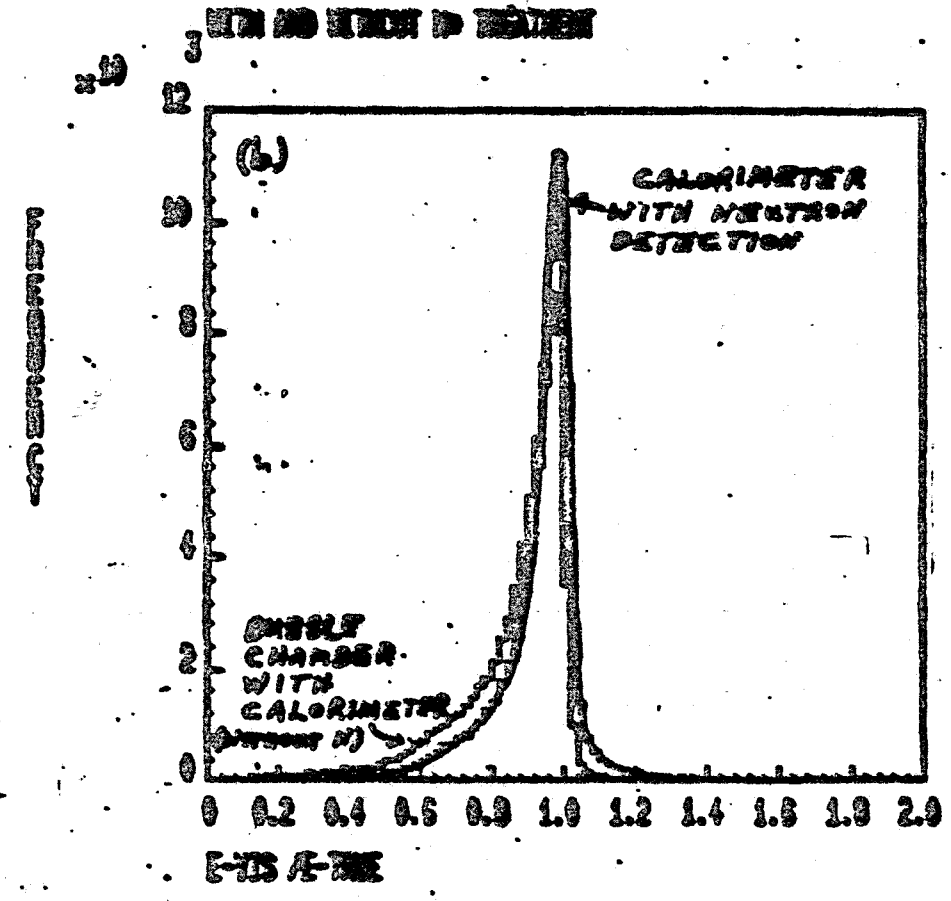
(b)
CALORIMETER
WITH NEUTRON
DETECTION
BUBBLE
CHAMBER
WITH
CALORIMETER
0 0.2 0.4 0.6 0.8 1.0 1.2 1.4 1.6 1.8 2.0

Fig. 5

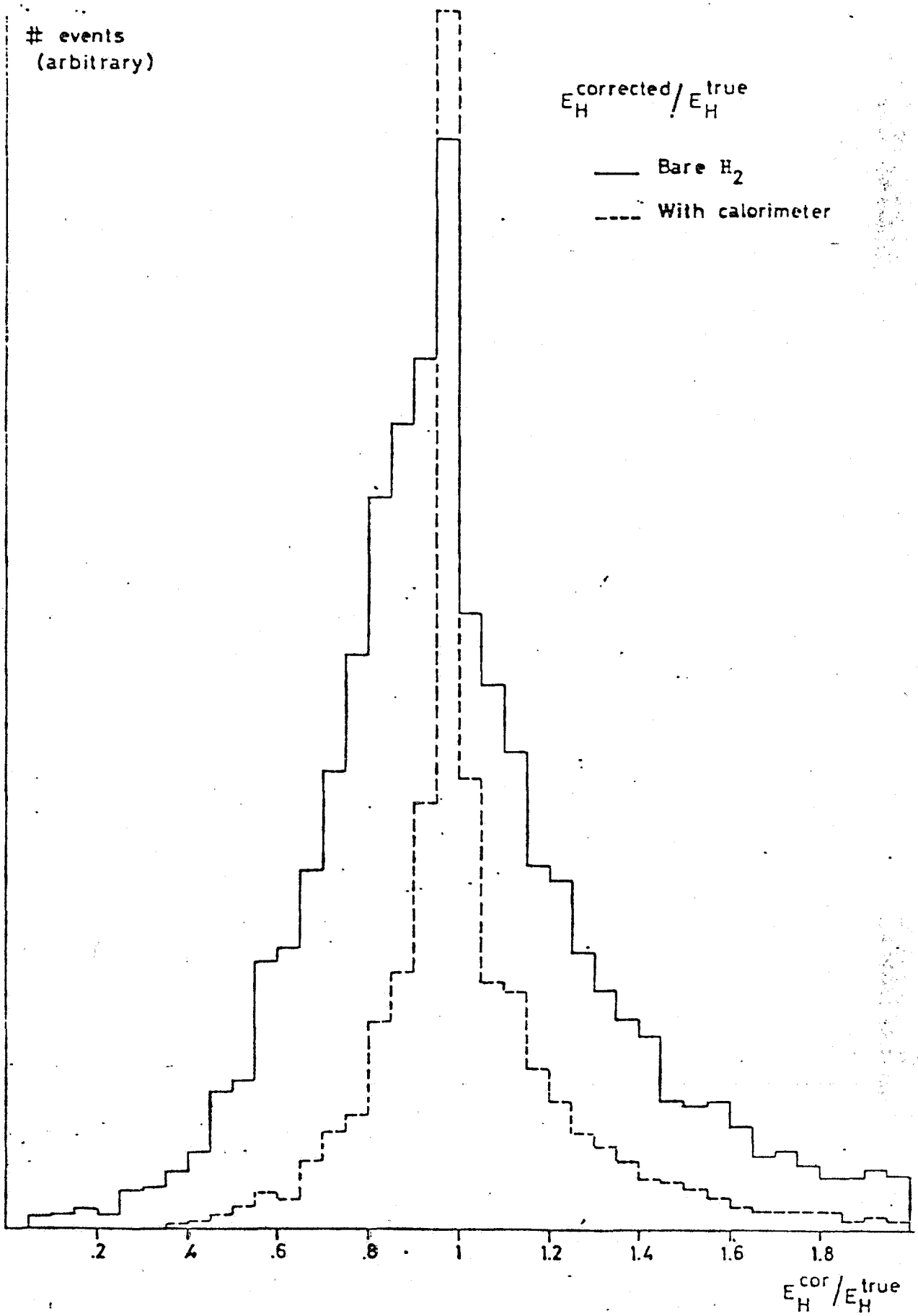
events
(arbitrary)
$E_H^{corrected}/E_H^{true}$
Bare H_2
With calorimeter
.2
.4
.6
.8
1
1.2
1.4
1.6
1.8
E_H^{cor}/E_H^{true}

Fig. 2

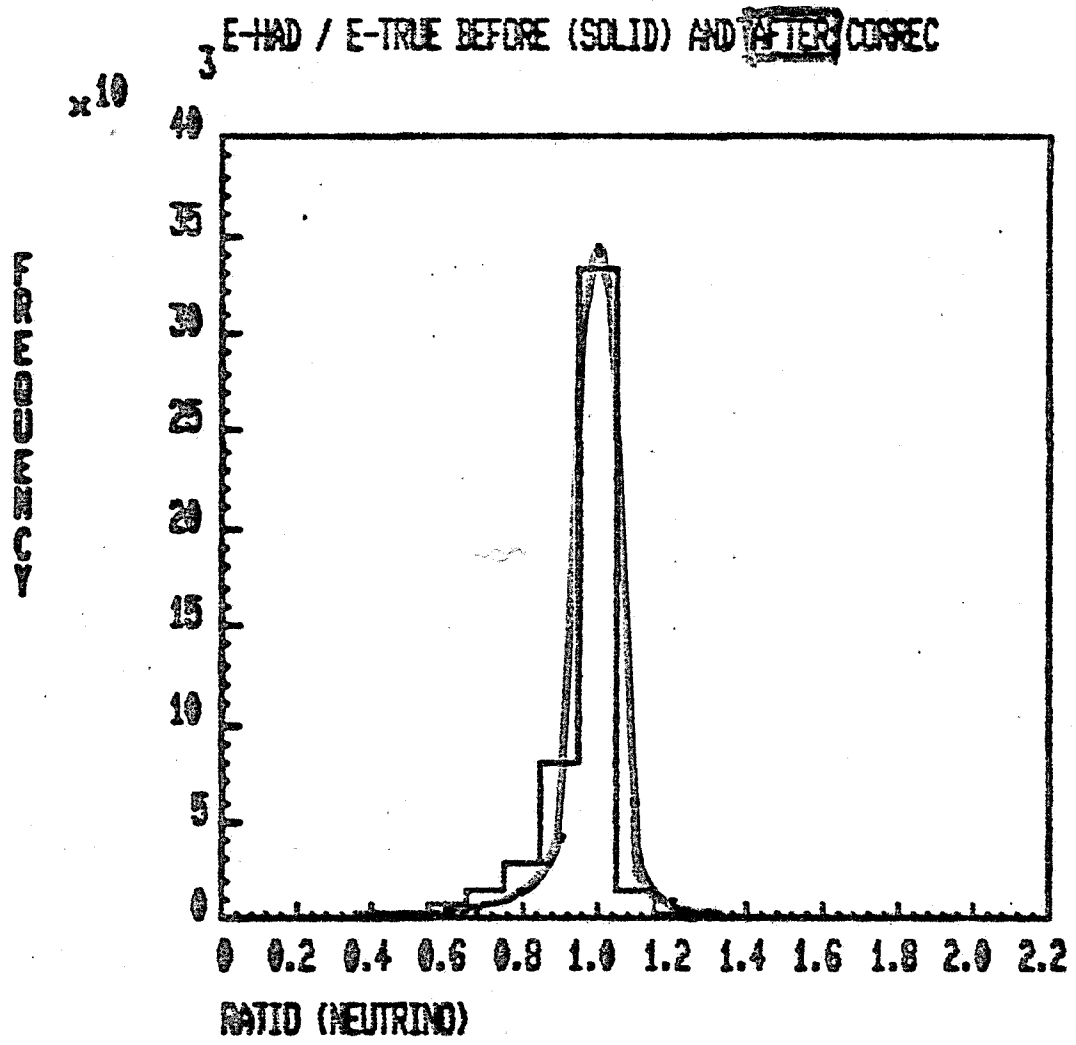
E-HAD / E-TRUE BEFORE (SOLID) AND AFTER CORREC
x10 3
40
35
30
25
20
15
10
5
0
FREQUENCY
0 0.2 0.4 0.6 0.8 1.0 1.2 1.4 1.6 1.8 2.0 2.2
RATIO (NEUTRINO)

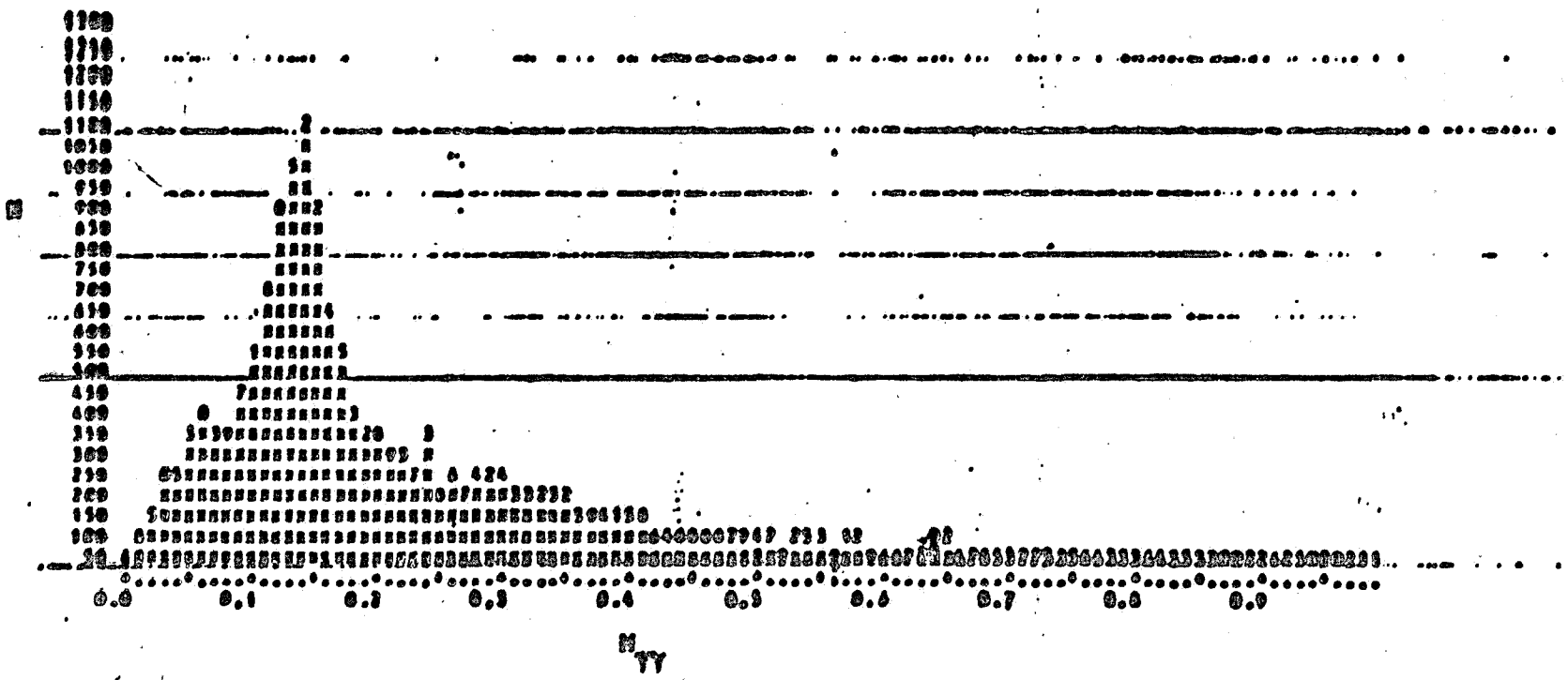

Fig. 4

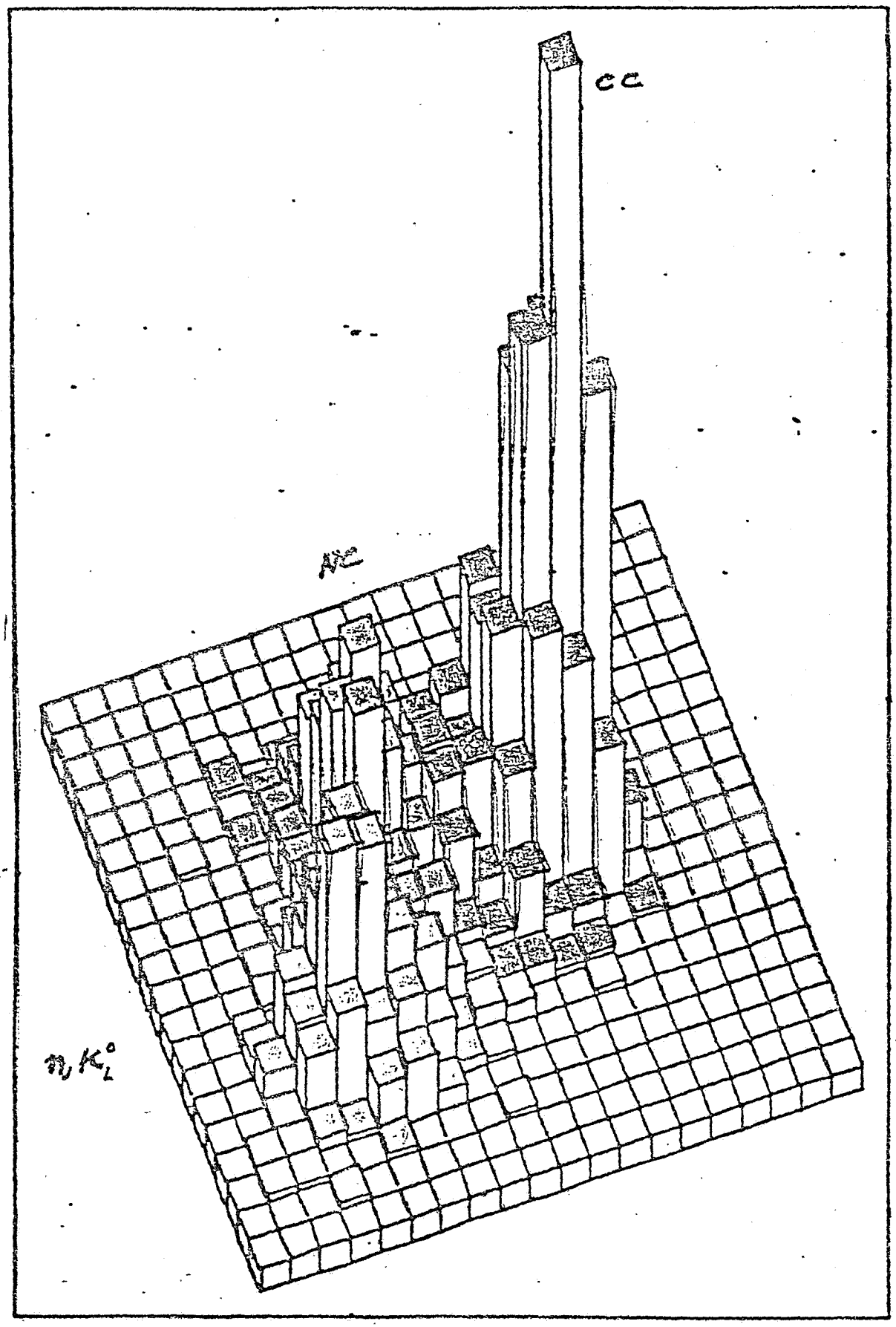

Fig. 12

Measuring $\sin^2\theta_W$

Llewellyn Smith has indicated 0.005 as precision needed in $\sin^2\theta_W$ to test higher order effects in Electroweak Theory.

Using $\sin^2\theta_W$ from $R_\nu = NC/CC$ gives

lowest order
$$\begin{cases} M_W = 78^{+2.7}_{-2.5}\ \text{GeV} \\ M_Z = 89^{+2.2}_{-2.0}\ \text{GeV} \end{cases}$$

radiative corrections plus second order mass formula
$$\begin{cases} M_W = 83.1^{+3.1}_{-2.8}\ \text{GeV} \\ M_Z = 93.8^{+2.5}_{-2.2}\ \text{GeV} \end{cases}$$

Errors are due to errors in $\sin^2\theta_W$. 0.005 measurement reduces them to ~ 1 GeV clearly separating the 2 sets of values. Then measure M_W, M_Z to similar precision

Radiative corrections on $\sin^2\theta_W$ are of order ~ 0.008. Measure it to half this.

L. S. Hen shows there are no theoretical obstacles to determining $\sin^2\theta_W$ from ν scattering on an isoscalar target. For only $u, d, \bar{u}, \bar{d}$

$$\frac{NC}{CC} = R_\nu = \frac{1}{2} - \sin^2\theta_W + \frac{5\sin^2\theta_W}{9} + \frac{5\sin^2\theta_W}{9} r$$

$$r = \sigma_{cc}^{\bar{\nu}} / \sigma_{cc}^{\nu}$$

Corrections for contributions of strange sea, charmed sea all deviations from QCD parton model all < 0.005.

In this experiment using MDA we can measure $\sin^2\theta_W$ to ~ 0.007. Purely a statistical limit. Double the experiment $\rightarrow$ 0.005.

Neutral Current Coupling Constants

Standard Model defines them precisely:

$$u_L^2 = (\tfrac{1}{2} - \tfrac{1}{3}\sin^2\theta_W)^2$$
$$d_L^2 = (\tfrac{1}{2} - \tfrac{2}{3}\sin^2\theta_W)^2$$
$$u_R^2 = (\tfrac{2}{3}\sin^2\theta_W)^2$$
$$d_R^2 = (\tfrac{1}{3}\sin^2\theta_W)^2$$

Van Doninck + collaborators at Brussels have carried out extensive Monte Carlo simulations since our proposal was submitted. They show that in order to make really significant improvement one needs not only R_ν and $R_{\bar{\nu}}$, but the π^+/π^- ratio in NC interactions.

Problem with π^+/π^- is proton contamination in π^+. However π^0/π^- is just as good. Calorimeter will do π^0 very well.

Pions should be in current region. Advantage of Tevatron - high W gives good separation of target and current region. How well we can separate them still to be studied via Monte Carlo simulations.

These slides (A to J) from P. Villain, Brussels.

Present data 1983 including current WA25 (BEBC D_2) WBB (D_2 stat. only!) $4\ 10^{18}$, $1.2\ 10^{18}$ (

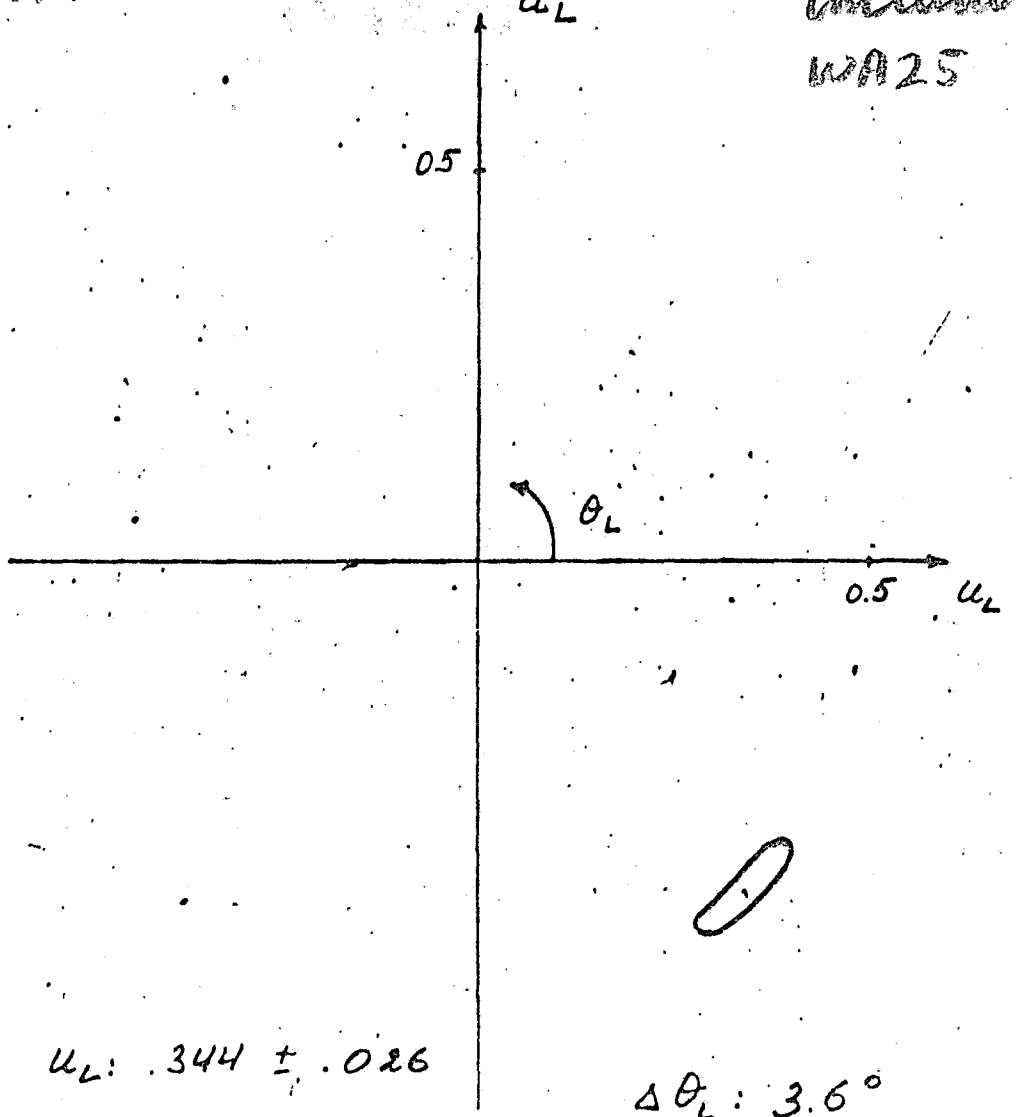

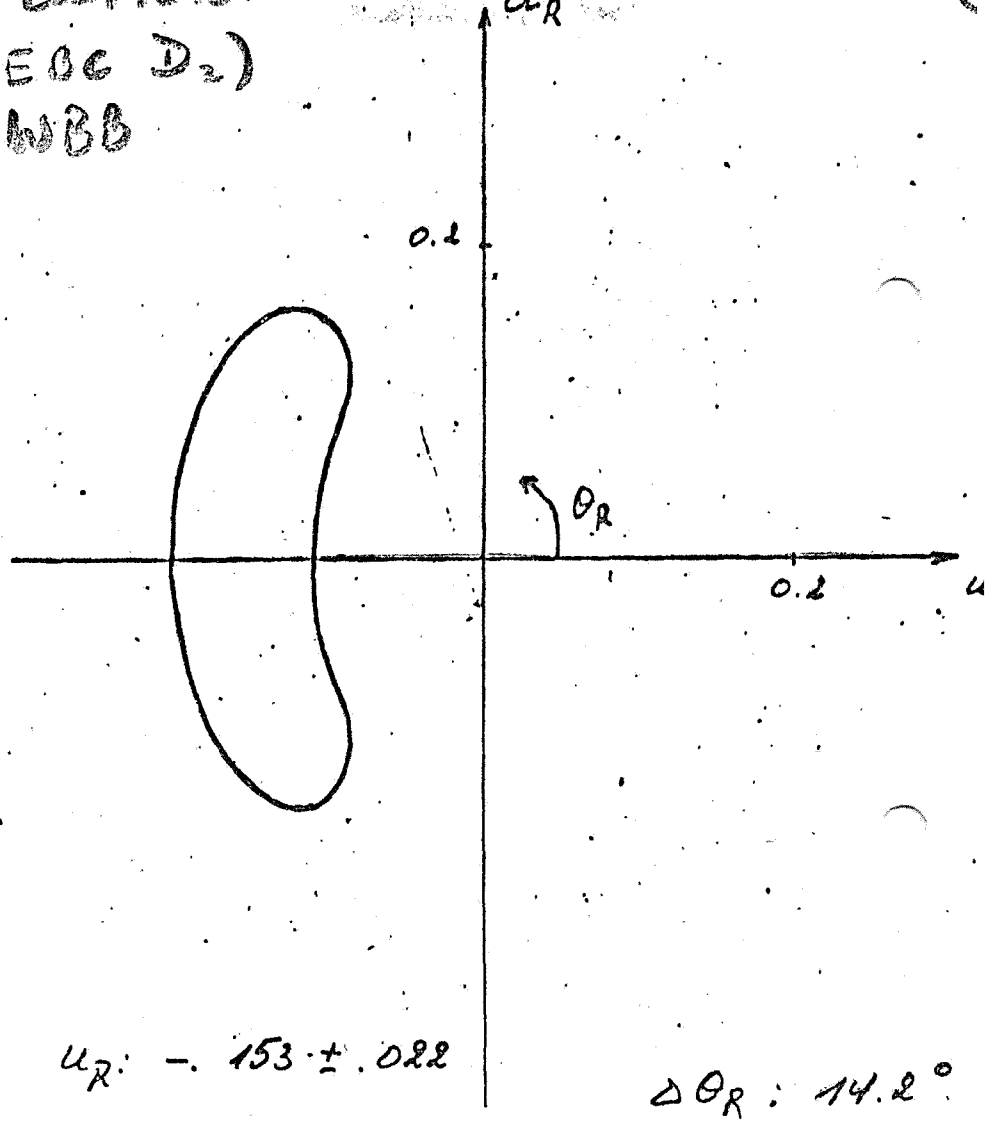

u_L: .344 ± .026

α_L: −.419 ± .022

$\Delta\theta_L$: 3.6°

u_R: −.153 ± .022

α_R: .076 ± .041

$\Delta\theta_R$: 14.2°

Present data

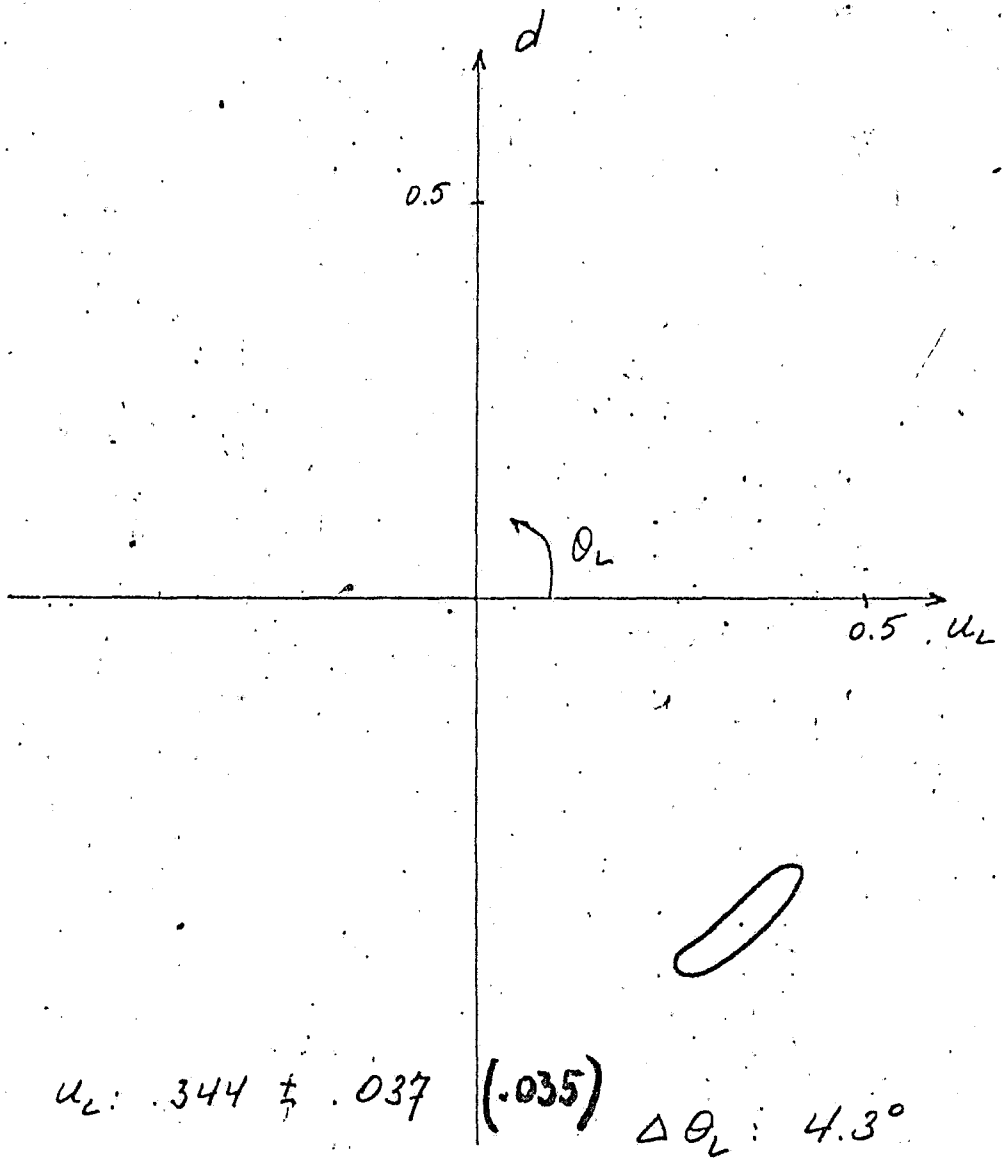

u_L: .344 ± .037 (.035) $\Delta\theta_L$: 4.3°

d_L: -.418 ± .031 (.029)

same as (A) but π^+/π^- removed (GGM); (only GGM PS removed

(B)

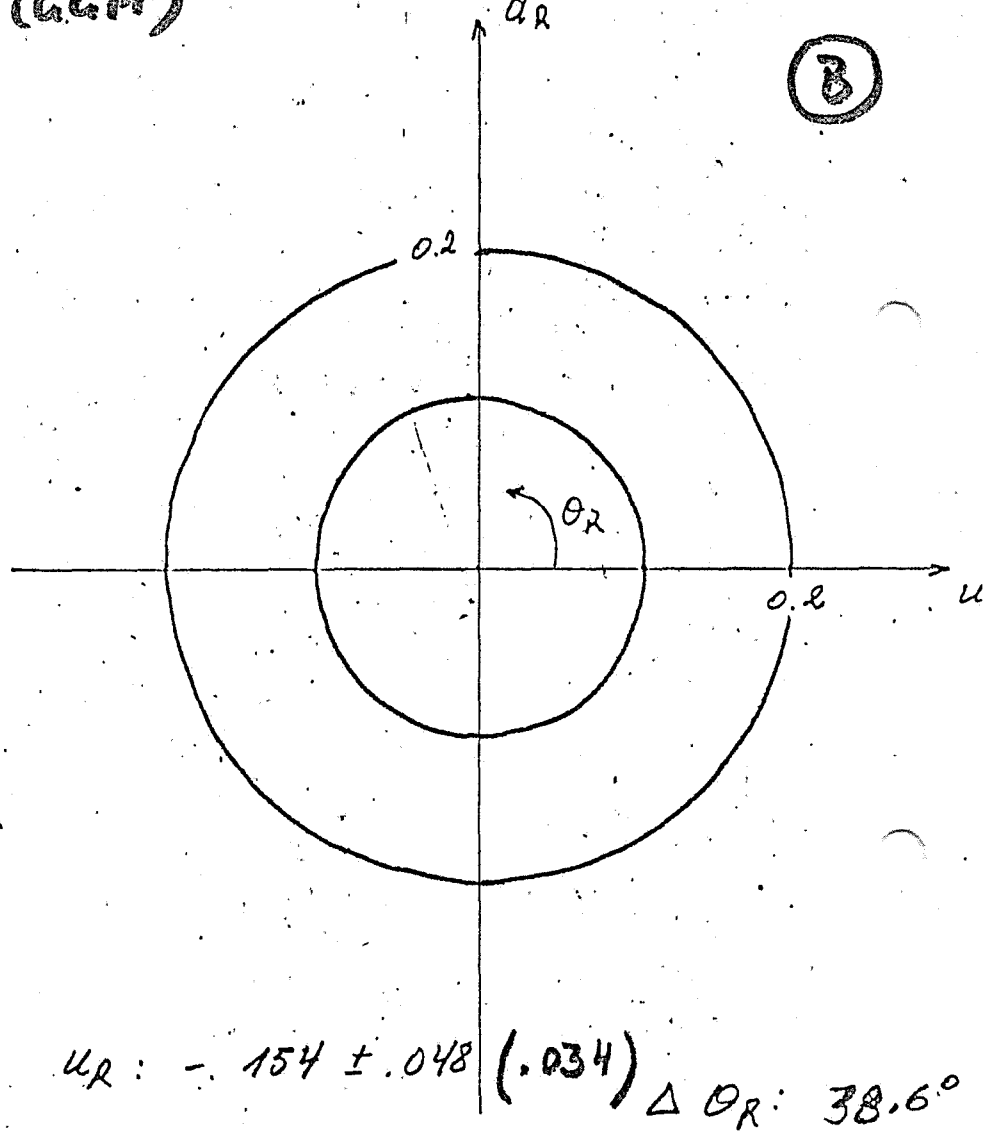

u_R: -.154 ± .048 (.034) $\Delta\theta_R$: 38.6°

d_R: .076 ± .099 (.069) (26.

(without π^0/η corr ps) ©

Data by 1985? (4x D_s without systematics!)

R_p { v .03 .08 .015
v .04 .020

R_n { v .02 .01 .010
v .10 .050

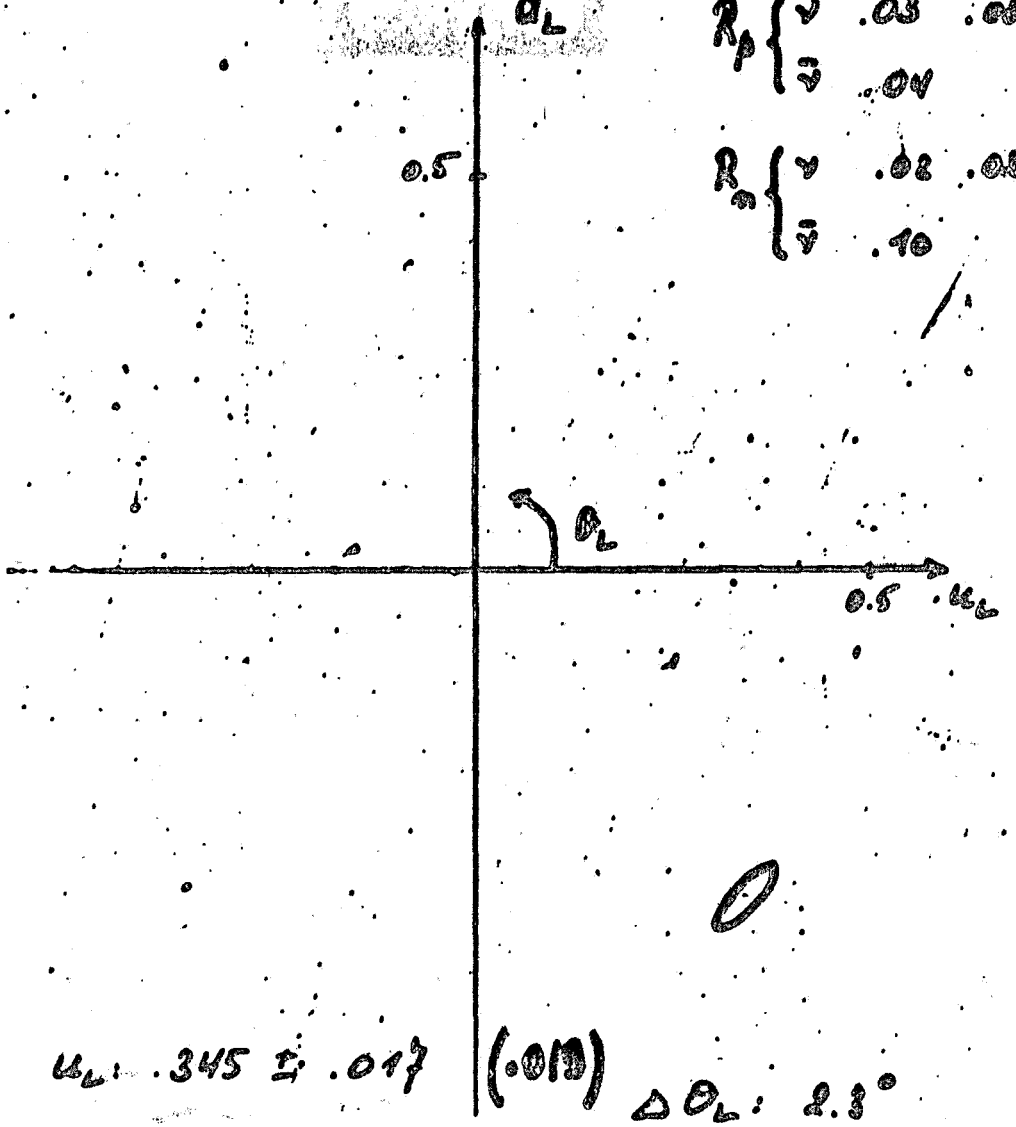

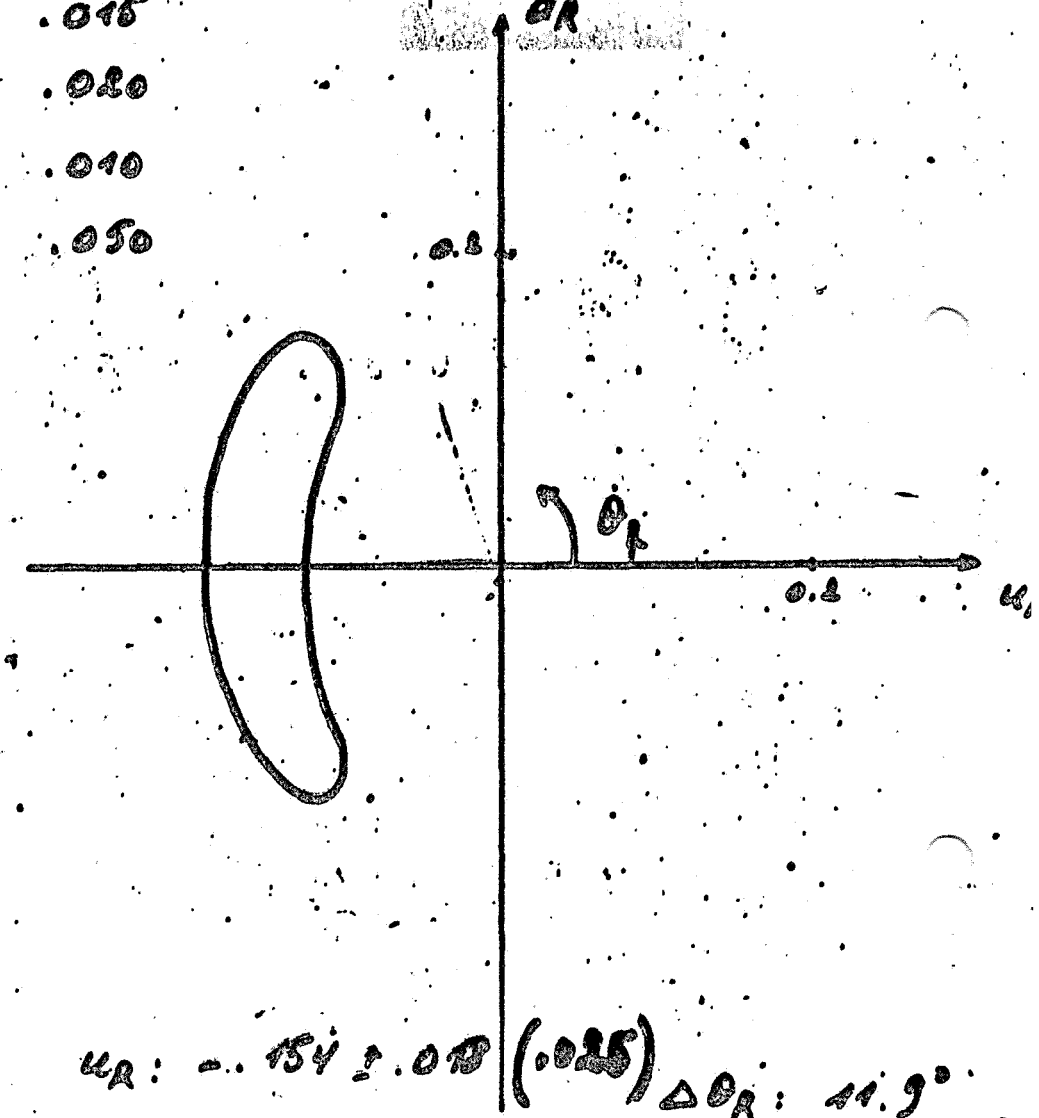

u_L: .345 ± .017 (.013) $\Delta\theta_L$: 2.3°

d_L: -.420 ± .015 (.016)

u_R: -.154 ± .018 (.025) $\Delta\theta_R$: 11.9° (18.9°)

d_R: .078 ± .015 (.009) "

D.I.S. ($\bar{x}=0$) +

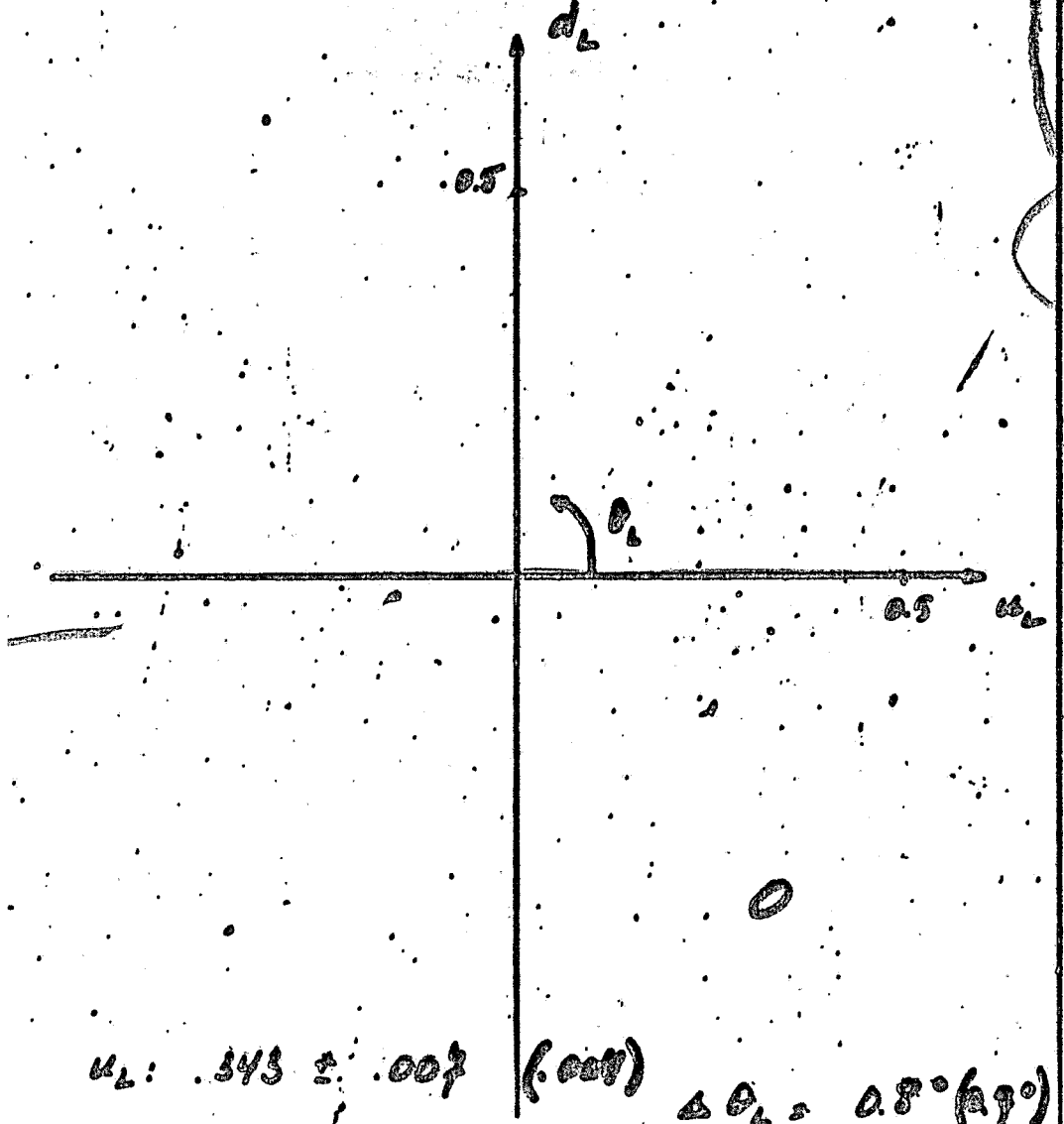

u_L: .343 ± .004 (cm) $\Delta\theta_L$ = 0.8° (typ°)

d_L: -.421 ± .006 (cm)

P36 only ($2\nu\beta\beta$; $4\nu\beta^-\bar{\nu}$) (+NB 2ν)

↑ BEBC NBB+cal

$R_e^{\nu,\bar{\nu}}$, $R_m^{\nu,\bar{\nu}}$ WBB

D2

NBB + cal. → x, y analyse

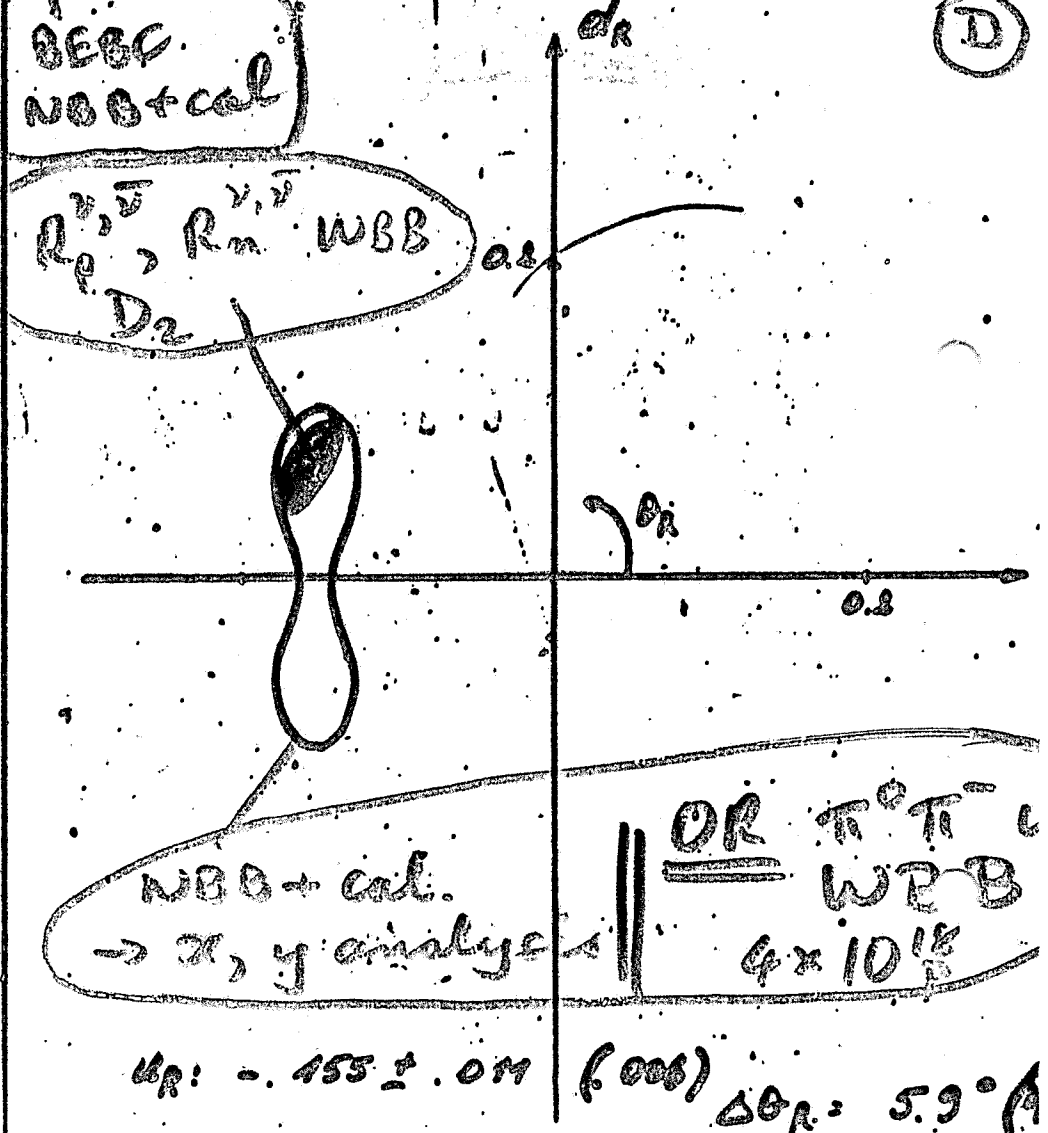

OR $\pi^0\pi^-$ WBB 4×10^{15}

u_R: -.455 ± .011 (cm) $\Delta\theta_R$ = 5.9° (

d_R: .077 ± .013 (cm)

Structure Functions

Some day (?) theorists will tell us how a nucleon is made of quarks and gluons.

The EMC Effect tells us that in order to verify this theory we are going to have to measure structure functions and parton distributions on nucleons, not on nuclei. ν and $\bar{\nu}$ experiments on hydrogen and deuterium targets are a vital part any program to do this.

Interesting things we can do now

1. The ratio $d(x)/u(x)$ from νn and νp, particularly as $x \to 1$.

QCD $d/u \to 0.2$

isospin + SU(6) sym. breaking $\to 0$

a certain diquark model $\to 0.27$

Improvement in smearing due to calorimeter should allow a 10-15% measurement at $x = 0.8$.

2. The sea, $\bar{u}(x), \bar{d}(x), s(x)$

$$\frac{d^2\sigma^{\nu p}}{dx\,dy} = \frac{G^2 M E}{\pi} 2x \left\{ u(x)(1-y)^2 + [\bar{d}(x) + \bar{s}(x)] \right\}$$

$$\frac{d^2\sigma^{\bar{\nu} p}}{dx\,dy} = \frac{G^2 M E}{\pi} 2x \left\{ d(x)(1-y)^2 + [\bar{u}(x) + \bar{s}(x)] \right\}$$

$$\frac{d^2\sigma^{\nu n}}{dx\,dy} = \frac{G^2 M E}{\pi} 2x \left\{ \bar{u}(x)(1-y)^2 + [d(x) + s(x)] \right\}$$

$$\frac{d^2\sigma^{\bar{\nu} n}}{dx\,dy} = \frac{G^2 M E}{\pi} 2x \left\{ \bar{d}(x)(1-y)^2 + [u(x) + s(x)] \right\}$$

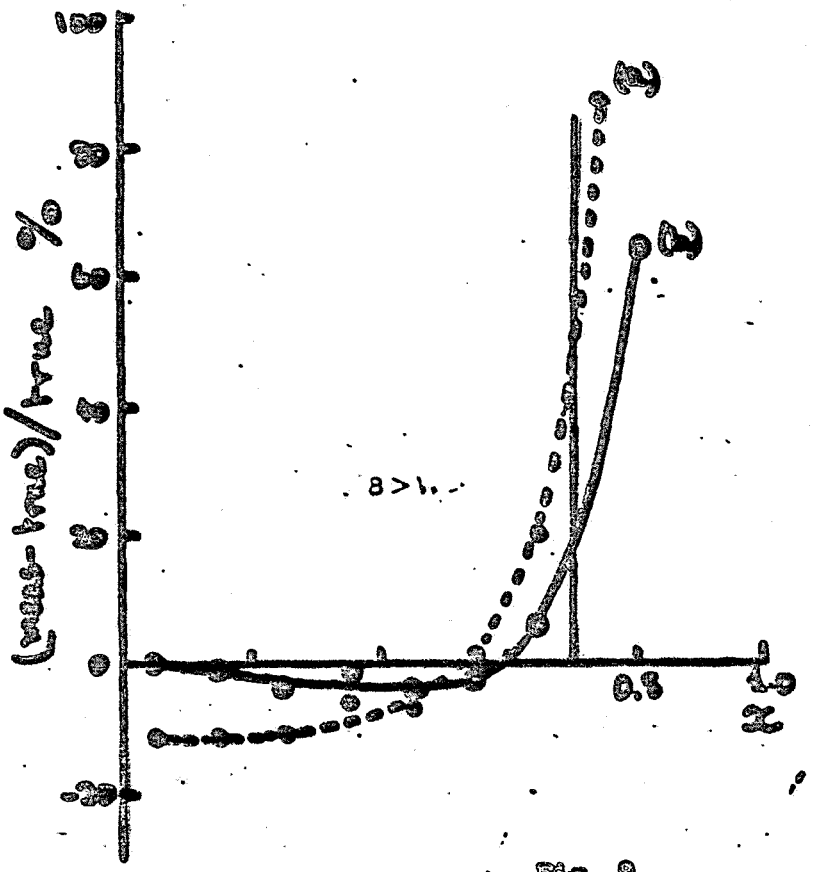
(meas-true)/true %
10
8
6
4
2
0
-2
0.5
1.0
x
(a)
(b)

Fig. 9

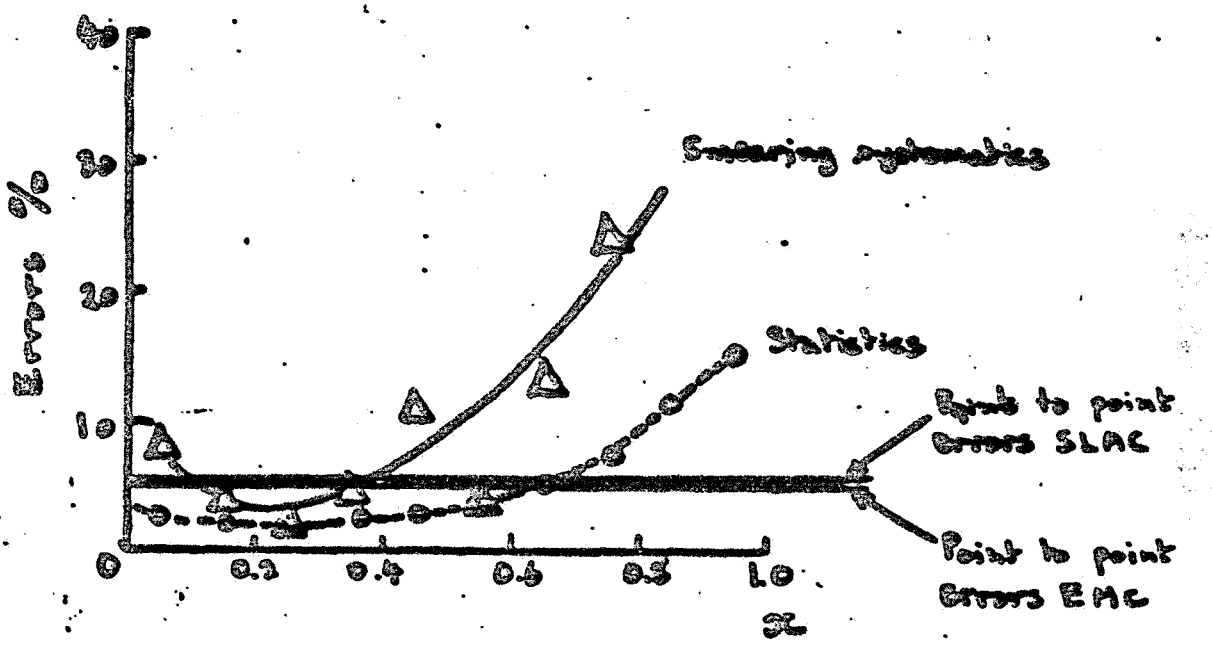
Errors %
30
20
10
0
0.2
0.4
0.6
0.8
1.0
x
Smearing systematics
Statistics
Bjork to point Errors SLAC
Point to point Errors EMC

Fig. 10

Does $\bar{u} = \bar{d}$? How big is $\bar{s}$ compared to $\bar{u}$ and $\bar{d}$. Accuracy?

Present νd exp. gives

$$\bar{d} + \bar{s} = 0.034 \pm 0.004$$
$$\bar{u} + \bar{s} = 0.021 \pm 0.003$$

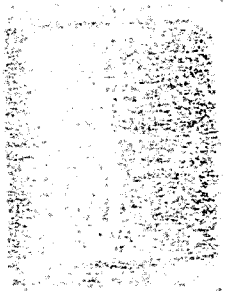

with SMC using MDA we will have better acceptance, less bias, and will do better. Also less smearing in y and essentially no double scattering contamination in γp.

QCD Effects

Higher, wider range of W^2, Q^2 of Tevatron and better resolution with SMC.

Repeat Q^2 evolution analysis of structure functions.

Look at gluon bremsstrahlung effects, such as p_t^2 widening of forward jet with W^2.

Look for higher twist effects: low Q^2, high x.

CHARM and BEAUTY

HRO + SNC + EMI gives ideal charm and beauty detection.

See the charm decays HRO

Get the electronic decays SNC

Get the muonic decays EMI

Get the nonleptonic neutral decay modes SNC

Beautiful signal for beauty

Two leptons from the $\bar{B}$ primary vertex plus a visible charm decay.

THE HADRONIC FINAL STATE

A MYRIAD OF VERY INTERESTING PHYSICS TOPICS FROM FRAGMENTATION FUNCTIONS TO DIQUARKS. SEE OUR PROPOSAL.

COST of CALORIMETER

Based on estimate prepared by BEBC group at CERN.

3 calorimeter modules (boxes)	$ 350,000
Interior Structures (insulation, cooling loops, lead and copper plates etc)	$ 400,000
Modifications to 15' chamber	$ 125,000
Cryogenics and controls	$ 125,000
Test-runs etc	$ 150,000
Electronics (5,100 channels @ $100/channel)	$ 510,000
Total	$ 1,660,000

Assumes no extra neon
no new dewar
much of design "in-house"
no inflation

Resources for Development.

① Rutherford Laboratory

— Cryogenics and Physics Apparatus Groups want to contribute to project.

— Have built bubble chambers and superconducting magnets.

— Prepared to tackle preliminary studies and outline cryogenic design in autumn 1983.

— Will have manpower for detailed design work at end of 1983.

— Can, in principle, supply technical personnel on 6mo to 1year secondment to instal and test.

— NEED APPROVAL FROM PAC TO PERSUADE THEM IT IS WORTHWHILE.

— AND TO CONVINCE OTHER U.K. GROUPS (I.C. LONDON, BIRMINGHAM) TO JOIN COLLABORATION.

— U.K. RESOURCES DEPEND UPON

(2) Ecole Polytechnique

- Very keen to develop electronics.
- Strong design group — have already investigated prototype readout system for calorimeter — now being adapted for a LEP experiment. (Also designed and developed LeCroy's CAB)

(3) Wes Smart has joined the collaboration

If any large part is built in U.K., France etc. then would expect that country to bear most of the cost (of that part)

Present collaboration could raise about ½ total cost.

For an approved experiment we expect to find more strong collaborators to share costs.

- Last year I said "approve us or we withdraw."

- Why am I here again? Especially since we cannot run before 1987.

- Two reasons

a) We asked Fermilab for money to help support R&D. They haven't offered enough, but it has kept us talking.

b) CERN fixed target workshop revealed many more physics topics for P 651 and its successors.

- CERN is now reconsidering the calorimeter for BEBC. 14 labs, including our collaboration and members of 632, are interested.
- Whether or not CERN goes ahead there will be a programme for the 15' chamber with calorimeter.

— Advantages of BEBC at CERN

a) Could run early in 1986

b) May wish to do large ν_e experiment at same time in WBB.

c) Repetition rate at 450 gev allows us to think of $\sim 1.5 \times 10^{19}$ protons over a 3 year period.

BUT LEP is coming, and CERN wants the BEBC resources for other things.

— Advantages of 15' at FNAL

a) Higher energy for high W^2 Physics, charm, beauty etc.

b) May eventually be able to get high statistics too with 150 Gev, 3 second cycle (if 15' can be made to cope).

c) Unique beam-dump facility being built. Our proposal 700 would match this with unique ν_e analysis (see last year's PAC presentation).

BUT Earliest scheduled run cannot be before 1987. <u>APPROVAL will make it look closer.</u>

P 651

SOLID NEON CALORIMETER — SNC

\+ 15' BUBBLE CHAMBER

\+ TEVATRON & HORN BEAMS, ν & "$\bar{\nu}$" — IDF

\+ INTERNAL PICKET FENCE

\+ EXTERNAL MUON IDENTIFIER — EMI

\+ HIGH RESOLUTION OPTICS (HOLOGRAPHY) — HRO

COLLABORATION

IIT
TUFTS
FERMILAB
} USA

U.C. LONDON
• I.C. LONDON
• BIRMINGHAM
} U.K.

(WITH R.A.L. ENGINEERS)

ECOLE POLYTECHNIQUE — FRANCE

• BOLOGNA — ITALY

\+ OTHERS .....

SPOKESMAN J.J. MILLER U.C. LONDON

CO-SPOKESMAN J. SCHNEPS TUFTS

SOLID NEON CALORIMETER

FOR DETAILS SEE FEB. 1983 VERSION OF P651
TEST RESULTS IN N.I.M. 215 p79 (1983)

SCHEMATIC DRAWING BY RUTHERFORD ENGINEER →

ALLOWS FIDUCIAL VOLUME OF 11 m^3
→ 1.5 TONS OF D_2

~5000 READOUT CHANNELS

SEGMENTED IN DEPTH ~5 LAYERS
FOR PARTICLE I.D.
e/π , π/μ
γ FROM CHARGED TRACKS
π OR K_L (~1.8 COLL. LENGTHS)

AND SIDEWAYS — MOSTLY STRIPS
~2cm wide
SOME PADS TO RESOLVE AMBIGUITIES.

ENERGY RESOLUTION ON E.M. SHOWERS
$\sim \pm \frac{13\%}{\sqrt{E}}$ (c.f. LIQUID ARGON)

ENERGY OF HADRONS IS NOT WELL MEASURED
BUT POSITION AND IDENTIFICATION IMPORTANT
FOR USING π AND K^0_L IN CC ANALYSIS.

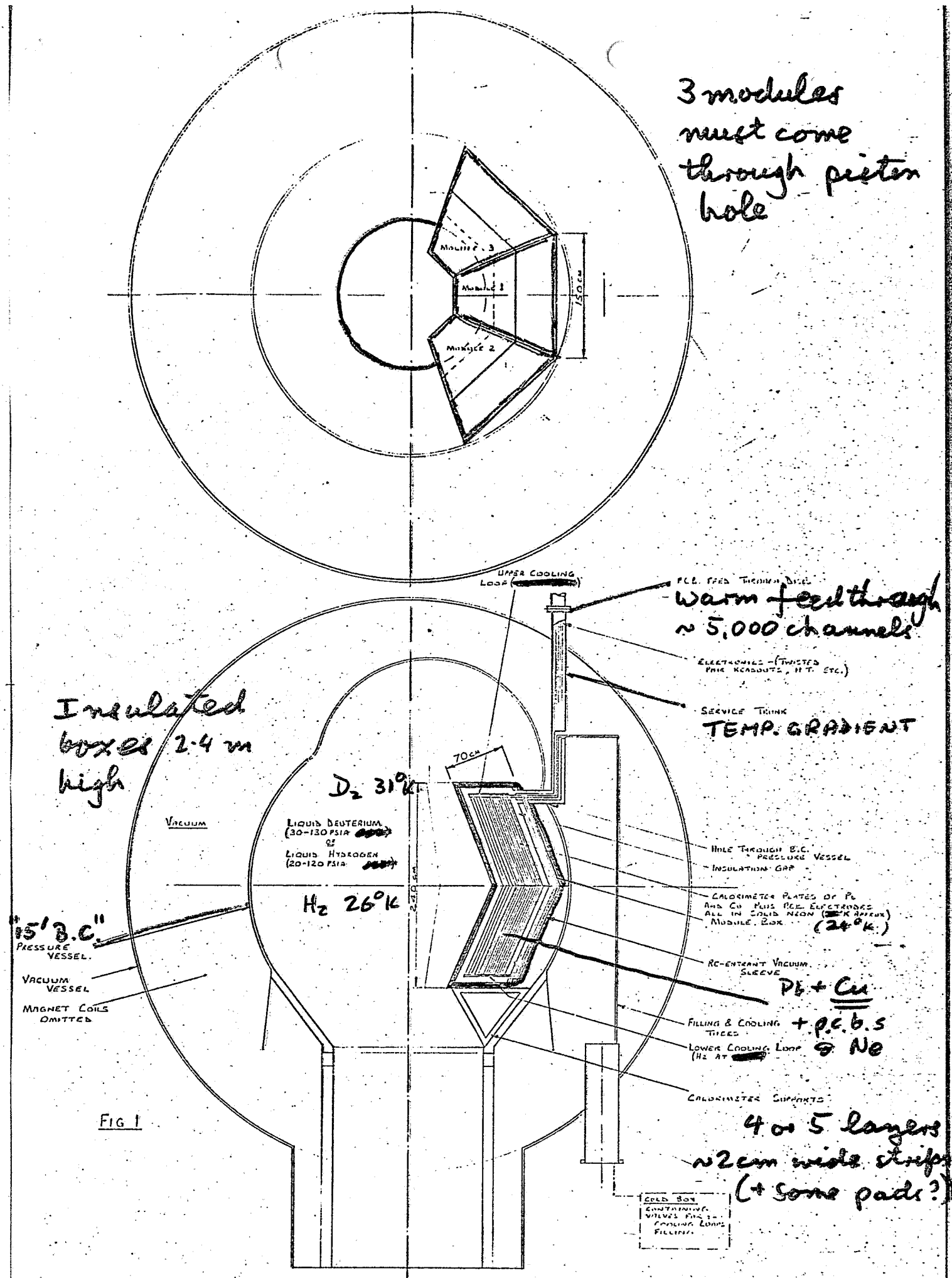

FIG 1

DIAGRAMMATIC LAYOUT OF SOLID NEON CALORIMETER

MOUNTED IN THE FERMILAB 15FT BUBBLE CHAMBER

BUILDING THE CALORIMETER

DOCUMENT AVAILABLE "OUTLINE OF PROGRAMME"

- ASSUMES MAJOR DESIGN OF BOX, CONTENTS ETC. DONE BY R.A.L. ENGINEERS
- MODIFICATIONS TO CHAMBER, SAFETY ASPECTS MUST BE HANDLED BY FNAL. (K & S THE RIGHT MEN — BUT THEY NEED PEOPLE).
- TIMESCALE

CONCEPTUAL DESIGN		MAY 1984
TEST WITH 1 MODULE IN CHAMBER	LIQUID SENSITIVITY CALORIMETER STABILITY MICROPHONY	1985
PHYSICS RUNNING		1987

- COST

DESIGN & TEST TO 1985	~$200,000
ELECTRONICS	~$ 500,000
OVERALL TOTAL	~$ 1.6 M.

TO GET U.K. DESIGNERS AND KEEP U.K. PARTICIPATION WE NEED STRONG SUPPORT FROM FNAL AND APPROVAL OF U.K. SELECTION PANEL ON DECEMBER 20TH.

COLLABORATORS CAN PROBABLY FIND ABOUT $100,000 PER LAB — IF APPROVED BY THEIR FUNDING AGENCIES

HORN BEAM

NUMBERS FROM MALBISKY & STUTTE

PAC ASKED WHAT WE COULD DO WITH

10^{18} p FOR ν IN H_2

" " $\bar{\nu}$ " H_2

" " ν " D_2

" " $\bar{\nu}$ " D_2

WE GAVE THE ANSWER*, BUT WE WOULD LIKE THESE 4×10^{18} p ON D_2 AS OUR FIRST CHOICE. TWO BIG RUNS OVER 2 OR 3 YEARS.

E.g. – EITHER (A) 2.15×10^{18} p $\nu D_2 \rightarrow$ 50,000 CC μ^-

and 1.85×10^{18} p $\bar{\nu} D_2 \rightarrow$ 11,200 CC μ^+ (+~11,000 CC μ^-)

– OR (B) 0.82×10^{18} p $\nu D_2 \rightarrow$ 19,200 CC μ^-

and 3.18×10^{18} p $\bar{\nu} D_2 \rightarrow$ 19,200 CC μ^+ (+~19,000 CC μ^-)

– ETC. ETC. (SOME νH_2 RUNNING?).

JUSTIFICATION FOR $1.7M PROJECT IS HIGH STATISTICS. ~80K EVENTS TO MEASURE.

WILL HAVE TO CHOOSE MOST IMPORTANT PHYSICS AT THE TIME OF THE RUN

(A) IS OPTIMISED TO MEASURE $\sin^2\theta_W$ to $\pm .005$

(B) WILL RESOLVE THE NC d_R COUPLING FROM ZERO

AND MEASURE $\bar{q}$ AND xF_3 (and F_2) ON NUCLEONS.

BOTH WOULD HAVE WELL RECONSTRUCTED CHARM, HIGHER TWIST TESTS, HIGH W^2 L^2, ETC. SEE PROPOSAL

RECOMPUTED RATES PER 10^{18} p ON TARGET

HORN BEAM. ATHERTON MODEL

AS CALCULATED BY MALENSEK & STUTTE

HAVE TAKEN — 11 m^3 OF FIDUCIAL LIQUID

— LAB B FLUX = 1.12 × LABC

	μ^- CC	μ^+ CC
νD_2	23,300	~1,200
"$\bar{\nu}$" D_2	~6,000	6,025
νH_2	7,000	~350
"$\bar{\nu}$" H_2	~3,000	3,400

	"WANTED" NC	"UNWANTED" NC
νD_2	7200	450
"$\bar{\nu}$" D_2	2200	1900
νH_2	2900	100
"$\bar{\nu}$" H_2	1000	1200

WHY A CALORIMETER ?

1. NC – CC SEPARATION

   USE MULTIVARIATE DISCRIMINANT ANALYSIS →

   SYSTEMATICS ON $R \sim 1\%$

2. p – π SEPARATION

   USE $\epsilon = \sum_i (E_i - P_{z_i}) - m_N$

   DISTRIBUTION.

   SYSTEMATICS ON $\frac{D}{ALL}$ TO 0.5%

3. KINEMATIC VARIABLES

   x, y, z_{vtx}. etc

   GREATLY REDUCES SMEARING →

MEASURES ENERGY EVENT BY EVENT IN A WIDE BAND BEAM

MULTIVARIATE ANALYSIS

DESCRIBED BY WA24 (JEBC+TST)

PHYS. LETTS. 123B, p448 (1983)

EACH EVENT CHARACTERISED BY A NUMBER OF VARIABLES :-

E.g. P_L LONGITUDINAL MOMENTUM OF EVENT

$P_\perp$ TRANSVERSE MOMENTUM OF EVENT

F_i FOR i^{th} TRACK (TO SELECT 'MUON')

$$= \frac{p_\perp^i \, p_{\perp_H}^i \, P_L^i}{\sqrt{\sum_{j \neq i} p_{\perp_H}^{j\,2}}}$$

(WHERE $p_{\perp_H}^i$ IS W.R.T. REST OF EVENT)

ϕ ABOUT ν DIRECTION BETWEEN 'MUON' AND REST OF EVENT.

etc. etc.

DISCRIMINANT ALGORITHM HAS DIFFERENT WEIGHTS FOR DIFFERENT VARIABLES.

INITIAL SETS OF CLEAN EVENTS ARE USED TO TUNE THE ALGORITHM

IN WA24 HAS - CLEAN CC FROM EMI

- NC' BY OMITTING μ FROM CLEANCE
- N^* FROM EVENTS FITTED TO π SCATTERING

OR neutral hadron EVENTS FROM π^0 RUN IN TST

IN PGS! WILL HAVE — CLEAN CC FROM EMI
— NC' BY OMITTING μ
— N^* FROM FITTED EVENTS

PLUS — NC EVENTS WITH NO μ CANDIDATE THROUGH CALORIMETER INTO IPF (GOOD FOR HIGH y)
— N^* FROM EVENTS IN SAME TIMESLOT AND DOWNSTREAM OF A 'WALL ON' (USING UPSTREAM IPF)

HAVING TUNED THE ALGORITHM THE THREE CATEGORIES OF EVENT ARE SEPARATED IN MULTIVARIATE SPACE.

SIMPLE EXAMPLE

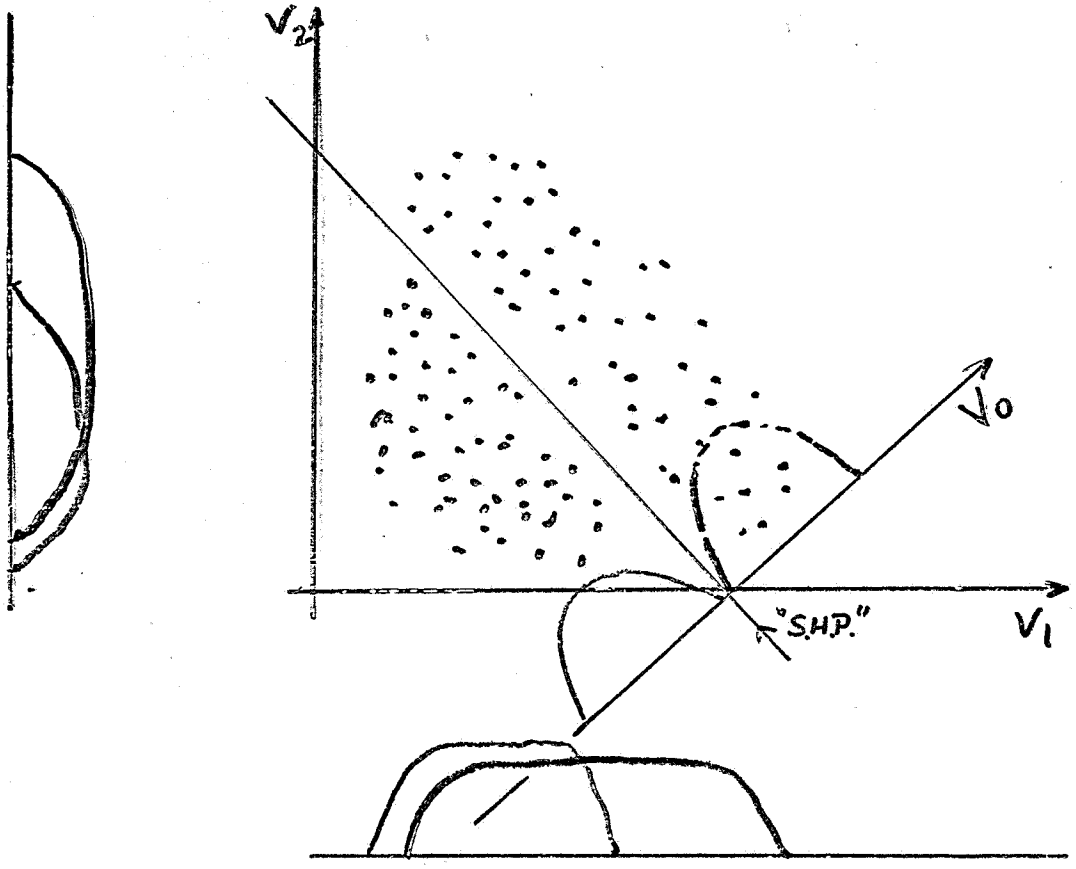

SHP ≡ SEPARATION HYPERPLANE

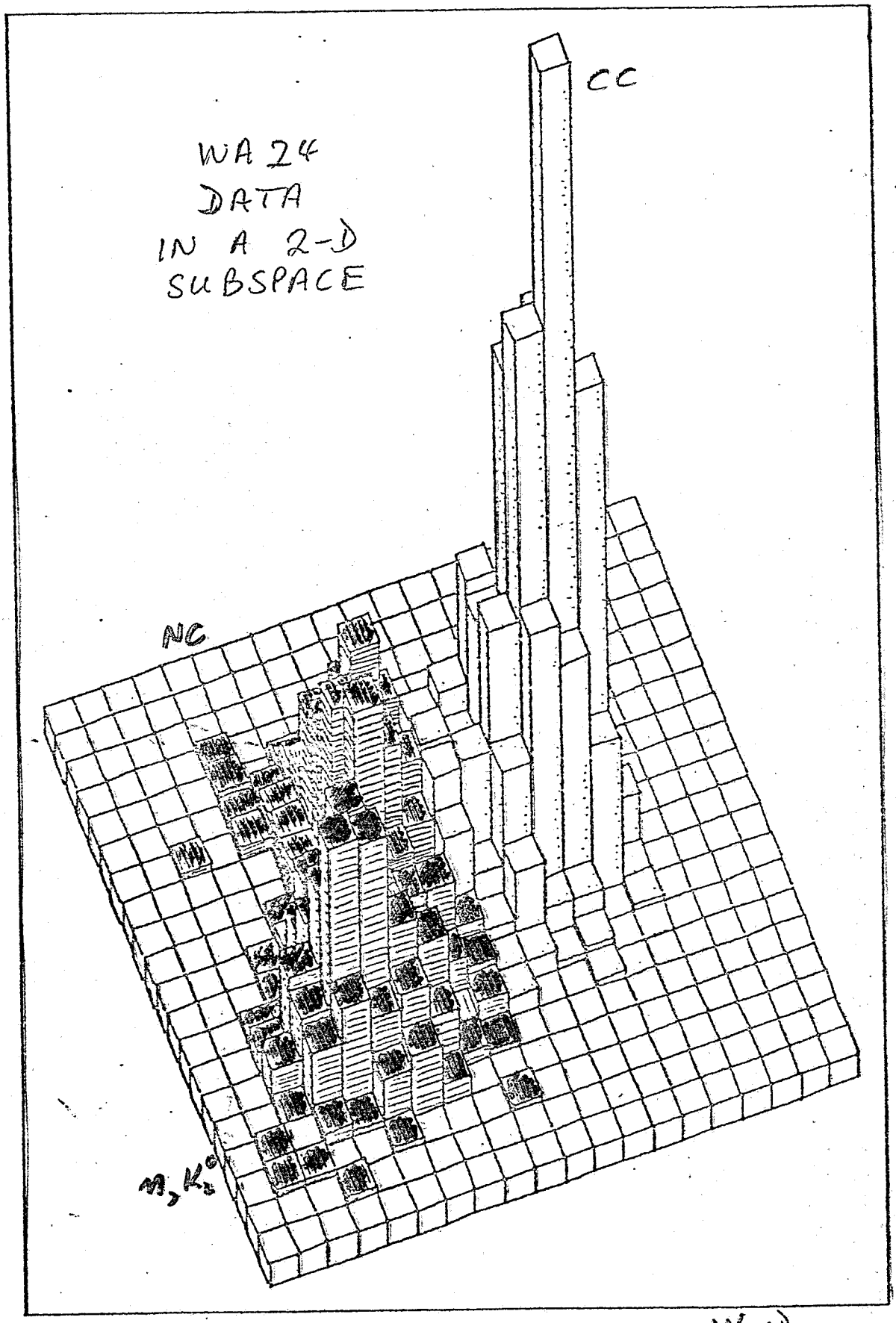

W.v.D.

WA 24

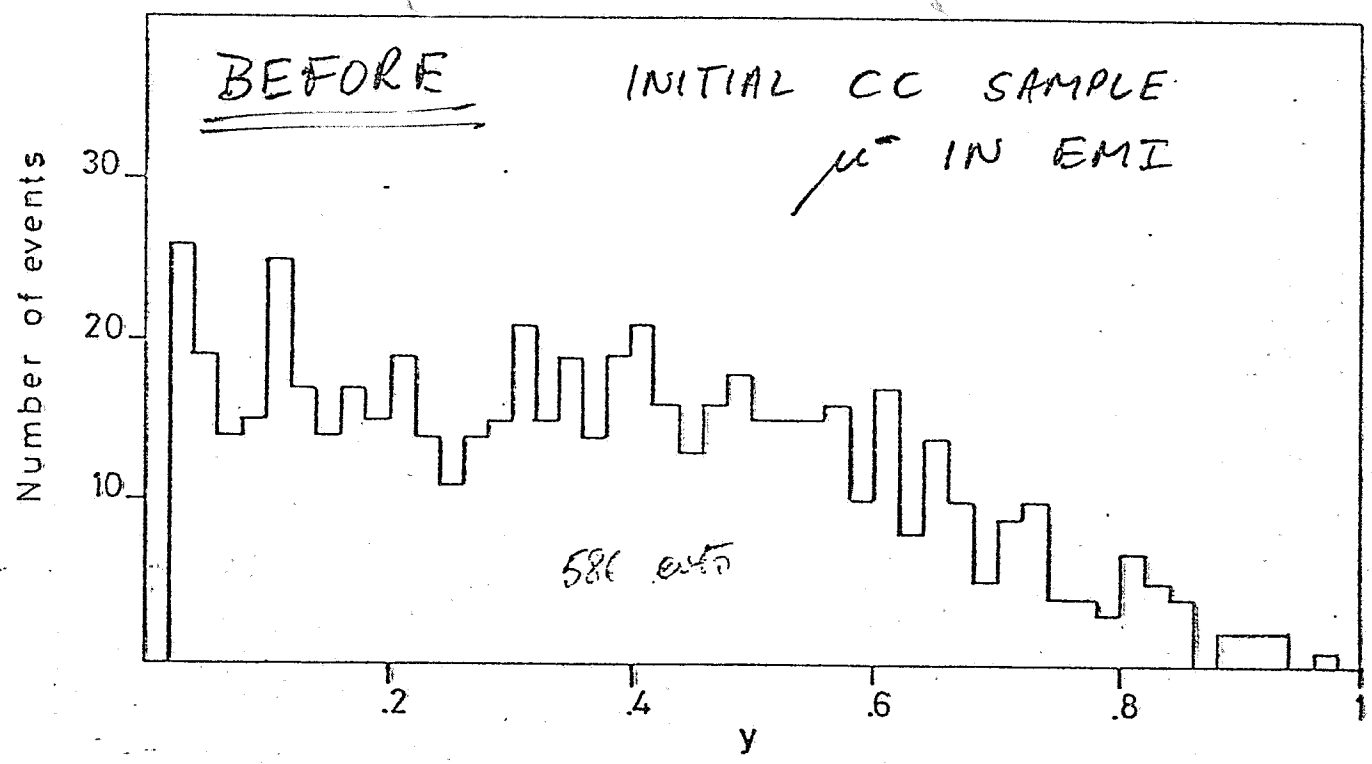

Fig. 4 a

Initial CC : μ^- in EM!

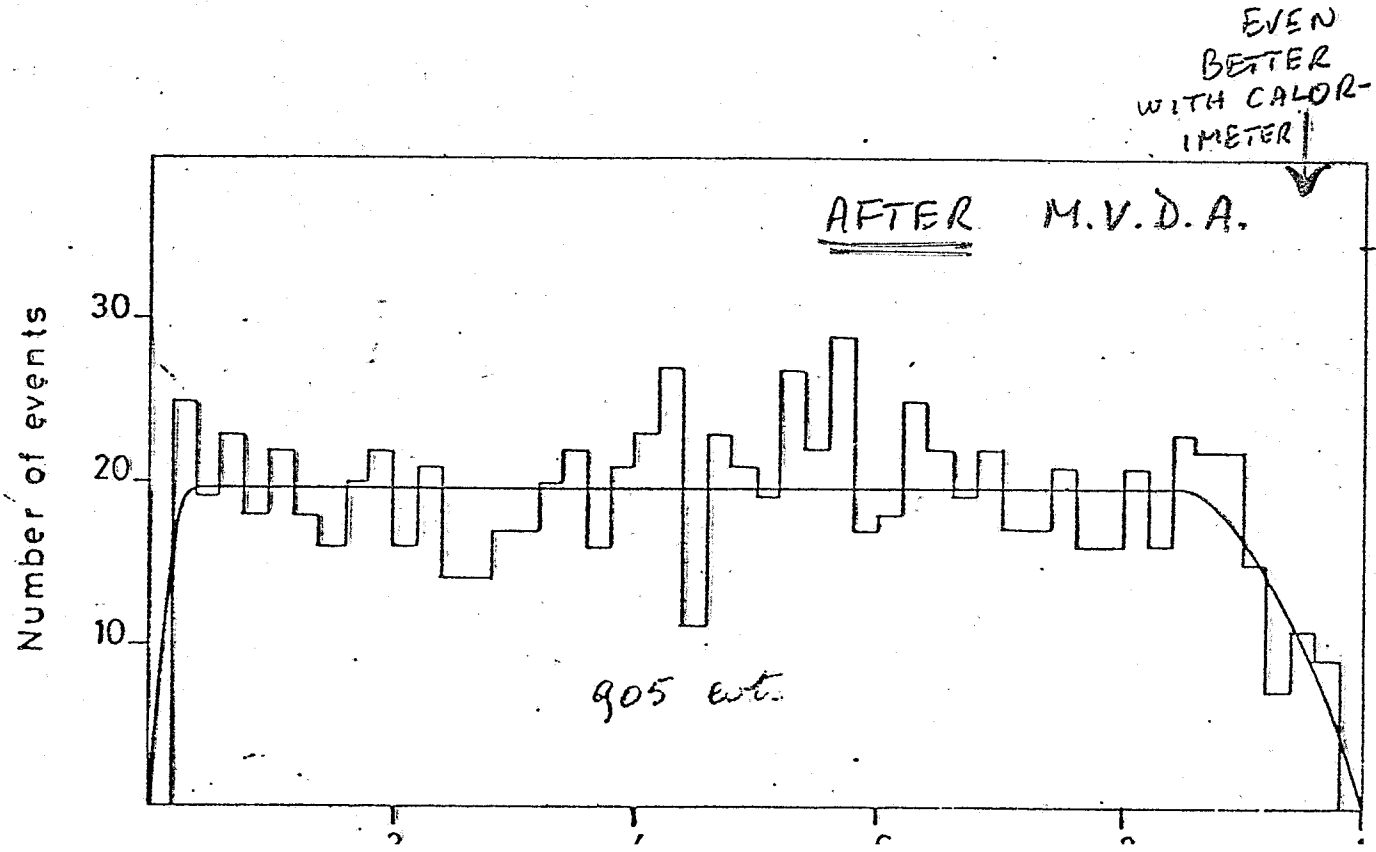

- MAXIMISE VARIANCE BETWEEN GROUPS
- MINIMISE VARIANCE WITHIN GROUPS. →

CONSISTENCY CHECKS SHOW THAT SEPARATION IS GOOD →

OVERLAP CORRECTIONS REMAIN W.D. DID MONTE CARLO STUDY OF OVERLAP

a) AGREED WITH WA24

$$\text{OVERLAP } \frac{(CC+NC)}{CC} = 8.7\%$$

b) OVERLAP WITH 'BARE' D_2 (NO CALORIMETER)

$= 14.8\%$

(HEAVY LIQUID SIMILAR. MANY PROBLEM EVENTS)

c) OVERLAP, D_2 + CALORIMETER

$= 2.1\%$

SYSTEMATICS ON SEPARATION

$$\left(\frac{\Delta R}{R}\right)_{syst} = \begin{array}{ll} 7.2\% & \text{BARE } D_2. \\ 0.8\% & D_2 + \text{Calorimeter} \end{array}$$

$$R = \frac{NC}{CC}$$

BONUS CAN SEPARATE CC DOWN TO VERY LOW P_μ. NO CUT NEEDED

$\therefore$ y DISTRIBUTION EVEN BETTER

$p-n$ SEPARATION IN ν_2

E 545 HAS DEVELOPED THE

VARIABLE $\epsilon_L = \sum_i (E_i - P_{L_i}) - m_N$

$-1 < \epsilon_L < +1$

WITH BARE CHAMBER THE ϵ DISTRIBUTION SHOWS SOME CLEAR DOUBLE SCATTERS

ON A "FREE" NUCLEON $-1 < \epsilon_L < 0$ →

WHY ?

a) ALL PARTICLES SEEN

$\sum_i E_i = E_\nu + m_{target}$

$\sum_i P_{L_i} = E_\nu$

$\therefore \epsilon = 0$ FOR 1 NUCLEON TARGET

$= 1$ FOR DEUTERON

b) FAST FORWARD γ OR ν MISSED

$E_i = P_{L_i}$ $\therefore \Delta\epsilon = 0$

c) SLOW PARTICLE MISIDENTIFIED

e.g. P called π

E_i TOO SMALL

$\Delta\epsilon$ <u>−ve</u>

d) SIDEWAYS (OR SLOW) PARTICLE MISSED, $E_i > P_{L_i}$ $(\Delta\epsilon$ −ve)

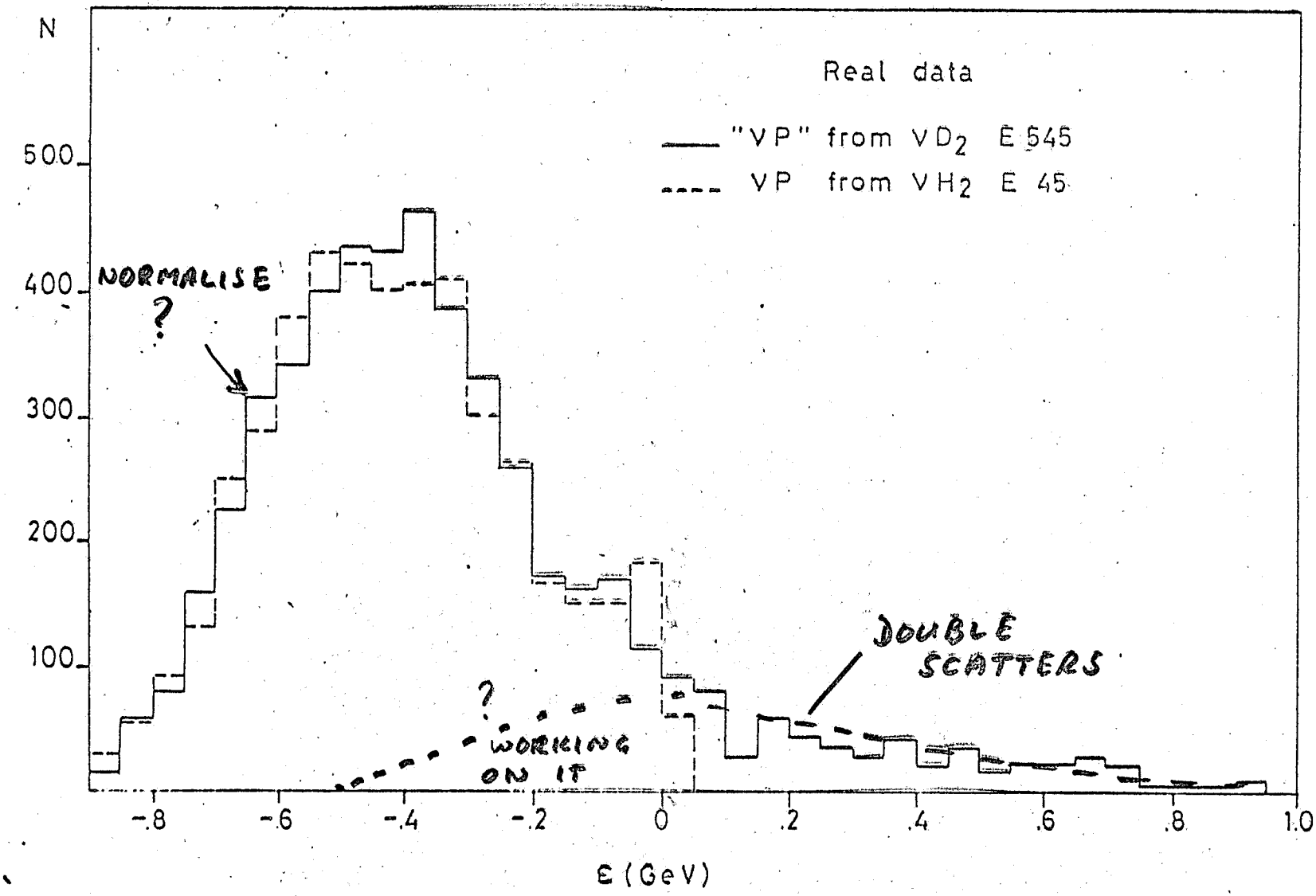
N
Real data
"VP" from VD_2 E 545
VP from VH_2 E 45
500
400
300
200
100
NORMALISE
?
DOUBLE SCATTERS
?
WORKING ON IT
-.8
-.6
-.4
-.2
0
.2
.4
.6
.8
1.0
E (GeV)

Fig. 5

CURRENT UNCERTAINTY ON AMOUNT OF DOUBLE-SCATTERING ~ ±3%

<u>BUT</u> – E 545 & WA25 BOTH WORKING ON IT.

– WA25 WILL BE ABLE (FROM WILLING) TO CROSS-NORMALISE TO WA 21 (BEBC H_2)

WITH CALORIMETER WE WILL LOOSE FAR FEWER LOW ENERGY γs. ALSO SEE π^0 & K^0_L. EXPECT TO GET NARROWER E DISTRIBUTIONS – EVEN BETTER SEPARATION OF DOUBLE SCATTERS.

0.5% SYSTEMATICS FEASIBLE

MUST BE BETTER THAN BARE BEBC

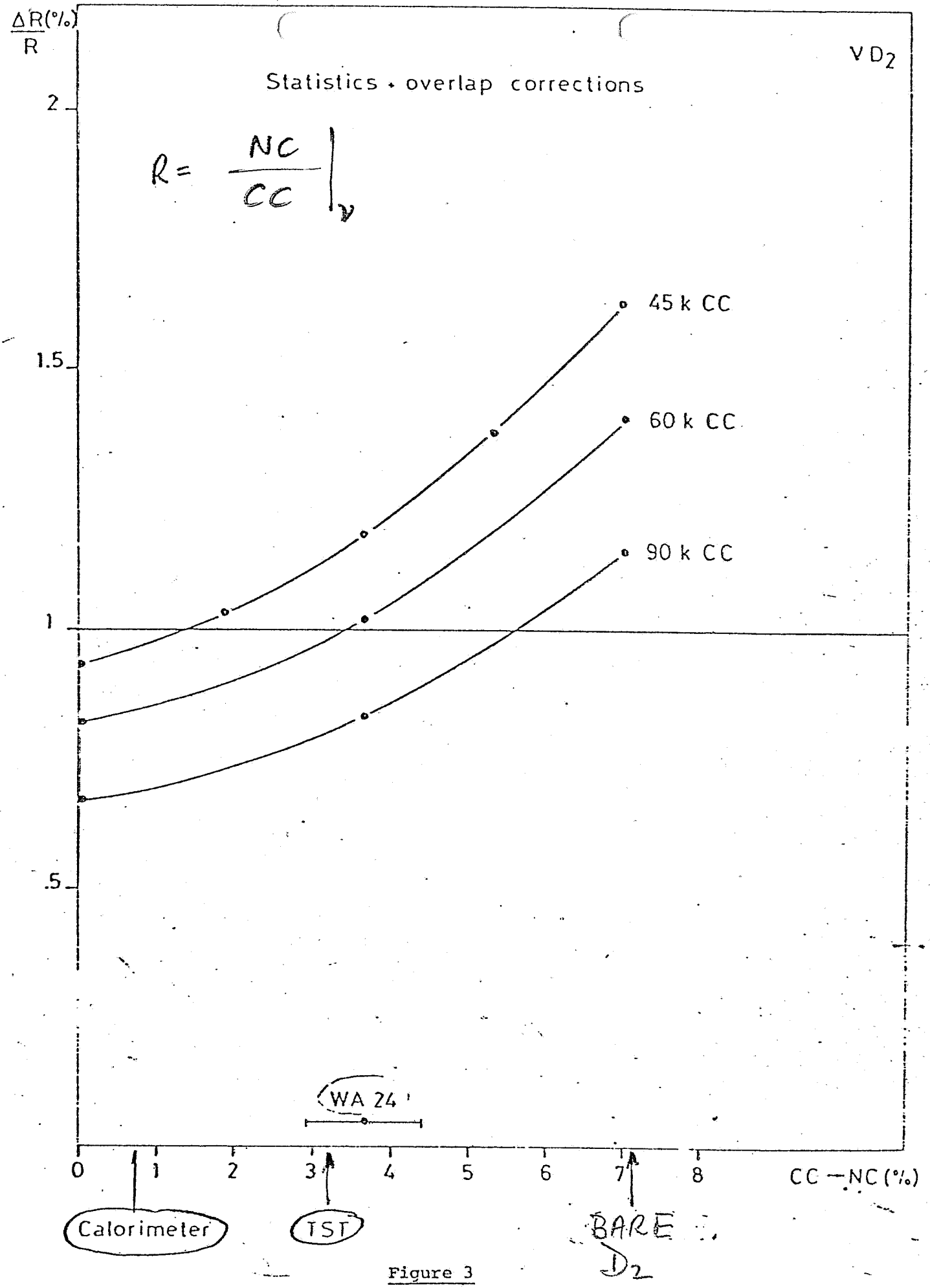
ΔR(%)
R
VD2
Statistics + overlap corrections
R = NC/CC |ν
2
1.5
1
.5
45 k CC
60 k CC
90 k CC
WA 24
0
1
2
3
4
5
6
7
8
CC — NC (%)
Calorimeter
TST
BARE D2

Figure 3

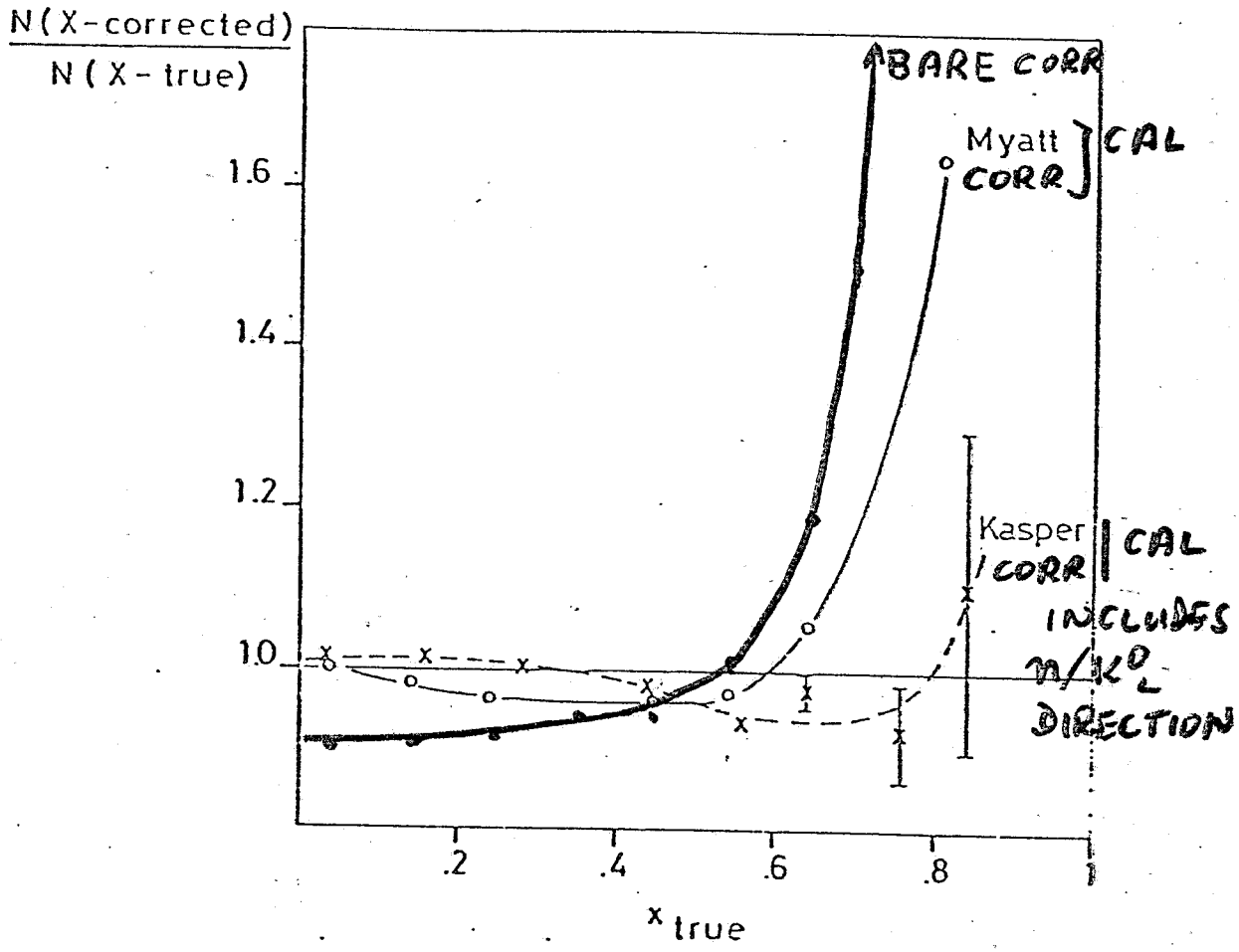
N(X-corrected)
N(X-true)
BARE CORR
Myatt CORR
CAL
1.6
1.4
1.2
1.0
Kasper CORR
CAL
INCLUDES
π/K⁰
DIRECTION
.2
.4
.6
.8
x true

Figure 2

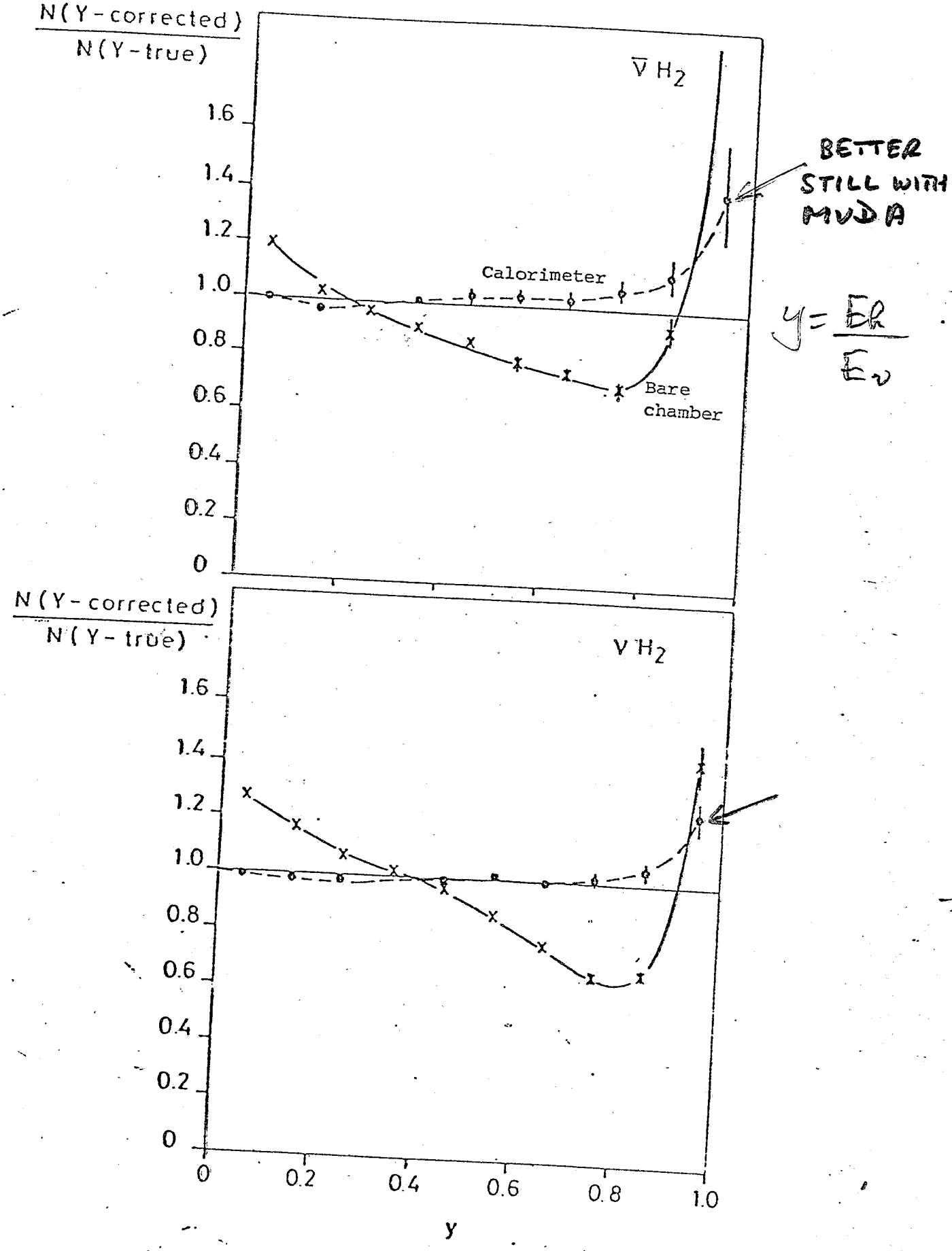
N(Y-corrected)
N(Y-true)
$\bar{\nu}$ H2
1.6
1.4
1.2
1.0
0.8
0.6
0.4
0.2
0
Calorimeter
Bare chamber
BETTER STILL WITH MUSA
y = Eh / Eν
N(Y-corrected)
N(Y-true)
ν H2
1.6
1.4
1.2
1.0
0.8
0.6
0.4
0.2
0
0
0.2
0.4
0.6
0.8
1.0
y

Figure 1

MAJOR PHYSICS AIMS

NOT NECESSARILY IN ORDER OF IMPORTANCE

(1) $\sin^2\theta_W$

FOR ± 0.005 NEED CALORIMETER
AND OPTION (A) — 50,000 CLEAN ν CC

OPTION (B) WILL HAVE 40,000 ν CC
+ 20,000 $\bar{\nu}$ IN ½ EXPERIMENT
SENSITIVITY $\sim \pm 0.007$

GOOD ENOUGH TO CHECK CDHS
(CDHS SYSTEMATIC ERRORS WORRY US)

IF STANDARD MODEL THEN MOST OF
RADIATIVE CORRECTION IS ELECTROMAGNETIC
BUT OTHER MODELS COULD GIVE BIGGER
ELECTROWEAK EFFECTS
" MEASUREMENT TO ~ 0.005 WELL WORTHWHILE "
C. QUIGG

CALORIMETER EXPERIMENT WILL BE SENSITIVE TO Θ_R IN TWO WAYS

a) TARGET QUARK FLAVOUR

$$\frac{NC(p)}{NC(n)}, \quad \frac{NC(p)}{CC(p)}, \quad \frac{NC(n)}{CC(n)}$$

ratios in ν and "$\bar{\nu}$" experiments.

PAC ASKED FOR EFFECT OF WRONG-SIGN BACKGROUND IN ANTINEUTRINO

NEW STUDY BASED ON SUMS OF ν & $\bar{\nu}$

i.e. $\dfrac{NC(p)_\nu + NC(p)_{\bar{\nu}}}{CC(p)_\nu + CC(p)_{\bar{\nu}}}$ etc

RAN EXPERIMENTS WITH

— 20K ν CC + 800 $\bar{\nu}$ CC WSB

and 20K $\bar{\nu}$ CC + 20K ν CC WSB

— MONTE CARLO STATISTICAL ERRORS AND SYSTEMATIC ERRORS

— FIT TO u_L, d_L, u_R, d_R AND WSB RATES. (OR TO $R_R, R_L, \Theta_R, \Theta_L$ EQUIVALENT)

— START FROM G.S.W. VALUES, BUT ERRORS CAUSE FIT TO CONVERGE TO DIFFERENT PLACES.

(2) NC CHIRAL COUPLINGS

SPRING 1983 DATA

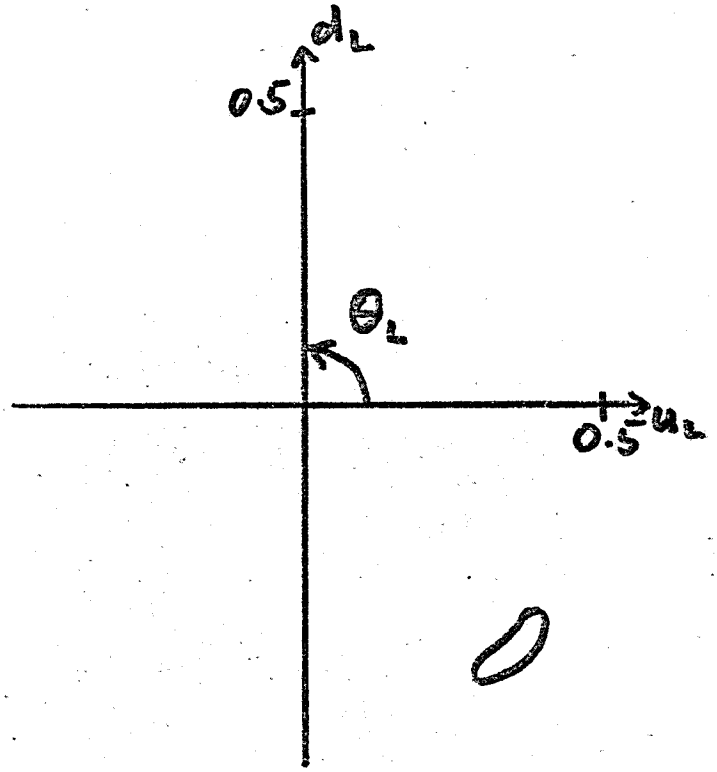

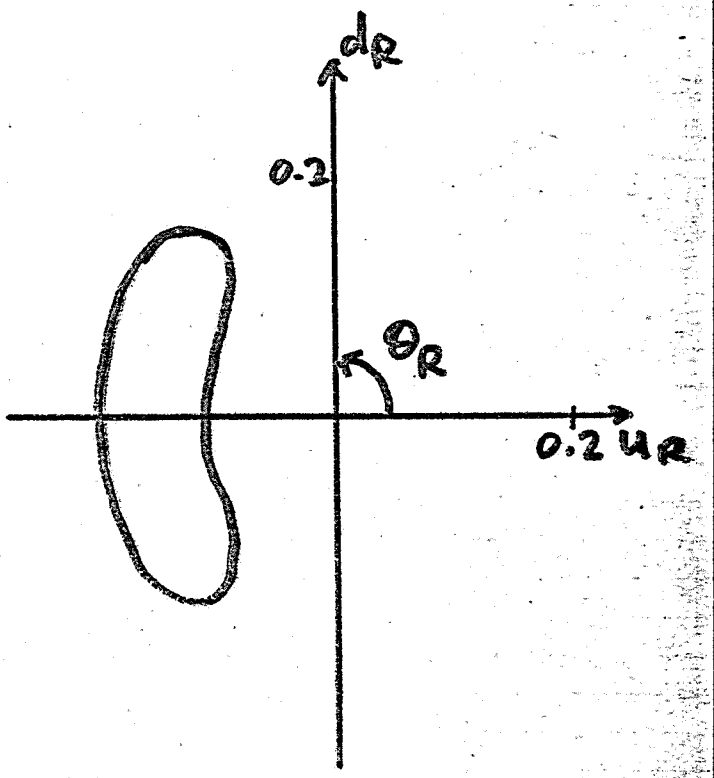

$u_L = 0.344 \pm 0.026$ $\quad u_R = -0.153 \pm 0.022$

$d_L = -0.419 \pm 0.022$ $\quad d_R = ?$

GSW MODEL SAYS $d_R = \frac{1}{3}\sin^2\theta_W$

BUT EXPERIMENT IS CONSISTENT WITH 0 FOR R.H. COUPLING OF d QUARK.

IN FACT, IF THE GARGAMELLE P.S. AND E180 PION FRAGMENTATION RATIOS ARE IGNORED, ONLY $(u_R^2 + d_R^2)$ IS DEFINED IN R.H. COUPLING PLANE — FROM

IN FACT, IF THE GARGAMELLE P.S. AND E180 PION FRAGMENTATION RATIOS ARE IGNORED, ONLY $(u_R^2 + d_R^2)$ IS DEFINED IN R.H. COUPLING PLANE - FROM ISOSCALAR RATIO $R_{\bar{\nu}} = \frac{NC}{CC}\Big|_{\bar{\nu}}$. NEED A FLAVOUR-SENSITIVE EXPERIMENT FOR d_R (OR θ_R)

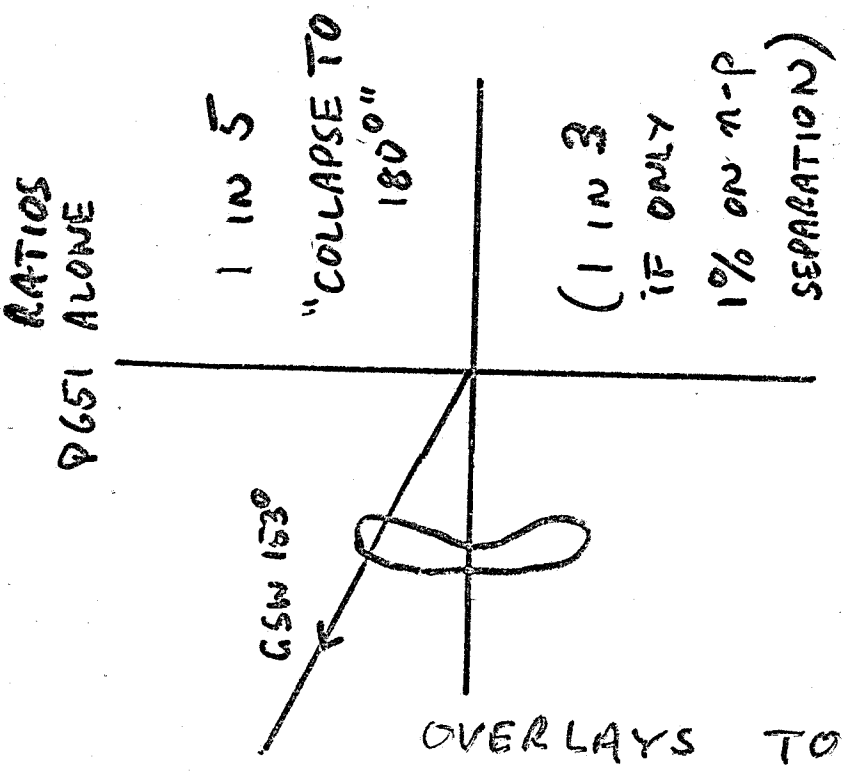

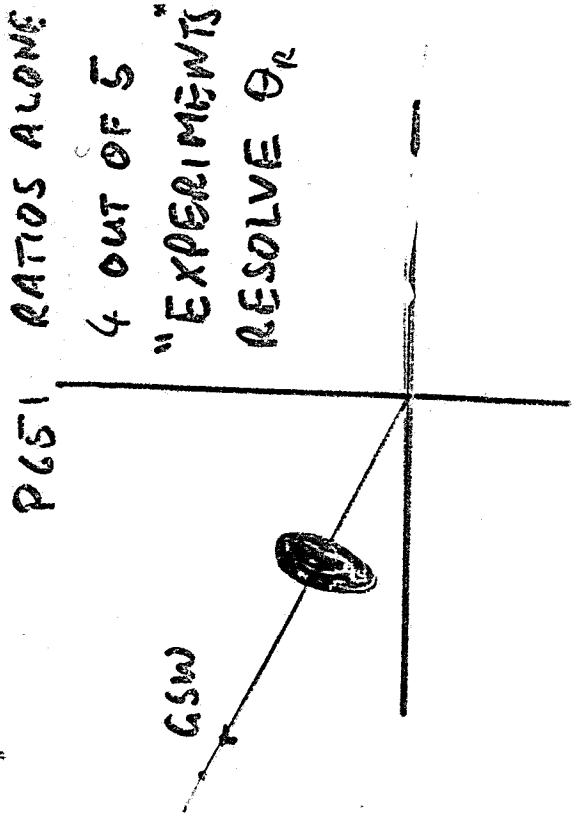

(b) $R^{+/-}_{\nu,\bar{\nu}}$

THE RATIO OF +VES TO −VES IN THE CURRENT FRAGMENTATION REGION − FLAVOUR OF FRAGMENTING QUARK.

STUDY IN WA 24 SHOWS THAT OPTION (B) WOULD GIVE

$R^{+/-}_{\nu}$ TO ~7%

$R^{+/-}_{\bar{\nu}}$ TO ~11% AFTER WSB UNFOLDING.

FITS WITH $R^{+/-}$ MOVED UP & DOWN 1 s.d. SHOW AGAIN 1 "EXPERIMENT" IN 5 WILL COLLAPSE TO 180° IN θ_R.

(USE CC EVENTS TO SEE PURE u OR d FRAGMENTS)

BUT METHODS a) & b) ARE INDEPENDENT

SO OPTION (B) { 20K ν CC
20K $\bar{\nu}$ CC + 20K WSB ν CC

HAS ~96% CHANCE OF RESOLVING d_R FROM ZERO.

~60% CHANCE OF DOING IT SIMULTANEOUSLY BY BOTH METHODS.

WILL ALSO GIVE PRECISE VALUES FOR u_L, u_d, u_R

W v D's estimate of 1985 situation
(after WA25, with all other expts
except new CDHS)

$u_L = 0.345 \pm 0.017$
$d_L = -0.420 \pm 0.015$ $\quad \Delta\theta_L = 2.3^\circ$

$u_R = -0.154 \pm 0.018$ $\quad \Delta\theta_R = 11.9^\circ$
d_R NOT RESOLVED

PG51 ALONE (DJM)

$u_L = 0.344 \pm 0.007$ $\quad \Delta\theta_L = 1^\circ$
$d_L = -0.424 \pm 0.007$

$u_R = -0.155 \pm 0.013$
$d_R = 0.077 \pm (0.03)$ $\quad \Delta\theta_R = 10^\circ$

COULD ALSO EXPRESS IN TERMS
OF SAKURAI'S VARIABLES —
(ISOVECTOR, ISOSCALAR)
× (AXIAL, VECTOR)

NEED PRECISION ON ALL OF u_L, d_L, u_R, d_R
TO FIX SAKURAI COMBINATIONS.

CHIRAL COUPLINGS ARE MUCH BETTER WITH D_2 + CALORIMETER THAN WITH EITHER HEAVY LIQUID OR BARE DEUTERIUM

BECAUSE

a) NC-CC SEPARATION WITHOUT CUTS GIVES $R_\nu = \left.\frac{NC}{CC}\right|_\nu^{I=0}$, $R_{\bar\nu} = \left.\frac{NC}{CC}\right|_{\bar\nu}^{I=0}$

TO BETTER PRECISION THAN ANYONE ELSE

$\longrightarrow (u_L^2 + d_L^2)$, $(u_R^2 + d_R^2)$

(COUNTERS NEXT BEST. HLBC OR BARE D_2 MUCH WORSE)

b) p − n SEPARATION USING WELL-MEASURED $\epsilon = \sum_i (E_i - p_{l_i}) - m_N$

GIVES SENSITIVITY TO TARGET QUARK FLAVOUR. IMPOSSIBLE IN H. L.
NOT SO GOOD IN BARE D_2

c) CAN MAKE CLEANER CUTS FOR $R^{+/-}$ WITH E_H WELL MEASURED — BETTER THAN BARE D_2.

HEAVY LIQUID HAS BAD SYSTEMATICS DUE TO RESCATTERING OF OUTGOING FRAGMENTS.

(3) FLAVOUR DISTRIBUTIONS

BECAUSE OF EMC EFFECT

F_2 IS WELL STUDIED

p AND n NOT

μ EXPERIMENTS GIVE F_2 ON NUCLEON

MUST USE NEUTRINOS FOR xF_3, $\bar{q}$

RECENT E 616 RESULT ON xF_3

HAD 23,000 $\bar{\nu}$ EVENTS(CC).

PGSI WILL HAVE 20,000 $\bar{\nu}$ CC
(OPTION B) 40,000 ν CC
HORN IMPORTANT

- ON D_2
- WITH ALMOST NO CUTS
- WITH BETTER x AND y RESOLUTION

FOR $\bar{q}$ PGSI IS ESPECIALLY WELL PLACED

FIT HIGH y EVENTS IN $\bar{\nu}$ D TO FIND $(\bar{u}+\bar{d}+2s)=\bar{q}$

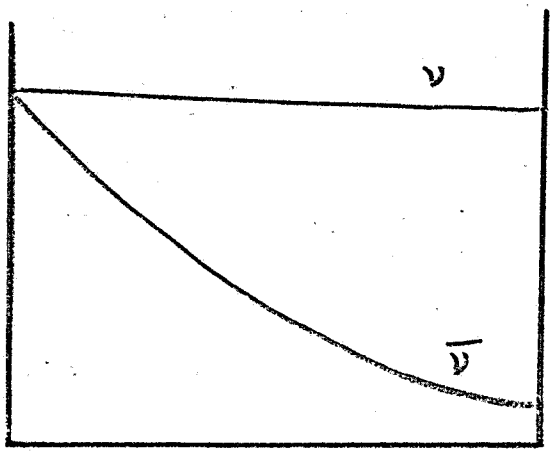

CALORIMETER ALLOWS V. LOW CUT ON P_μ — MVDA AND MEASURES y DIRECTLY

CAN ALSO SEPARATE

$\bar{q}$ IN p FROM $\bar{q}$ IN n

— GET $\bar{u}$, $\bar{d}$ DIFFERENCE

(IF ANY)

ν STATISTICS $\sim 1/6.5$ CDHS, $\sim 1/2.5$ CHARM

BUT SYSTEMATICS WILL BE

BETTER (POINT TO POINT).

$\therefore$ WILL HAVE ACCURATE VALUES ($\sim 14\%$)

FOR $\bar{q}(x)$ IN BROAD Q^2 BANDS

- COMPARE WITH Fe FOR EMC EFFECT
  (PRESENT CDHS H_2 RESULT IS SUBJECT TO GREAT EXPERIMENTAL DIFFICULTIES)

REAL TEST OF MODELS

- COMBINE WITH xF_3 AND F_3 FOR ALTARELLI–PARISI FIT TO GLUE

- DETERMINE $\bar{q}$ DISTRIBUTIONS FOR USE IN $\bar{p}p$ COLLIDERS. (KANE CTY 20 TEV?)

LARGE x, LOW Q^2 (HIGHER TWIST)

STATISTICS LIMITED BUT WE

CAN MAKE MEASUREMENTS UP TO

BEYOND $x \sim 0.8$

COLLABORATORS AT I.C. LONDON HAVE

PION STRUCTURE FUNCTION

$$\frac{(\text{DRELL-YAN})_N}{(\text{D. I. S.})_N} = K$$ FOR NUCLEON STR. FN.

$(\text{DRELL-YAN})_\pi$ HAS BEEN MEASURED

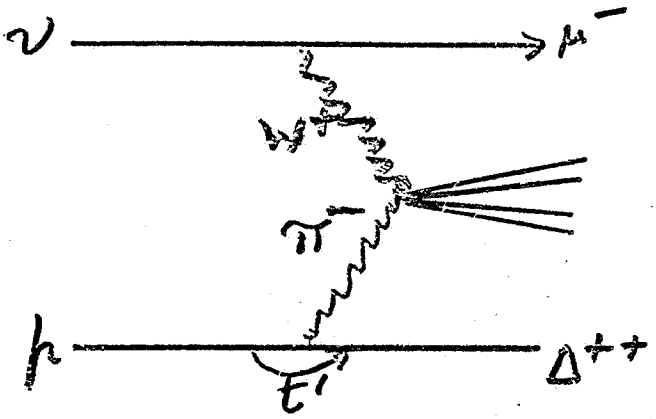

SELECT LOW t' FOR π

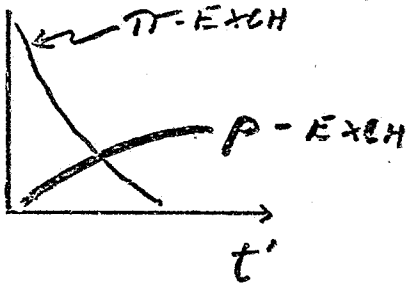

$W^+ d$
$W^+ \bar{u}$
} WILL INTERACT

∴ MEASURE VALENCE + SEA.

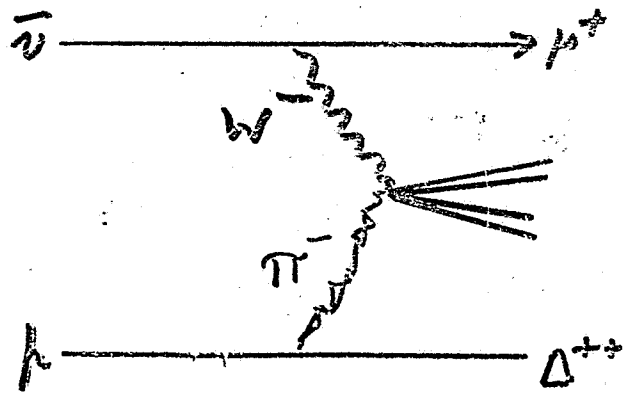

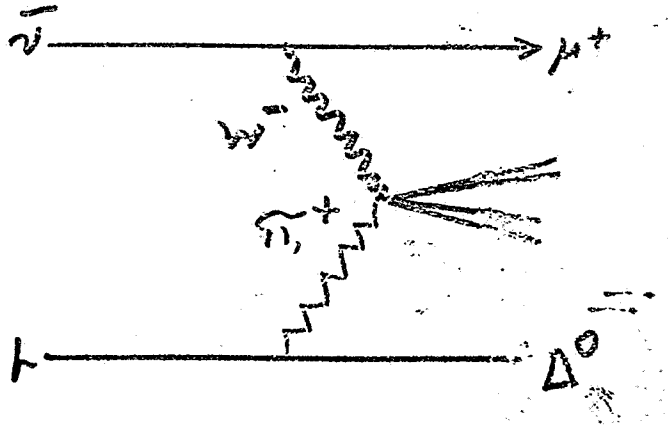

$W^- d$
$W^- \bar{u}$
} DO NOT INTERACT

$W^- u$
$W^- \bar{d}$
} DO INTERACT

∴ STUDY VALENCE + SEA

$W^- \bar{d}$
$W^- u$
} DO INTERACT

STUDY SEA OF PION

PRELIMINARY

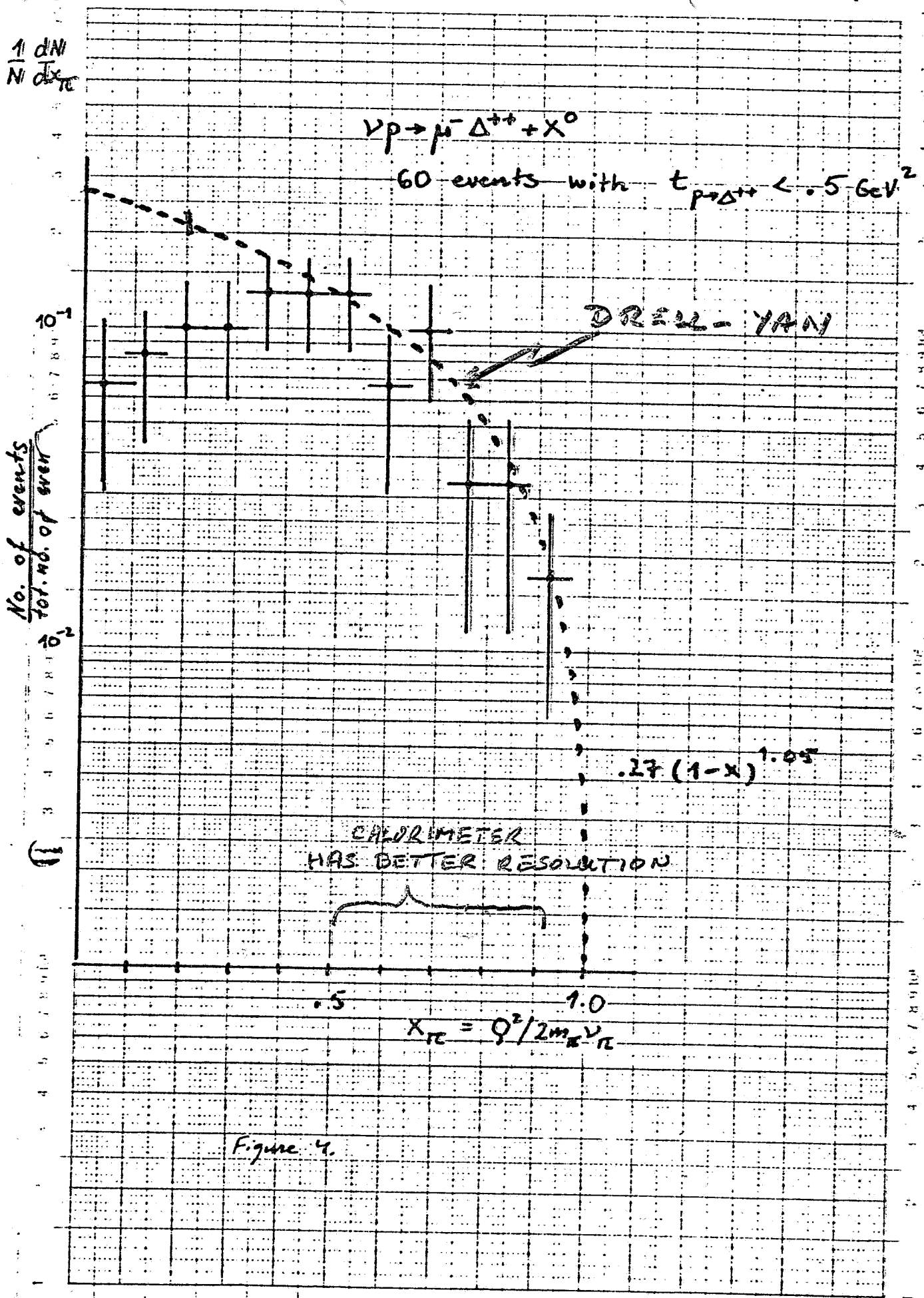

Figure 4.

ONLY HAD ~1000 ν +~1000 $\bar{\nu}$ BUT WERE MEASURING $\frac{\partial F_2}{\partial(\log Q^2)}$ OUT TO $x \sim 0.8$

SEE SUGGESTION OF ANOMALLY AT END OF RANGE.

? GSI WILL HAVE ~20× STATISTICS*!!
MUCH BETTER x RESOLUTION

---

* MAYBE SLIGHTLY REDUCED FIDUCIAL VOLUME FOR HIGH ENERGY MUONS.

DYDAK AT CORNELL

"CERN HAS DECIDED NOT TO CONTINUE WITH THE STUDY OF THE QUARK STRUCTURE OF NUCLEONS"

WITH P GSI FERMILAB COULD FILL THE GAP.